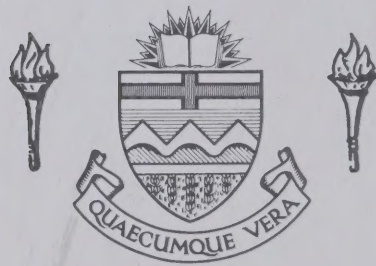


For Reference

NOT TO BE TAKEN FROM THIS ROOM

Ex LIBRIS
UNIVERSITATIS
ALBERTAENSIS



THE UNIVERSITY OF ALBERTA

A DETAILED PALEOMAGNETIC INVESTIGATION OF GEOMAGNETIC
SECULAR VARIATION IN WESTERN CANADA

by



ISMAIL B. HUSSIN

A THESIS

SUBMITTED TO THE FACULTY OF GRADUATE STUDIES AND RESEARCH
IN PARTIAL FULFILMENT OF THE REQUIREMENTS FOR THE DEGREE

OF MASTER OF SCIENCE


IN

GEOPHYSICS

DEPARTMENT OF PHYSICS

EDMONTON, ALBERTA

FALL, 1978



Digitized by the Internet Archive
in 2023 with funding from
University of Alberta Library

<https://archive.org/details/Hussin1978>

to my wife were thicker because of

SUJANAH

and to my parents

JURIAH HAJI IDRIS & HUSSIN HAJI IMAM,

without whose continuing encouragement and loyal support

without whose continuing encouragement and loyal support
this thesis would not have been written.

this thesis would not have been written.

ABSTRACT

The intensity and direction of the geomagnetic field vector not only vary from place to place on the surface of the Earth, but they also show variation with time. The long term variations due to causes within the Earth are referred to as secular variation. The rather brief historical records can be extended backwards by sampling sequences of dated sediments. In this study paleomagnetic specimens were collected from a 7 metre thick section representing some 9,000 years, which is part of a much thicker sequence of strata laid down during the Olympia Interglaciation (43,000-20,000 yrs.B.P.). The specimens carry a stable remanent magnetization, and the overall mean direction is $D=005.7^\circ$, $I=+65.4^\circ$ ($N=94$, $R=93.3099$, $k=135$, $\alpha_{95}=1.3^\circ$), which is significantly different from the present geomagnetic field vector at the sampling locality ($D=022.3^\circ$, $I=+72.6^\circ$). The mean of the virtual geomagnetic poles lies at $0.0^\circ E$ and $85.6^\circ N$ ($N=94$, $R=92.7032$, $K=72$, $A_{95}=1.7^\circ$) and is statistically distinct from the Earth's spin axis being both 'right-handed' and 'far-sided'. There is no evidence of the recently reported Mono Lake and Lake Mungo 'excursions' even though the age of the above events are spanned by the sequence. Instead a sequence of smooth declination and inclination oscillations are observed with major

periodicities of a few thousand years. These trace out a remarkable pattern in which three-quarters of an open loop is first traversed counterclockwise, then clockwise, and finally counterclockwise again. The most likely explanation involves an easterly biased non-dipole field and a geocentric dipole which undergoes a linear oscillation with a period of about 5,000 years.

ACKNOWLEDGEMENTS

I wish to express my sincere thanks to my supervisor Dr. M. E. Evans who introduced me to the subject. I am also grateful for his invaluable advice and guidance at various stages of this project.

I am also thankful to Dr. G. S. Hoyer for the assistance given in the collecting of the specimens.

During the course of this study, financial support was received from the Universiti Teknologi Malaysia and the University of Alberta.

TABLE OF CONTENTS

	Page
CHAPTER 1 INTRODUCTION	
1.1 Geomagnetism and Secular Variation	1
1.2 Archaeomagnetism and Paleomagnetism	10
1.3 Organization of Thesis	12
CHAPTER 2 Detailed Paleomagnetic Results from a Quaternary Section in British Columbia	
2.1 Geological Details	14
2.2 Field and Laboratory Techniques	18
2.3 Results	21
2.4 Comparison of Sampling Methods	28
2.5 Comparison of the Present Study with Oberg's Reconnaissance Results	35
CHAPTER 3 The Nature of the Remanent Magnetization	
3.1 Remanence Removed by Partial Demagnetization	42
3.2 Viscous Remanent Magnetization	47
3.3 Magnetic Mineralogy	53
CHAPTER 4 Analysis of the Riggins Road Paleomagnetic Data	
4.1 Introduction	59
4.2 Site Means and Overall Mean Paleomagnetic Field Directions	59
4.3 Declination and Inclination Oscillations	75
4.4 Spectral Analysis	85
4.5 Discussion	95
CHAPTER 5 Summary and Conclusions	106
BIBLIOGRAPHY	112

	Page
APPENDIX 1 List of Data Used in Chapter 2	118
APPENDIX 2 Carved Specimens Data	129
APPENDIX 3 Viscous Remanent Magnetization Data	131
APPENDIX 4 IRM Build-Up Data	133
APPENDIX 5 High Temperature Data	134

LIST OF TABLES

Table	Page
1.1 The spectrum of temporal variations of the geomagnetic field of internal origin.	5
2.1 Comparison of sampling techniques.	36
3.1 Viscous remanent magnetism of four specimens.	50
3.2 VRM's and vectors removed by AF demagnetization.	52
4.1 Site means at 0, 10 and 20 mT.	61
4.2 Periods and sense of looping with different filter lengths.	91
4.3 Periods and sense of looping of the divided data set.	94

LIST OF FIGURES

Fig.		Page
1.1	The non-dipole field for 1945.	3
1.2	Secular change of declination and inclination at Baltimore, Boston, London and Paris from observatory measurements.	7
1.3	Variation of geomagnetic dipole moment from archaeomagnetic studies.	8
1.4	Probabilistic model for reversals..	9
2.1	Stratigraphic succession at the Riggins Road exposure.	15
2.2	Mean (and range) of the AF demagnetization for the 10 pilot specimens.	23
2.3	Angular shift between successive AF demagnetization steps for the 10 pilot specimens.	24
2.4a-j	Rates of angular shift ($d\theta/dH$) and Zijderveld plots for the 10 pilot specimens.	25
2.5a-c	Declination, inclination and intensity magnetograms for all the 376 specimens at 0, 10 and 20 mT.	29
2.6	Site means results from laboratory carved sites and the corresponding sites carved in situ.	33
2.7	Comparison of intensity profiles of the present study with Oberg's reconnaissance study.	38
2.8	Comparison of the site mean intensity, declination and inclination of the present study with Oberg's reconnaissance study.	40
3.1a	Mean of the 94 site means at 0, 10 and 20 mT.	43

Fig.		Page
3.1b	Mean of the 94 site means removed vectors at 0-10 mT and 10-20 mT.	43
3.1c	Removed vectors for the 10 pilot specimens.	43
3.2	Acquisition of viscous remanent magnetization (VRM).	49
3.3	Mean (and range) of the AF demagnetization curves of the 100 hours VRM.	51
3.4a-d	IRM build-up curves for specimens HAH04, HAR04, HAS04 and HBB02.	54
3.5a-d	Variation of intensity with temperature.	57
4.1a-c	Site means; declination, inclination, intensity and Fisher's precision parameter (k) at 0, 10 and 20 mT.	63
4.2	A plot of Fisher k versus the lateral spread of specimens at each site.	67
4.3	Virtual geomagnetic poles (VGP's) for all 94 horizons with their mean and its circle of 95% confidence.	69
4.4	Mean common site longitude (CSL) pole position for the Quaternary and for the Riggins Road data with their respective circles of 95% confidence.	71
4.5	ΔD_0 anomaly averaged by 30° longitude sectors.	74
4.6a,b	Magnetograms of three-point and five-point moving averages.	78
4.7a	Azimuthal equidistant plot of the 94 site means.	81
4.7b,c	Three-point and five-point moving averages of the data shown in (a).	81

Fig.		Page
4.8a,b	Declination and inclination power spectra obtained by Fourier analysis.	86
4.9	Plot of FPE versus prediction error filter length.	89
4.10a-c	MEM power spectra of the complex time series.	90
4.11a-c	MEM power spectra of the divided data set.	93
4.12	Secular variations pattern obtained at latitude 50°N by letting the 1945 non-dipole field drifts westward.	96
4.13	Secular variations pattern when the dipole is allowed to precess counterclockwise around the spin axis at distances of 6° and 12° .	97
4.14a	Temporal variations of inclination when the pole is allowed to 'nod' back and forth along the meridian of the observer.	98
4.14b,c	Temporal variations of declination and inclination when the pole is allowed to 'nod' back and forth along a meridian at 45° to the meridian of the observer.	98
4.14d,e	Temporal variations of declination and inclination when the pole is allowed to 'nod' back and forth along a meridian at 90° to the meridian of the observer.	98
4.15	<p>Azimuthal equidistant plot of secular variations pattern obtained from a model whereby the observer is situated at 50°N and</p> <ul style="list-style-type: none"> (i) the dipole oscillates with a period $T_{\text{DO}} = 8,250$ years (ii) the dipole nods along the meridian of the observer with a period $T_{\text{DN}} = 5,500$ years (iii) the non-dipole is biased 	

Fig.		Page
	eastwards and oscillates with a period $T_{\text{NDO}}=2,300$ years.	102
4.16	Standing part of the non-dipole east component.	104

CHAPTER 1

INTRODUCTION

1.1 Geomagnetism and Secular Variation

The Chinese, probably as early as the second century B.C., invented the earliest known form of magnetic compass (Needham, 1962). In Europe the directional properties of the lodestone were referred to by Alexander Neckham in 1190, and Petrus Peregrinus discovered the dipole nature of the magnet in 1269. The magnetic declination was known to the Chinese in the eighth century A.D. (Needham, 1962; Smith & Needham, 1967), and was rediscovered in Europe in the latter part of the fifteenth century. The magnetic inclination was discovered independently by Georg Hartman in 1544 and Robert Norman in 1576. In 1600, William Gilbert synthesized these observations in his well known treatise 'De Magnete'. Gilbert described the Earth's magnetic field as that of a uniformly magnetized sphere. By 1839 global coverage was sufficient for C.F. Gauss to undertake the first thorough mathematical analysis of the field. His spherical harmonic analysis showed that more than 99.5% of the Earth's magnetic field is internal in origin and all subsequent analyses have confirmed this finding. This type of analysis further shows that approximately 80% of the Earth's field can be

attributed to a single geocentric dipole inclined at 11.5° to the axis of rotation with a magnetic moment of about 8×10^{22} A.m². Approximately 85% of this axial dipole field is attributed to a single dipole along the rotation axis and the remaining 15% to two orthogonal dipoles lying in the equatorial plane. When the best fitting dipole field is subtracted from that observed over the Earth's surface the residual is termed the non-dipole field. At present there are some eight non-dipole features (foci or anomalies) of continental dimensions displaying either positive or negative values with typical amplitudes of 10^{-5} T (Fig. 1.1). Lowes (1955) and Alldredge & Hurwitz (1964) represented the dipole and non-dipole fields by a central dipole and an array of 8 to 10 smaller eccentric radial dipoles with moments ranging from less than 1×10^{22} A.m² up to 5×10^{22} A.m².

As yet there is no completely satisfactory answer to the problem of the origin of the Earth's magnetic field. The most plausible theories involve some form of dynamo action (Elasser, 1946; Bullard, 1949). The Earth's core is both a fluid and a good electrical conductor. In other words it permits both the flow of electrical current and mechanical motions: the resulting interactions are thought to generate a self sustaining magnetic field. A comprehensive recent review is given by Gubbins (1974).

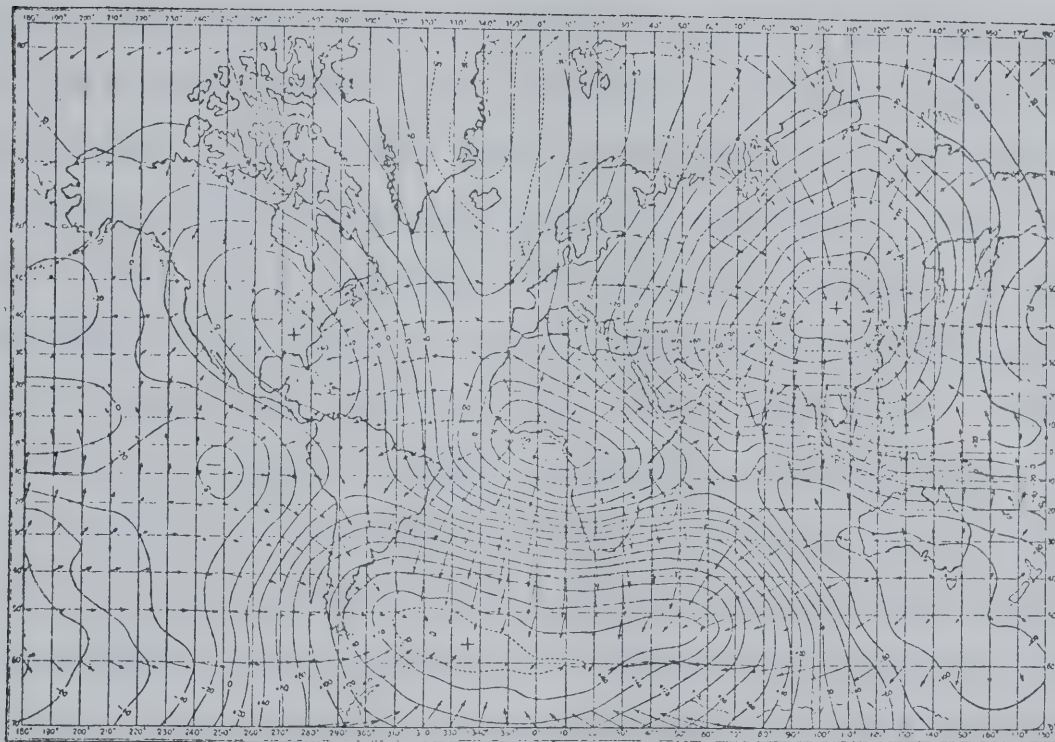


Fig. 1.1 The non-dipole field for 1945. The arrows indicate the direction and magnitude of the horizontal component. The contours give the vertical component at intervals of 2.0×10^{-6} T (after Bullard et al., 1950).

The intensity and direction of the magnetic field vector not only vary from place to place on the Earth's surface but they also show variation with time. There are two distinct types of temporal change; transient fluctuations and long term variations. The transient fluctuations arise from causes outside the Earth; they are very small and produce no enduring changes in the geomagnetic field. They are of no consequence in the present study. On the other hand the long term variations, often referred to rather loosely as secular variation, are of prime interest to us. These are due to causes within the Earth and the net effect over long intervals of time may be considerable. The 'spectrum' of temporal variations of internal origin exhibits periods ranging from less than 10^2 years to 10^6 years or more (Table 1.1).

At the surface of the Earth the non-dipole component of the field, although much weaker than the dipole, changes more rapidly, with periods as short as decades. There seems to have been a general westward drift of approximately 0.2° of longitude per year, over the first half of this century (Bullard et al., 1950) but paleomagnetic studies have indicated the presence of both eastward as well as westward drifts (Yukutake, 1962; Skiles, 1970). Examples of historically recorded changes in declination and inclination

Table 1.1 The Spectrum of Temporal Variations of the Geomagnetic Field of Internal Origin (after Jacobs, 1975 and McElhinny & Merrill, 1975).

Types of variation	Period
Minimum observable period	3.7 years
Secular variation of non-dipole field	
'High frequency' oscillations	< 100 years
'Medium frequency' oscillations	100 - 5,000 years
'Westward drift'	~ 2,000 years
Secular variation of dipole field	
Dipole 'wobble' (eastward drift)	1,200 - 1,800 years
Field strength oscillations	9,000 years
Main field generation mechanism	$10^3 - 10^4$ years
Magnetic Excursions	$10^3 - 10^4$ years
Polarity Reversals	
Change in field direction	1,000 - 4,000 years
Change in intensity	3,000 - 10,000 years
Time interval between polarity changes	$10^5 - 10^7$ years
Bias in favour of one polarity	$10^8 - 10^9$ years

at several observatories are illustrated in Fig. 1.2. These patterns usually take the form of open loops, and Runcorn (1959) and Skiles (1970) have shown that clockwise looping results from westward drift of non-dipole features and vice versa.

One of the most significant discoveries in paleomagnetic studies is that of reversals of the Earth's magnetic field. In the dynamo theory a field could be produced in either direction. There is no a priori reason why the magnetic field of the Earth should have a particular polarity and there is no fundamental reason why its polarity should not change. The observed field reversals are highly irregular and therefore have been modelled as a non-stationary random process. Cox (1968) developed a probabilistic model to explain reversals in which it is assumed that the changes in polarity result from an interaction between random processes and steady oscillations. The steady oscillator is the dipole component (Fig. 1.3) whilst the random variations are due to the non-dipole field. The random variations serve as the triggering mechanism that results in a reversal whenever the non-dipole to dipole ratio exceeds a critical value (Fig. 1.4). Cox (1975) suggests that the non-dipole sources are not randomly distributed with respect to latitude. During times of normal polarity, flux emerges from the core in localized regions

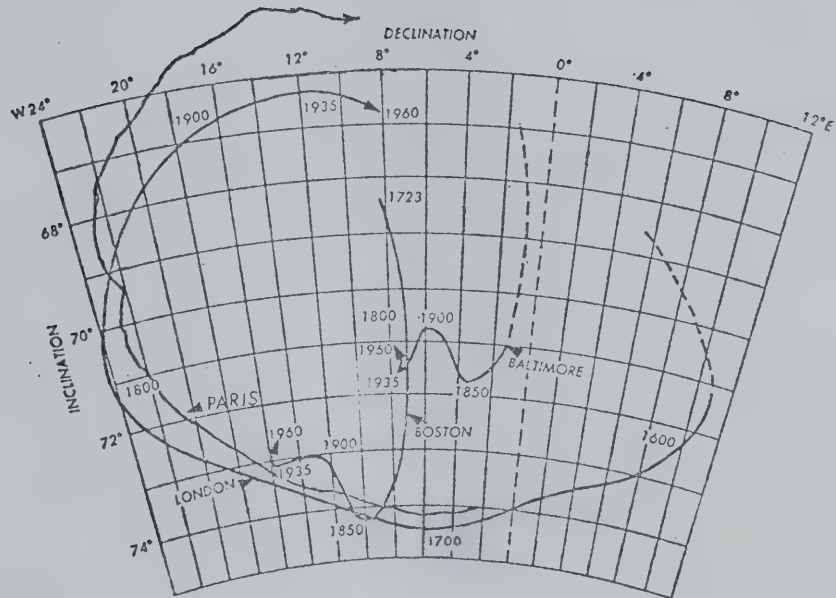


Fig. 1.2 Secular change of declination and inclination at Baltimore, Boston, London and Paris from observatory measurements. Note the same clockwise motions even though the size of the loops vary (after Nelson et al., 1962).

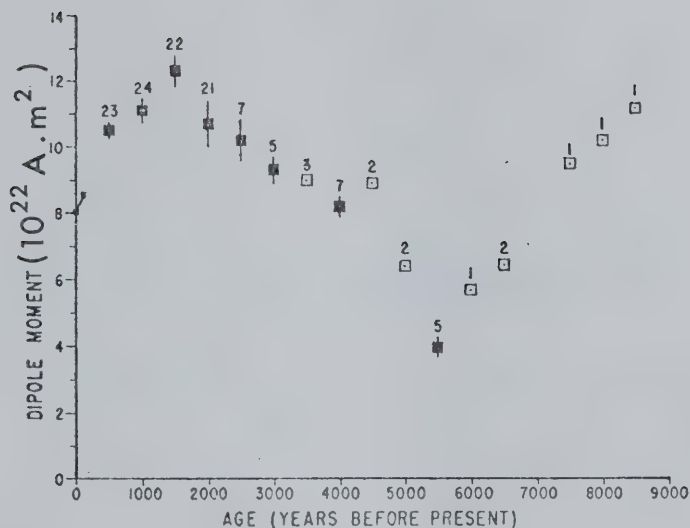


Fig. 1.3 Variation in geomagnetic dipole moment from archaeological studies. The short bar near the ordinate represents change during the past 130 years as determined from spherical harmonic analysis. The archaeological results are averages over 500 year intervals. The number of averaged data is shown above each point and the vertical lines indicate the standard error of the mean. Unshaded squares refer to intervals containing too few data to provide meaningful statistics (after Cox, 1968).

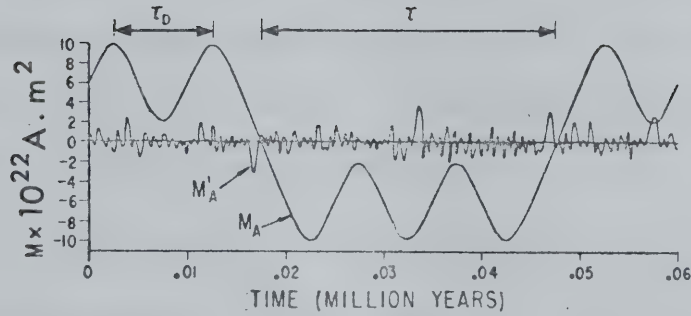


Fig. 1.4 Probabilistic model for reversals. τ_D is the period of the dipole field and τ the length of a polarity interval. Whenever the quantity $(M_A + M_A')$ changes sign a polarity change will occur. M_A is the moment of the dipole field and M_A' is the axial non-dipole moment (after Cox, 1968).

near the equator and reenters the core in localized regions approximately 55° from either pole. On the other hand during times of reversed polarity this entire pattern is reversed suggesting that the toroidal field also reverses when the dipole field reverses itself. The latitudes at which the large features of the non-dipole field are generated by convective cells or fluid motions therefore appear to be linked to the polarity of the dynamo.

Apart from reversals, the Earth's field appears to undergo 'excursions' which seem to represent a kind of enhanced secular variation but are not total reversals. Barbetti & McElhinny (1976) give a summary of localities and ages of geomagnetic excursions recorded over the past 40,000 years. However in a recent review Verosub & Banerjee (1977, p.153) "do not feel that the existence of any proposed excursion is yet sufficiently well established for its reality to be beyond question."

1.2 Archaeomagnetism and Paleomagnetism

The records of long term variations (>100 years) of the Earth's field can be extended backwards for a few thousand years using remanence preserved in historically dated lavas and archaeological material. The main difficulty encountered is the precise dating of the samples, the intermittent

extrusion of lava flows and the sporadic rise and fall of past civilizations. An alternative method is to sample sequences of dated sediments, especially in the Late Quaternary where the C^{14} method of age determinations can be used. The geomagnetic record in these sediments is primarily acquired by a process known as detrital remanent magnetization (DRM) (for a recent review see Verosub, 1977). Depositional DRM is the process whereby magnetic particles eroded from preexisting rocks are aligned by the ambient field as they settle. The process of rotation of such particles into the ambient field direction when they are in the water-filled interstitial holes of a wet sediment prior to consolidation is termed post-depositional DRM. Johnson et al. (1948), King (1955) and Griffiths et al. (1960) have investigated the depositional process under controlled laboratory conditions whilst Irving & Major (1964) and Blow & Hamilton (1977) have investigated the post-depositional process. The laboratory studies of post-depositional DRM show impressive agreement between the direction of the applied field and that of the magnetization of the sediment, however studies of depositional DRM often indicate an 'inclination error', i.e. even though the declination is faithfully recorded by the sediment, the sediment inclination is less than the applied field inclination. Irving (1957, 1967) and Opdyke (1961) have confirmed that

these effects do not seem significant for most rocks of paleomagnetic interest since any inclination error acquired during the deposition of the particles is 'corrected for' by subsequent post-depositional DRM.

1.3 Organization of Thesis

The present work is a detailed follow up study of a reconnaissance investigation by C.J.Oberg (1978). A Quaternary section which spans some 9,000 years was sampled at stratigraphic intervals representing approximately 100 years to achieve a high resolution data base suitable for investigation of secular variation patterns and application of spectral analysis techniques.

The subject matter is divided as follows:

Chapter 2 gives an account of the field and laboratory techniques employed. The rock magnetic properties and mineralogy of the magnetic carriers are discussed in Chapter 3. Analysis of the paleomagnetic results is discussed in Chapter 4. The maximum entropy method is used to obtain improved knowledge of the geomagnetic spectrum since it is a radically new approach to power spectrum estimates which obviates several limitations of conventional methods and is especially suitable for short time series. Worldwide geomagnetic secular variation results during the Late

Quaternary are summarized in relation to the present study in Chapter 5.

The standard statistical techniques due to Fisher (1953) are used in analysing the data presented. Fisherian statistics are essentially an analogue of Gaussian statistics adapted to distributions on a sphere. The most important parameter involved is the precision parameter, $k = (N-1)/(N-R)$ (N = number of unit vectors and R = length of the resultant of the N unit vectors) which corresponds to the Gaussian invariance. At a probability level of $(1-P)$, the true mean direction of the population lies within a circular cone about the vector resultant R with a semi-angle $\alpha_{(1-P)} = \cos^{-1} \left[1 - \frac{N-R}{R} \left\{ (1/P)^{1/(N-1)} - 1 \right\} \right]$. For small α , the circle of 95% confidence is given by $\alpha_{95} = 140/(kN)^{1/2}$.

S.I. units are used throughout the thesis. Since much geophysical literature is still written in c.g.s units, conversions for the most common parameters are given below.

Magnetic dipole moment, $1 \text{ A.m}^2 = 10^3 \text{ emu}$

Intensity (moment/unit mass), $1 \text{ A.m}^2/\text{kg} = 1 \text{ emu/gm}$

Magnetic induction, $10^{-9} \text{ Tesla} = 10^{-5} \text{ gauss} = 1 \text{ gamma}$

CHAPTER 2

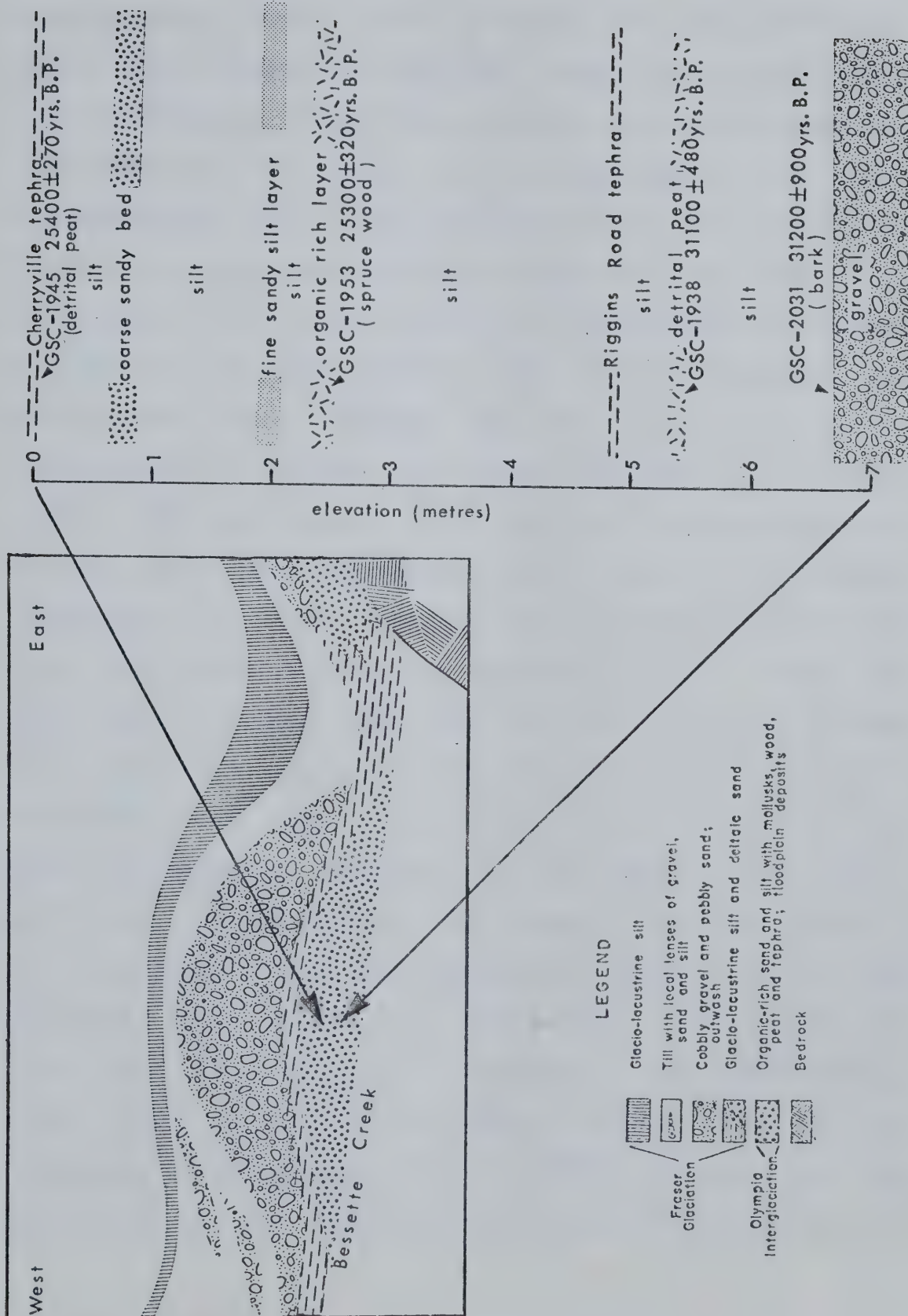
Detailed Paleomagnetic Results from a Quaternary Section in British Columbia

2.1 Geological Details

The late Quaternary geologic/climatic units in southern British Columbia and northwestern Washington State record a sequence of glacial and interglacial episodes, usually referred to as Postglacial (10,000-0 yrs.B.P.), Fraser Glaciation (20,000-10,000 yrs.B.P.), Olympia Interglaciation (43,000-20,000 yrs.B.P.) and Okanagan Glaciation (>43,000 yrs.B.P.) (Westgate and Fulton, 1975). The Olympia Interglacial sediments in the interior plateau region of British Columbia contain several thin layers of rhyolitic and dacitic tephra which represent the distal portions of widespread airfall eruptive units. Each tephra layer, being of regional extent and distinctive chemical character, serves as a useful time-parallel stratigraphic marker.

In this study paleomagnetic specimens were collected from a 7 metre thick section which itself is part of a much thicker sequence of strata laid down during the Olympia Interglaciation (Fig. 2.1). The outcrop sampled forms a stream-cut escarpment on the edge of Bessette Creek

Fig. 2.1 Stratigraphic succession at the Riggins Road exposure. The section sampled is part of a sequence laid down during the Olympia Interglaciation (43,000 - 20,000 yrs.B.P.). The four radiocarbon dates are shown.



approximately 10 km east of Lumby, B.C. (lat. $50^{\circ}7'55''\text{N}$, long. $118^{\circ}51'45''\text{W}$), and consists of dark organic-rich flood plain sediments. With the exception of a coarse sandy bed approximately 0.3 m thick, and a fine sandy silt layer approximately 0.2 m thick near the top of the section, the sediment is remarkably uniform in character and there is no evidence of any major change in depositional environment during the time span sampled. The section contains four radiocarbon dated horizons and two tephras, namely the Cherryville and Riggins Road tephras (Westgate and Fulton, 1975). The radiometric dates are vital for estimating the average rate of deposition, which assumes considerable importance in later analysis and discussion. Two of the dates were obtained from wood specimens, but the other two were from detrital peat. Some time may have passed between the death and deposition of any biological material, therefore both wood and detritus dates may be too old for their stratigraphic position, but they cannot be too young. The wood, having retained its integrity, is less likely to have undergone a long pre-depositional history. Since both detritus dates appear too old relative to the wood dates (the upper one is even out of sequence), the sedimentation rate given by the two wood dates is likely to be the most accurate. The lower wood date ($31,200 \pm 900$ yrs.B.P.) lies at the base of the section. The upper wood date ($25,300 \pm 320$

yrs.B.P.) lies 4.50 m above this, giving an average deposition 'slowness' of 13 ± 2 yrs/cm (deposition rate of 0.77 ± 0.01 mm/yr). The discrepancies between the various dates are not large - a linear regression using all four dates yields a deposition 'slowness' of 10 yrs/cm. The age of the oldest specimens is nominally 31,200 yrs.B.P., and extrapolation of the estimated deposition rate yields an age of 22,100 yrs.B.P. for the youngest specimens collected. Thus the total time span represented is slightly over 9,000 years.

2.2 Field and Laboratory Techniques

The specimens were collected in commercially available plastic cubes of 2 cm edge. Two small holes were drilled close to the base of each cube to let out air whilst the cube was being pressed or tapped gently into the vertical face of the outcrop. Each cube was painted on one face in a way which permitted unique orientation. Specimens were oriented by measuring three angles, strike, dip and roll with a Brunton compass-clinometer, as described in detail by Oberg (1978). Over the course of six days sampling, forty magnetic sun bearings were taken giving an average local magnetic declination of $21.7^\circ\text{E} \pm 0.8^\circ$ (s.d.). These data allow the orientation scheme to be assessed. The mean agrees quite well with the regional average (22.3°E , Canadian Isogonic

Chart for 1975.0), indicating that adequate accuracy was achieved. Likewise, the small variance, of less than a degree, indicates that good precision was attained.

After removal from the outcrop, each specimen was capped and sealed to prevent dessication. A total of ninety four sites (i.e. stratigraphic horizons) with four independently oriented specimens per site was sampled, beginning immediately below the Cherryville tephra. Sample spacing was as uniform as the outcrop allowed; of the ninety three intervals between sites, eighty nine were 7 cm, two were 9 cm, one was 12 cm and one was 18 cm. The sedimentation 'slowness' (13 ± 2 yrs/cm) indicates that the sampling interval is about 100 years, with each specimen representing 20-30 years. At each site the lateral spread was typically 30 cm but ranged from 10 to 60 cm. All stratigraphic elevations in this thesis are measured downwards from the Cherryville tephra (Fig. 2.1). The layer which extends from 0.63 m to 0.93 m was sandy and tended to crumble upon sampling, however the occurrence of a thin silt layer within this sandy layer allowed us to avoid too large a sampling gap. A total of eight sites were sampled within the hard compact silt layer which extends from 4.40 to 4.89 m. These specimens were obtained by carving stumps protruding from the vertical face of the outcrop over which plastic cubes could be snugly fitted. A comparison of data

from 'carved' versus 'tapped' specimens indicates that any distortion taking place as the cube penetrates the sediment is minimal and its magnetic effects negligible. The data involved in this test are brought together and discussed in section 2.4.

The specimens were stored in a magnetically shielded room (field strength approximately 40 nT, Reid, 1972) and taken out only for remanence measurement using a Digico balanced fluxgate magnetometer. All measurements were carried out with an integrating time of 37 seconds (i.e. 2⁸ spins), and instrument calibration was repeated every six measurements (i.e. approximately every 30 minutes). Empty cubes, painted and unpainted, gave no detectable signal above the noise level expected when the spinner is operated with no sample present (Molyneux, 1971). The specimens themselves are at least two, and generally three, orders of magnitude stronger than this.

Schmidt (1976) constructed Helmholtz coils to cancel the effect of flux concentration at the top of the mumetal shield of the magnetometer, which amounts to about twice the Earth's field. This potential problem was investigated by exposing a typical specimen to a field twice that of the Earth (approximately 0.1 mT) for periods from 10 minutes to 4 hours. No detectable remagnetization was observed and

therefore the flux concentration claimed by Schmidt does not seem to be a problem in this study. Perhaps Schmidt suffered from strong but very soft and unstable material.

Routine stepwise alternating field demagnetization studies were undertaken using the apparatus described by Murthy (1969) which is essentially identical to that developed by McElhinny (1966).

2.3 Results

To attempt isolation of the primary magnetization from magnetic 'noise', incremental demagnetization was undertaken. It is both impracticable and unnecessary to carry out complete demagnetization analysis of every specimen in an extensive collection such as this, instead the routine procedure of investigating selected pilot specimens in detail was followed. The treatment which best isolated the stable directions was then applied to the remainder of the collection. Ten pilot specimens were selected (one each from sites HAA 0 m, HAK 0.75 m, HAO 1.07 m, HBF 2.28 m, HBI 2.49 m, HBT 3.28 m, HCE 4.05 m, HCO 4.75 m, HDD 5.80 m and HDL 6.36 m) and subjected to stepwise AF demagnetization in peak fields of 2.5, 5.0, 10, 15, 20, 30, 40, 50 and 60 mT. At this point three specimens (HAK02, HAO03, HBT04) remained stable and were therefore treated in

higher fields; however they all underwent large angular shifts at 80 mT. Median destructive fields (MDF's) range from 10 to 30 mT with an average close to 20 mT (Fig. 2.2). Up to 30 mT, successive directional shifts were small (mean=2°, maximum=7°) ; beyond 30 mT some, but not all, specimens became unstable (Fig. 2.3). The results are illustrated by the Zijderveld (1964) convention in Fig. 2.4a-j. Also plotted is the rate of angular shift between successive demagnetization steps which has been used by some authors as a measure of stability (Symons & Stupavsky, 1974; Lowrie & Alvarez, 1977). As a result of the pilot investigation 10 and 20 mT were chosen as appropriate fields for AF cleaning of the remaining 366 specimens. Again, angular movements are small (mean=2° , for both the 0 to 10 mT and 10 to 20 mT steps), and the overall means at 10 mT and 20 mT are not significantly different. It thus appears that these samples carry a stable remanence, whose origin and significance is the subject of the following chapters. Prior to cleaning, intensities ranged from 2.94×10^{-6} to 4.28×10^{-4} A.m²/kg with a geometric mean of 2.77×10^{-5} A.m²/kg. After cleaning in peak fields of 10 and 20 mT, the geometric mean intensities are 2.12×10^{-5} and 1.45×10^{-5} A.m²/kg respectively. An archive of all the data (1,208 individual determinations of remanence) is given in Appendix 1. The results are illustrated in terms of magnetograms in

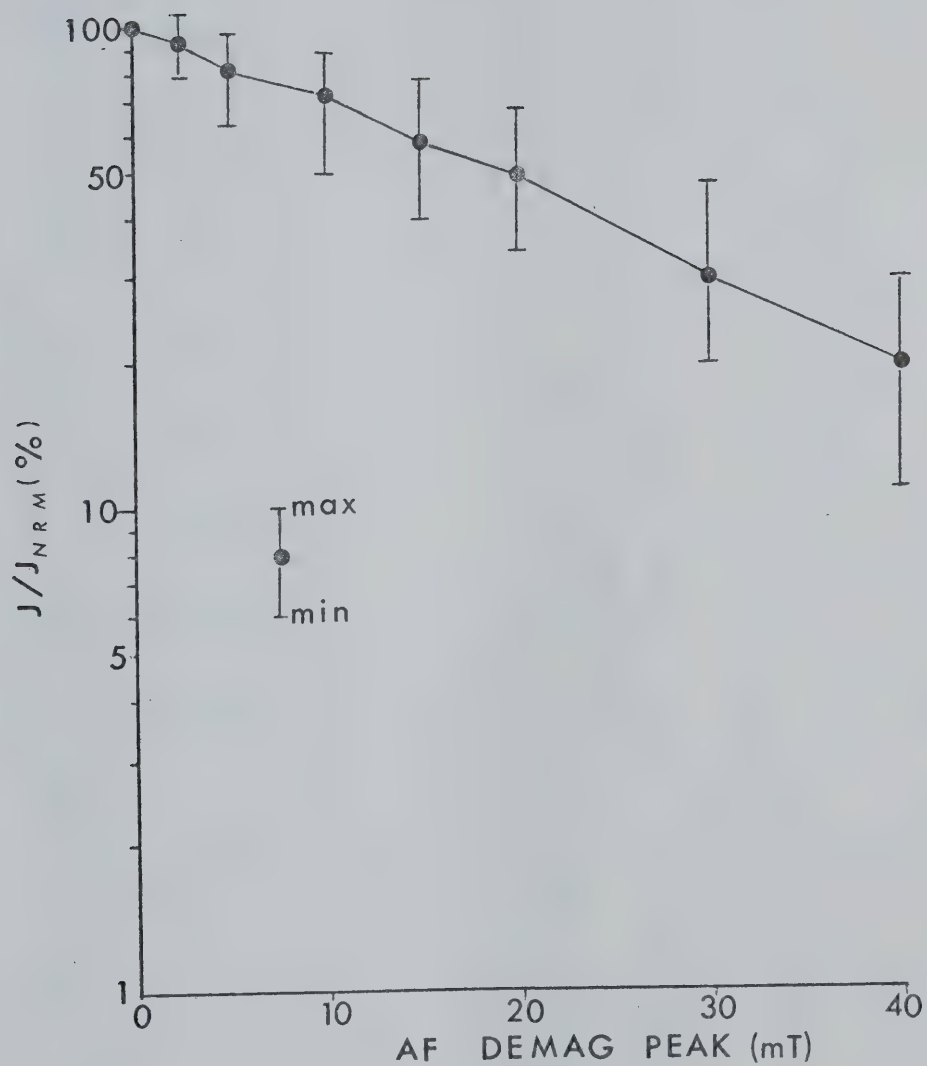


Fig. 2.2 Mean (and range) of the AF demagnetization curves for the 10 pilot specimens.

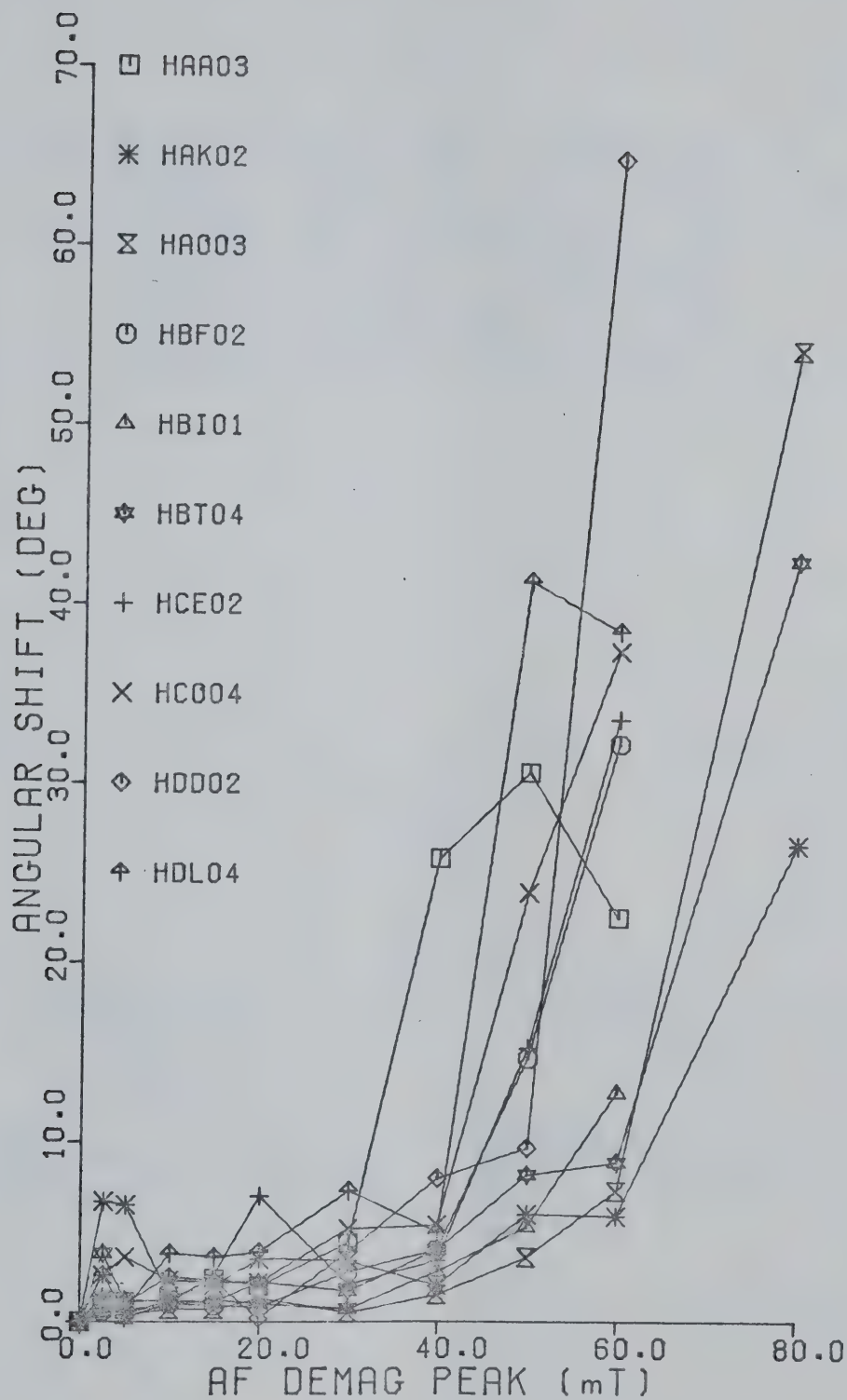
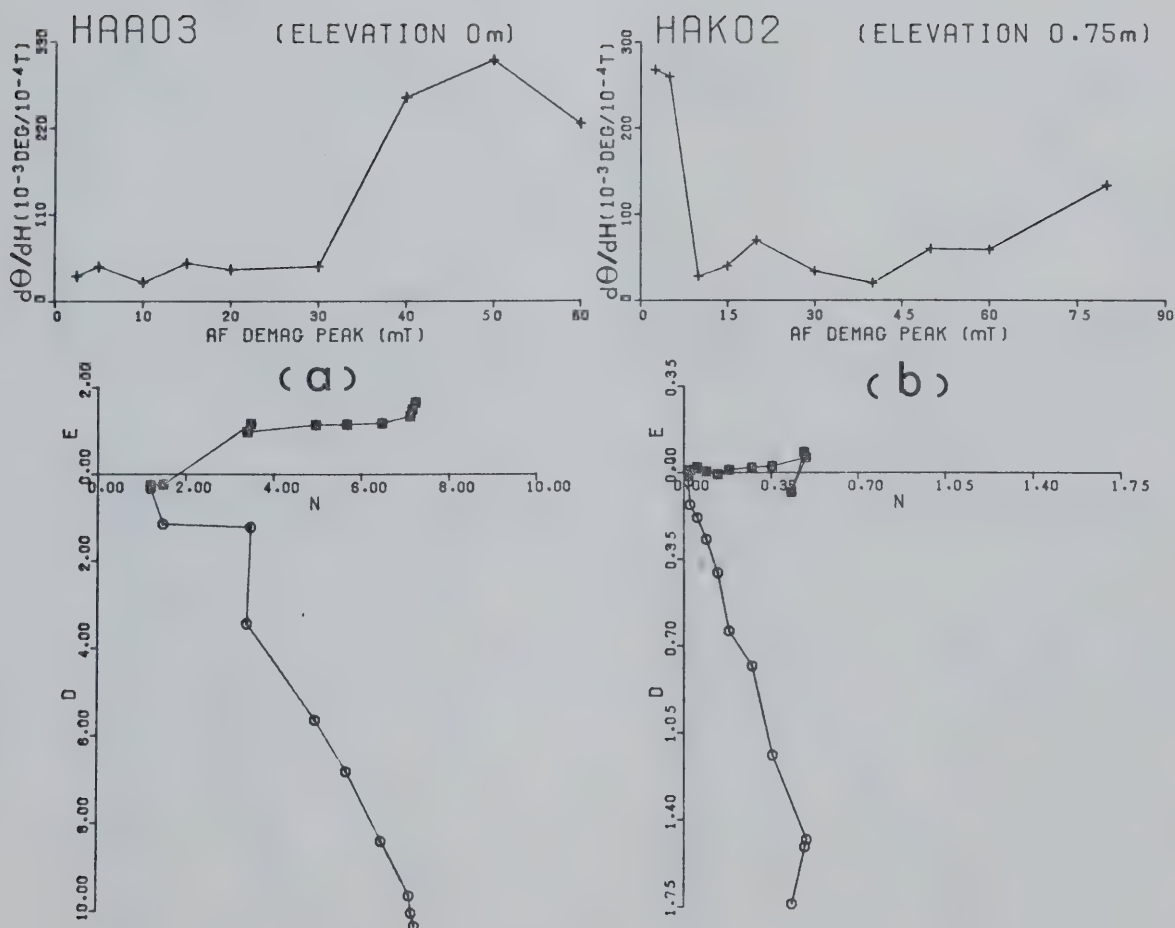
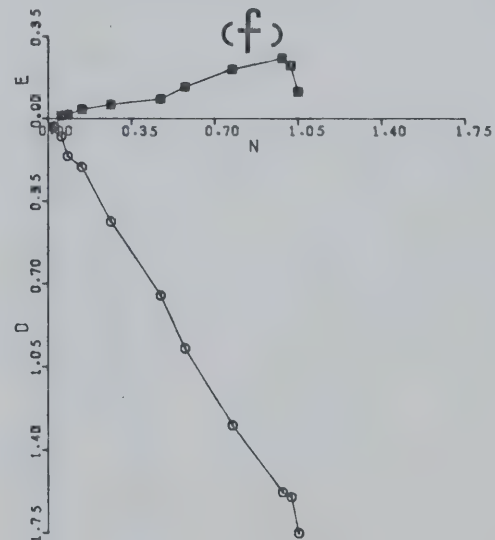
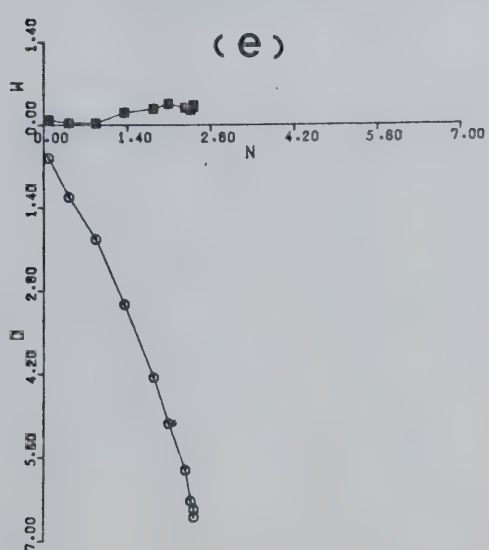
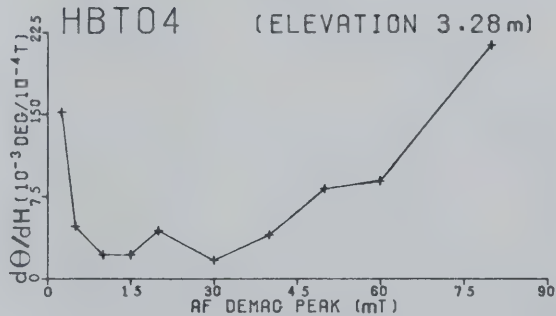
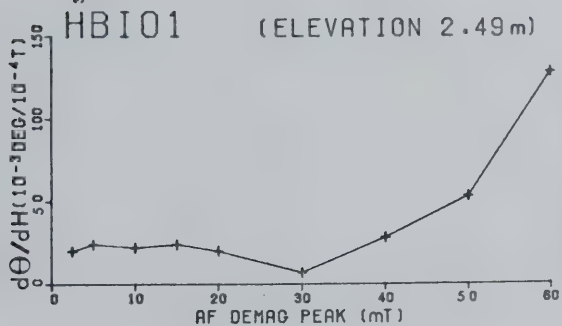
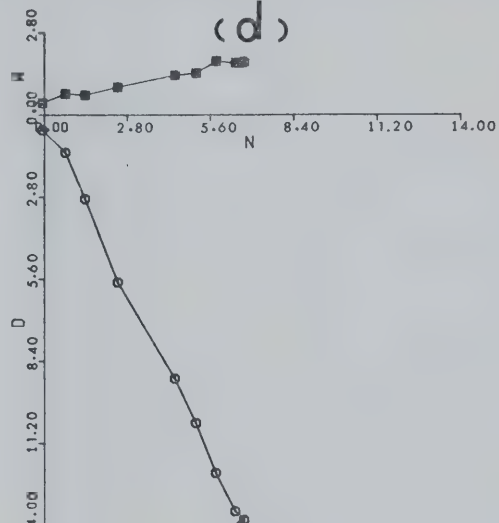
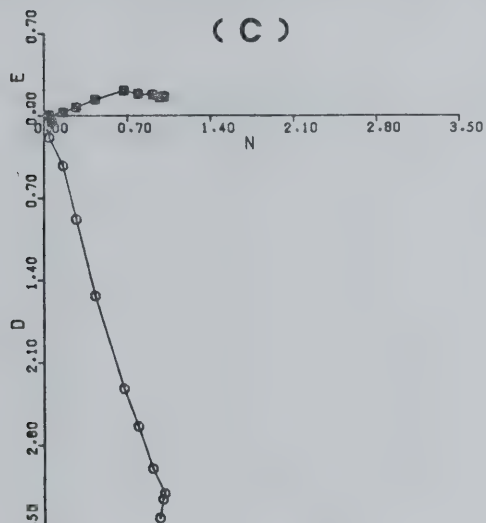
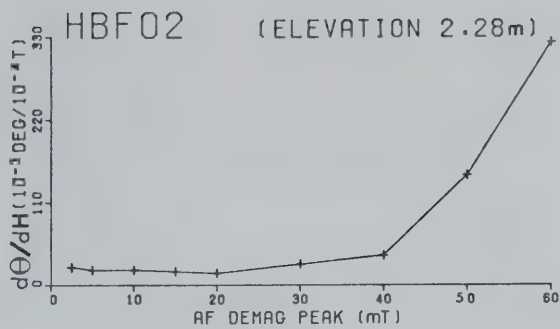
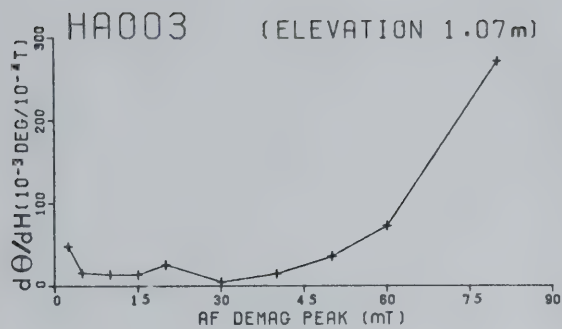


Fig. 2.3 Angular shift between successive AF demagnetization steps for the 10 pilot specimens.

Fig. 2.4a-j Rates of angular shift ($d\theta/dH$) and Zijderveld plots for the 10 pilot specimens. Units for $d\theta/dH$ are $10^{-3} \text{ deg} / 10^{-4} \text{ T} \equiv \text{mdeg} / \text{oe}$; the value for a particular demagnetization interval is plotted at the higher field value involved. Units for the Zijderveld plots are $1 \times 10^{-5} \text{ A.m}^2 / \text{kg}$.





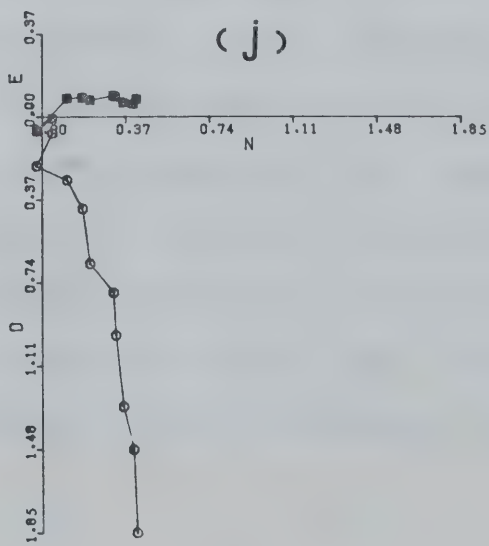
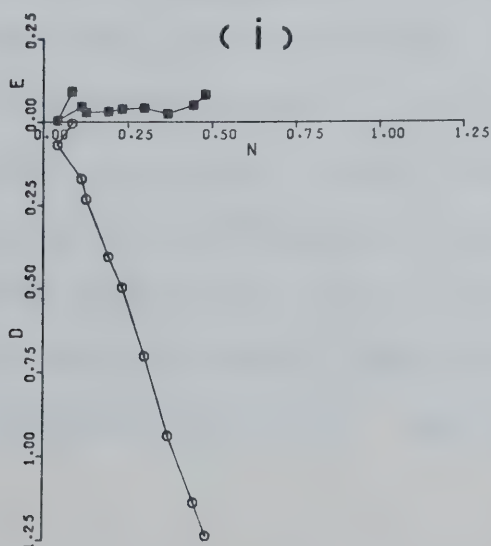
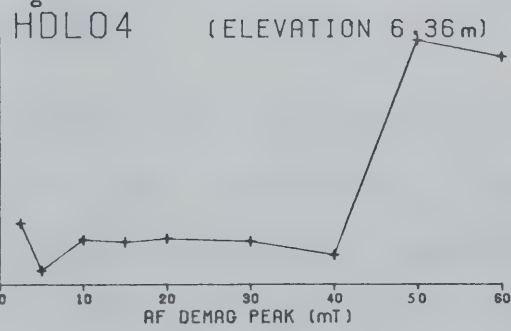
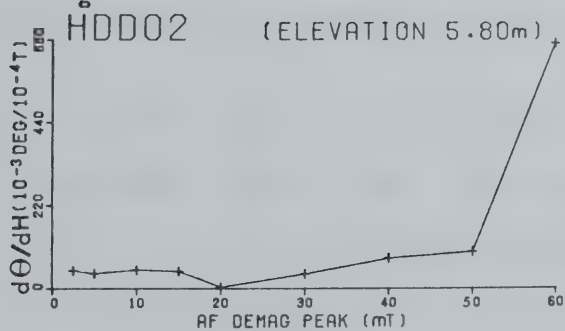
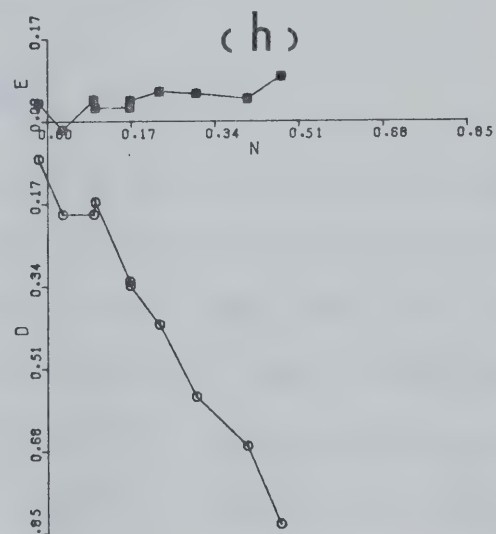
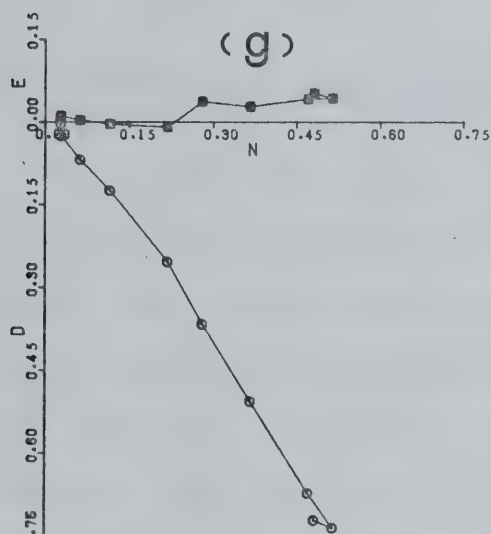
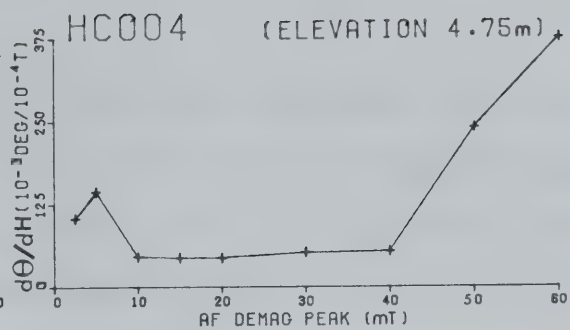
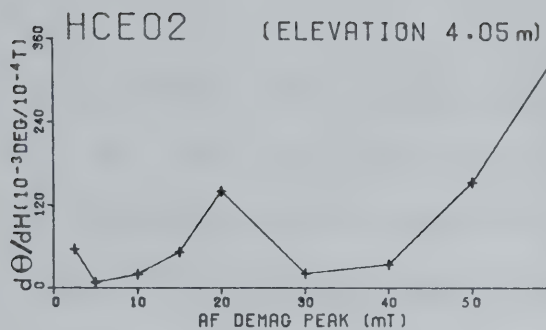


Fig. 2.5a-c, which show all the individual specimen data at 0, 10 and 20 mT. It is clear that smooth declination and inclination oscillations are present and the significance of these will be discussed in chapters 4 to 5.

2.4 Comparison of Sampling Methods

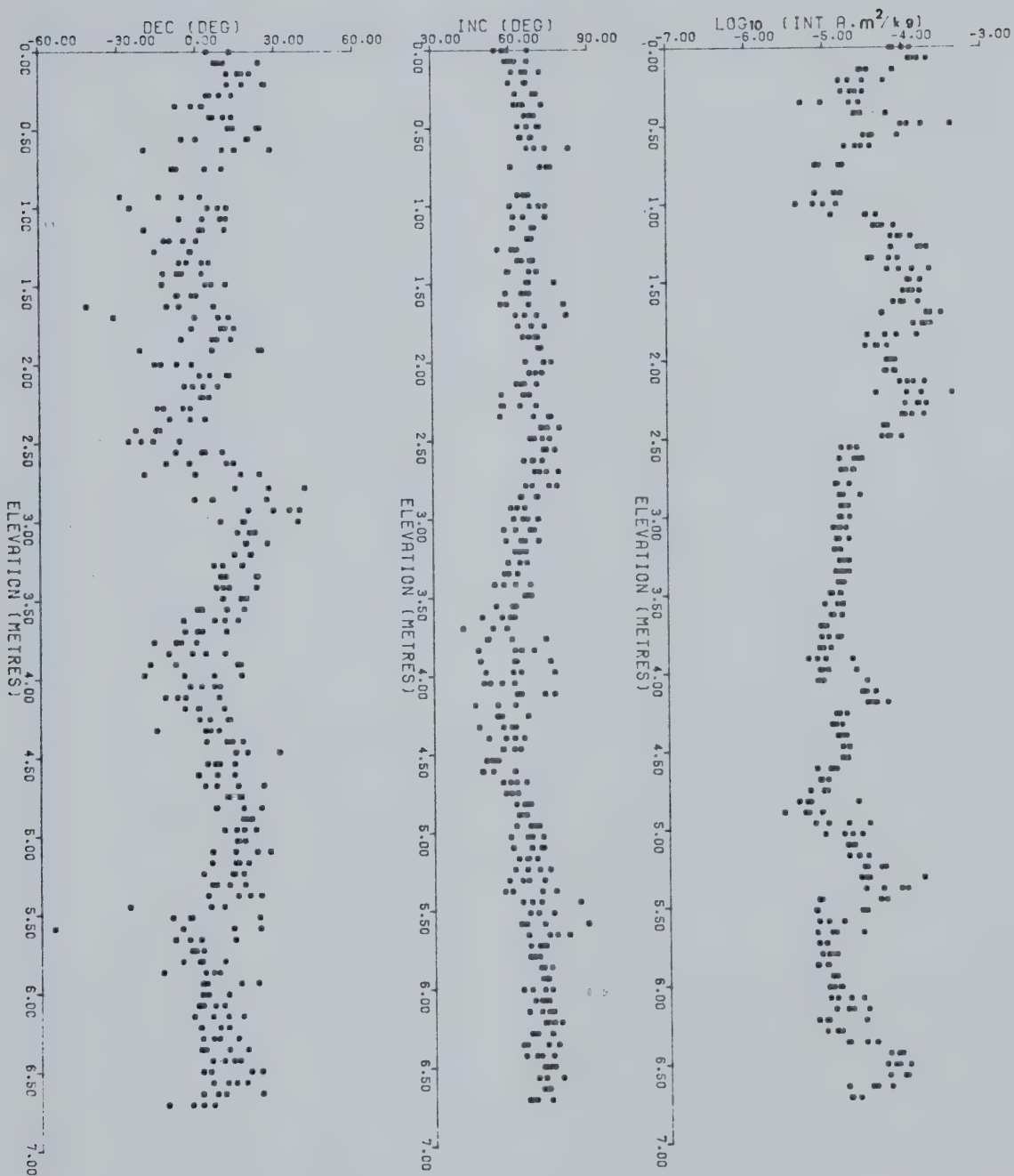
As discussed above, two sampling techniques were employed. The majority of specimens were collected by tapping the plastic cubes directly into the face of the outcrop, but where the sediments proved too hard carving was used. We also collected a large coherent block spanning the interval 1.28 m to 1.40 m. The results obtained by these different techniques are now assessed.

From the large block a total of five sites (four specimens each) were carved in the laboratory. The declination and inclination of these five sites in relation to adjacent collecting horizons are shown in Fig. 2.6. It is clear that the two data sets are in close agreement. Orientation error of the block, whose frontal face is not perfectly planar, is the most probable cause of the slight systematic differences observed. The elevation of one of these five sites (HEG) corresponds exactly to site HAS. Two other horizons (HEB = HBE, elevation 2.21 m; HEA = HDC, elevation 5.73 m) were sampled by both methods in the

Fig. 2.5a-c Declination, inclination and intensity magnetograms for all the 376 specimens at 0, 10, and 20 mT. (The declination of specimens HCY03 (0, 10, 20 mT ; elevation 5.45 m) and HDA04 (10 mT ; elevation 5.59 m) lie outside the scale used and are not plotted. This results from their high inclinations (81° to 88°). For complete details see Appendix 1).

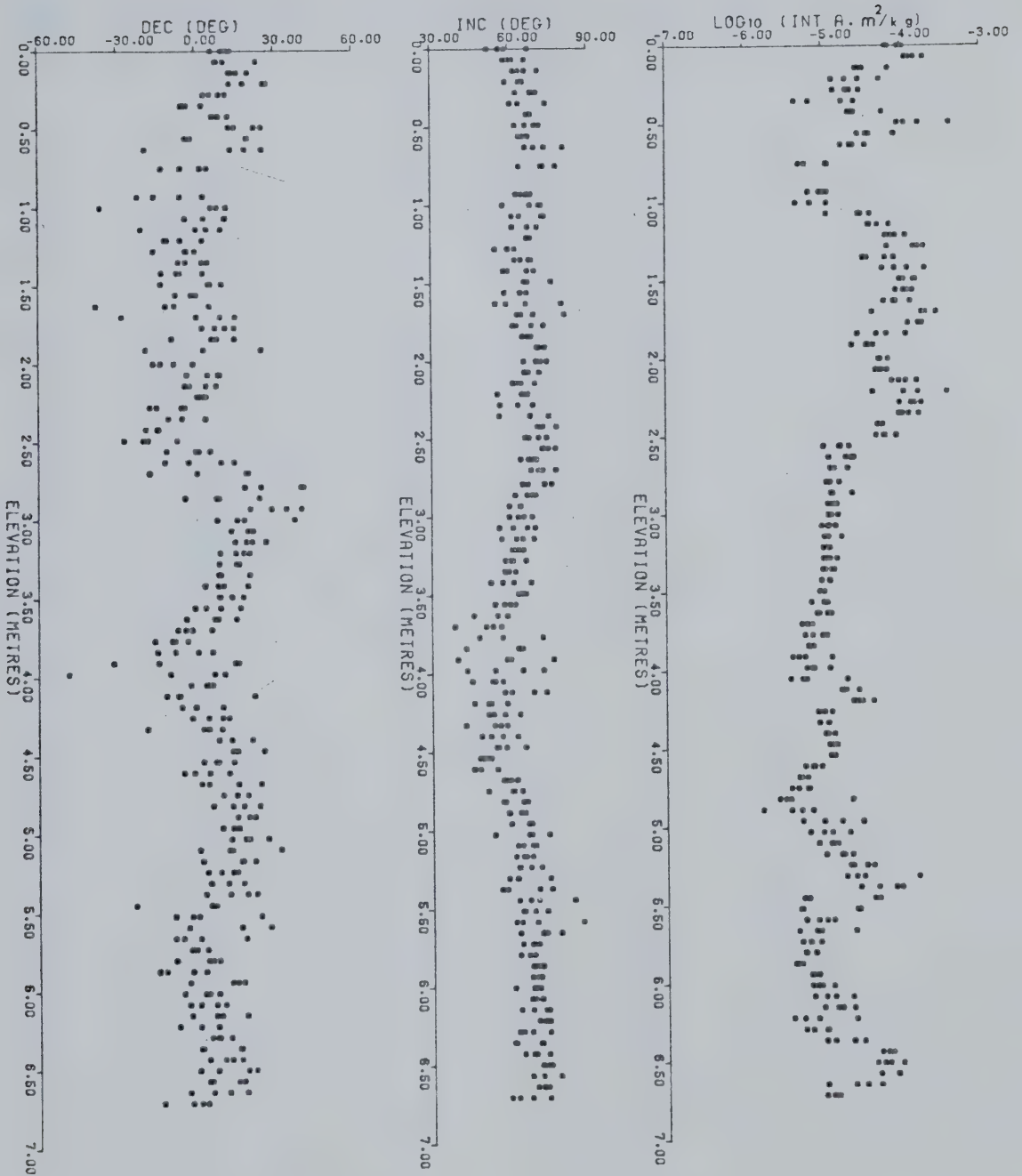
(a)

RIGGINS ROAD (0 mT)



(b)

RIGGINS ROAD (10mT)



(C)

RIGGINS ROAD (20mT)

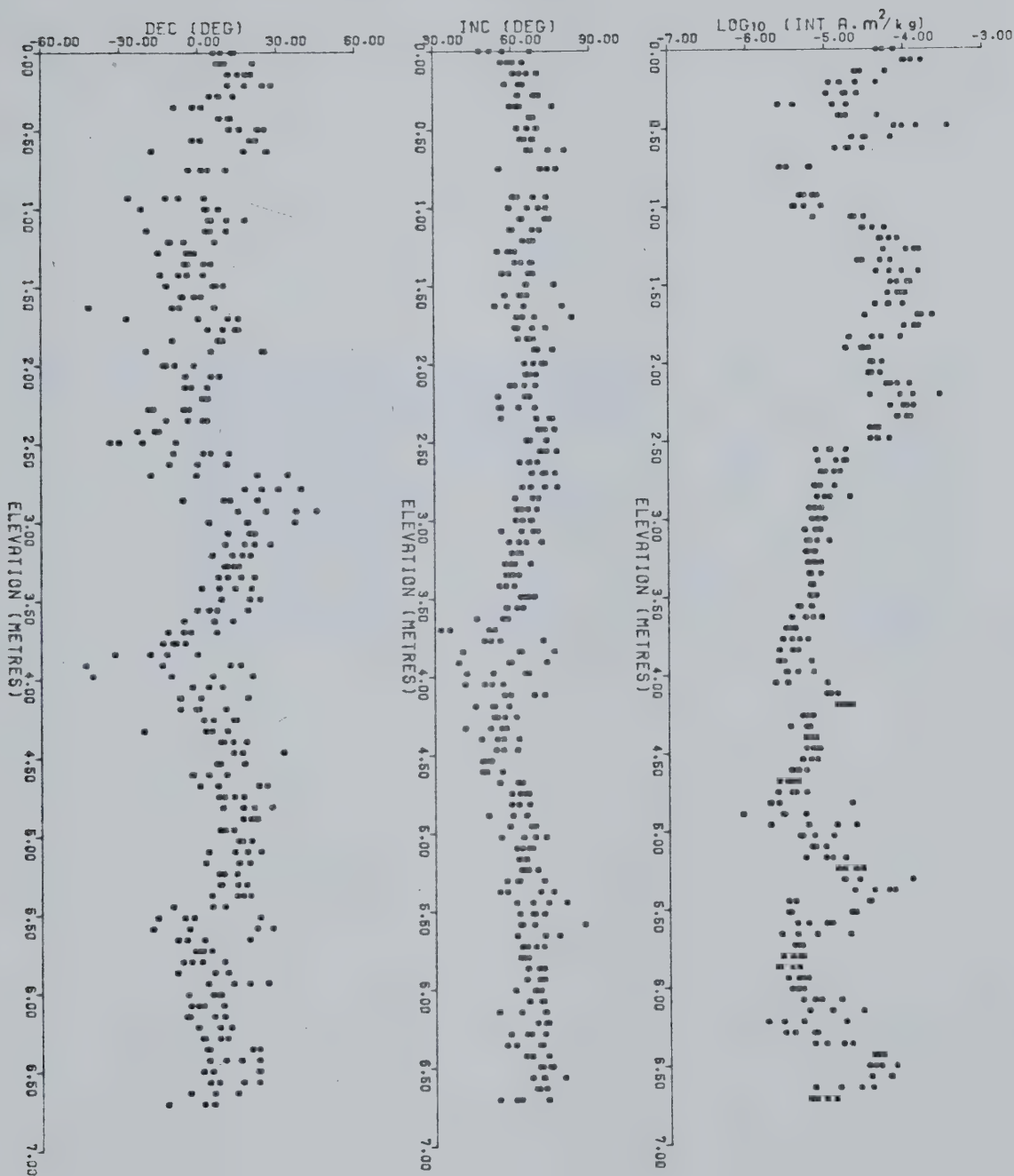
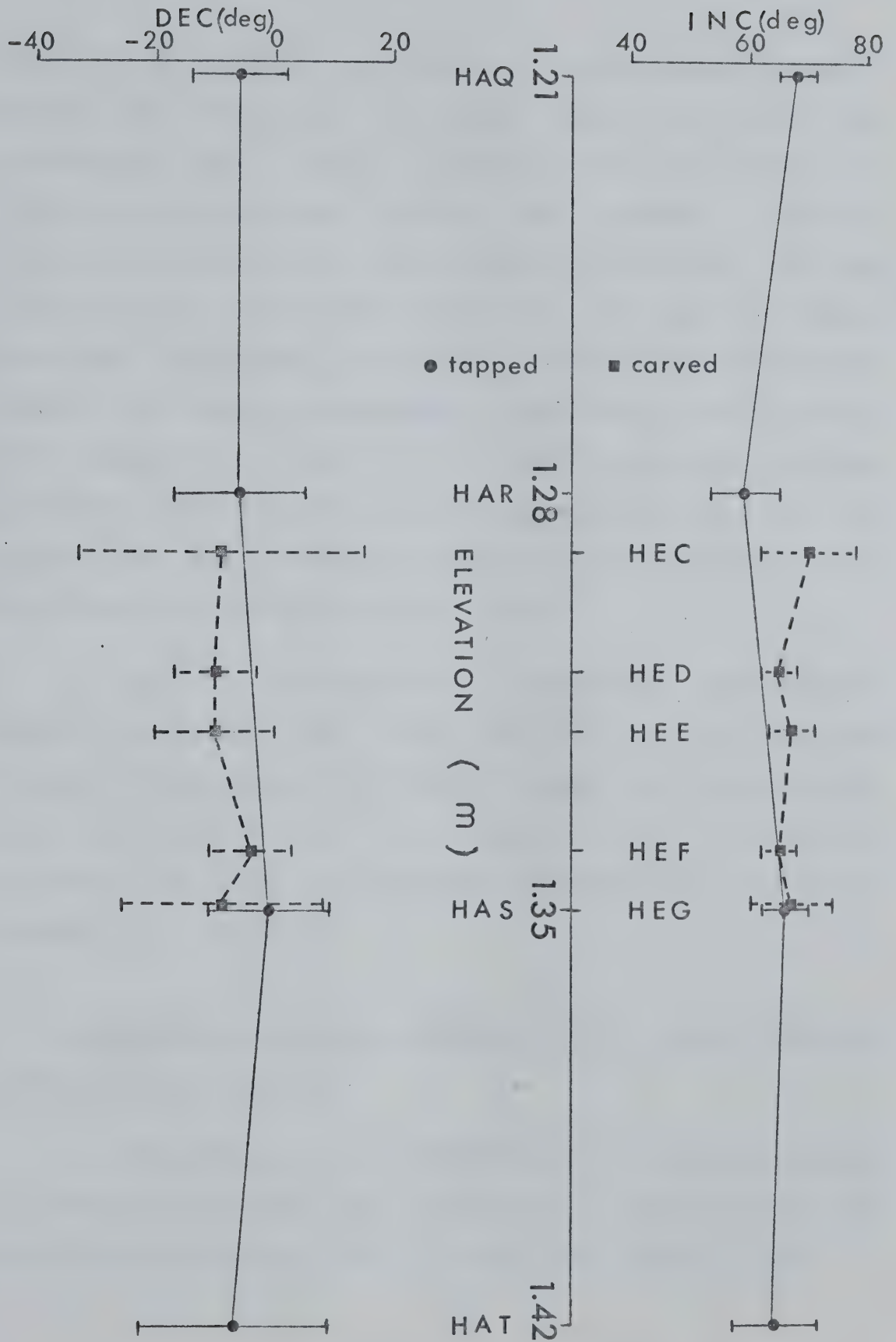


Fig. 2.6 Site mean results from laboratory carved sites and the corresponding sites sampled in situ. Tapped specimens were demagnetized at 10 mT. The large coherent block from which the carved specimens were obtained was not stored in the magnetically shielded room. The end points of these specimens were established at 20 mT, except for specimens from site HEG where the end points were at 35 mT (see footnote to Table 2.1). The bars indicate δD and δI where $\delta D = \alpha_{95}/\cos I$ and $\delta I = \alpha_{95}$.



field. It is therefore instructive to quantitatively compare results from these three elevations. Table 2.1 gives the appropriate data; again it is clear that differences are very small. The standard F-ratio test (Watson & Irving, 1957) indicates that these small differences are not statistically significant. The data of all the carved specimens are given in Appendix 2. One further comparison between the sampling techniques is provided by the within-site dispersions. For the 86 'tapped' sites the precision parameter (k) ranges from 20 to 5,242 with a mean of 342 whilst for the 8 'carved' sites it ranges from 140 to 568 with a mean of 274 (all data at 10 mT).

A point of considerable geomagnetic significance emerges from the data illustrated in Fig. 2.6. The finer sampling scale reveals no prominent geomagnetic features and this implies that the 7 cm spacing used is generally adequate and that no persistent high frequency content is missed.

2.5 Comparison of the Present Study with Oberg's Reconnaissance Results

A comparison is now made between the present results and those reported by Oberg (1978). The distance between the Cherryville tephra and the top of the gravel layer is

Table 2.1 Comparison of sampling techniques

Elev (m)	Site	Method	Fisher k	Dec °	Inc °	Δ°	F ratio
2.21	HBE	Tapped	226	002.3	63.5	4.7	+2.78
	HEB	Carved (in field)	2684	012.1	65.6		
5.73	HDC	Tapped	892	359.7	67.7	0.5	+0.04
	HEA	Carved (in field)	482	000.8	67.4		
1.35	HAS	Tapped	511	358.9	65.9	3.5	+1.01
	HEG	Carved (in lab)	199*	351.0*	67.4*		

All data refer to AF treatment at 10 mT except site HEG (data marked by asterisk). The specimens from this site were unintentionally placed close to a strong magnet for a period of almost one week, and thus required further AF treatment. The end points were established after treatment at 35 mT.

Δ angular difference

$$F = \frac{\sum N_i - B}{B - 1} \cdot \frac{\sum R_i - R_B}{\sum N_i - \sum R_i}$$

where B number of sites

N_i number of specimens at each site (i.e. 4)

R_i length of the resultant vector at each site

and R_B length of the vector sum of the resultant at each site

reported by Oberg to be 6.91 m, whilst in this study it is 6.71 m. Since the previous investigation was a reconnaissance study only (all the sampling was done in a single day), the present elevation measurements are considerably more reliable.¹ A comparison of the two intensity profiles shows remarkable similarities, reflecting the same underlying lithological variations (Fig. 2.7). When the former data are compressed by a factor of 0.97 (i.e. 6.71/6.91) the agreement becomes extremely good (Fig. 2.8), giving one much confidence in the results. The corresponding declination and inclination magnetograms are also shown. The present data exhibit oscillations of somewhat larger amplitude at certain elevation intervals, but on the whole, the agreement is satisfactory.

¹Oberg and his field party agree that this is the case.

Fig. 2.7 Comparison of intensity profiles of the present study (right) with Oberg's reconnaissance study (left). All data refer to AF treatment at 10 mT.

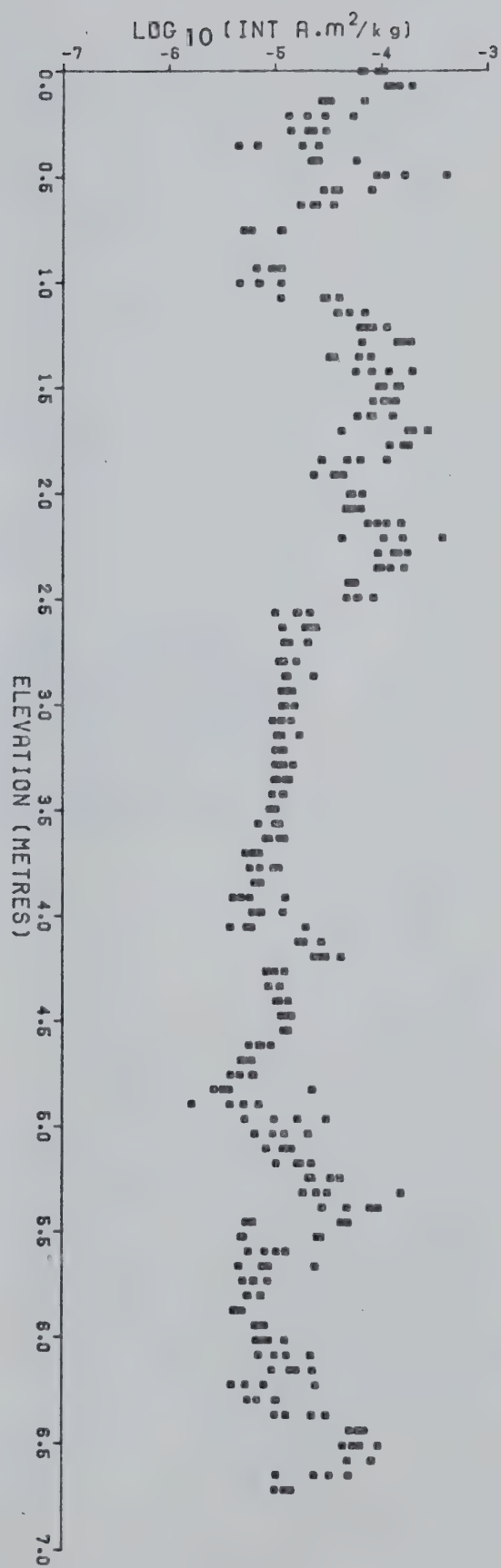
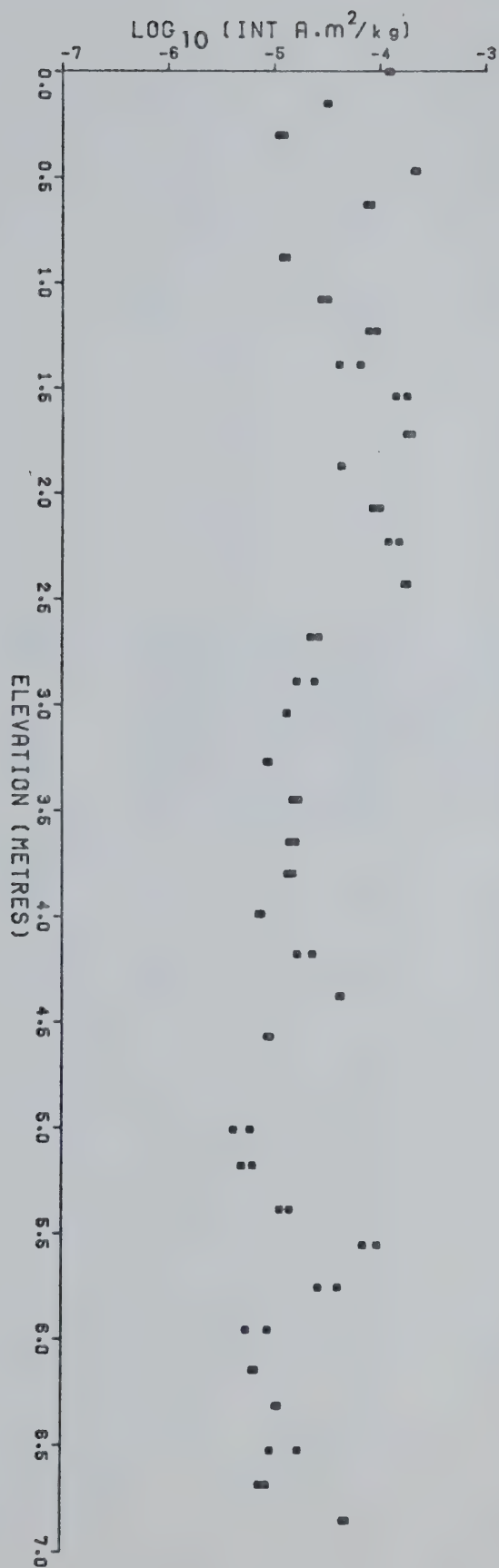
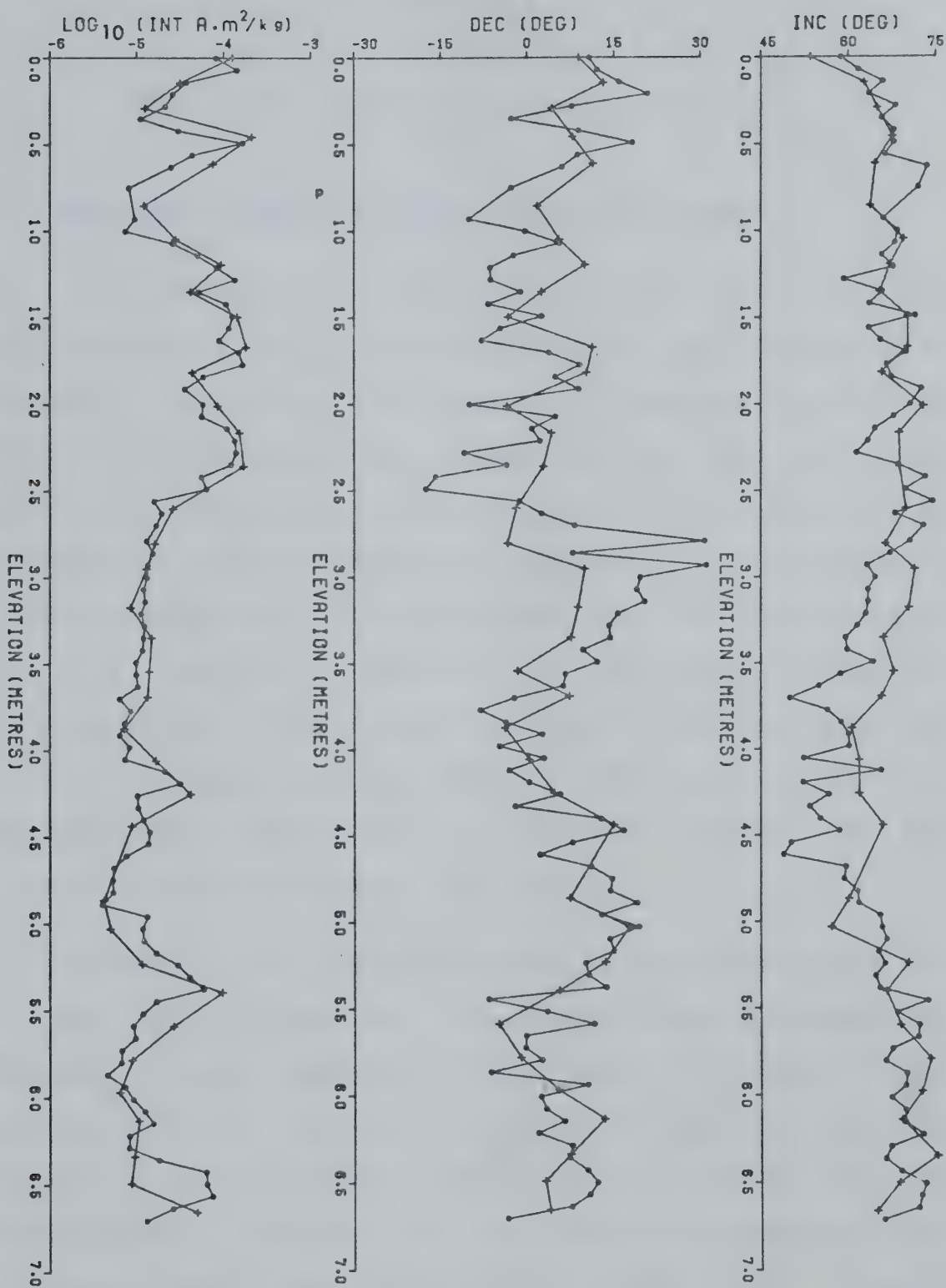


Fig. 2.8 Comparison of the site mean intensity, declination and inclination of the present study with Oberg's reconnaissance study. The elevation of the previous study has been compressed by a factor of 0.97 (i.e. $6.71/6.91$, see text) . (● present data ; + reconnaissance data)



CHAPTER 3

The Nature of the Remanent Magnetization

3.1 Remanence Removed by Partial Demagnetization

In paleomagnetic studies it is important to enquire if the remanence finally isolated by partial demagnetization is 'primary' (i.e. aligned parallel to the ambient field at the time of formation). The direction and magnitude of the remanence removed by demagnetization can yield useful information about the nature of any secondary magnetization. Simple vector subtraction yields the direction and intensity of the remanence removed at each step by partial demagnetization. Such calculations have been performed on the 94 sites of the Riggins Road data in the AF demagnetization ranges of 0 to 10 mT and 10 to 20 mT. The results are illustrated in Fig. 3.1a-c.

Consider first the means of all 94 site means after 0 , 10 and 20 mT treatment (Fig. 3.1a); these represent the average vectors remaining after these treatments (see section 4.2 for detailed discussion), not the vectors removed by the treatments. The 10 and 20 mT data are not significantly different, but the NRM data are very slightly displaced towards the present field vector. This suggests

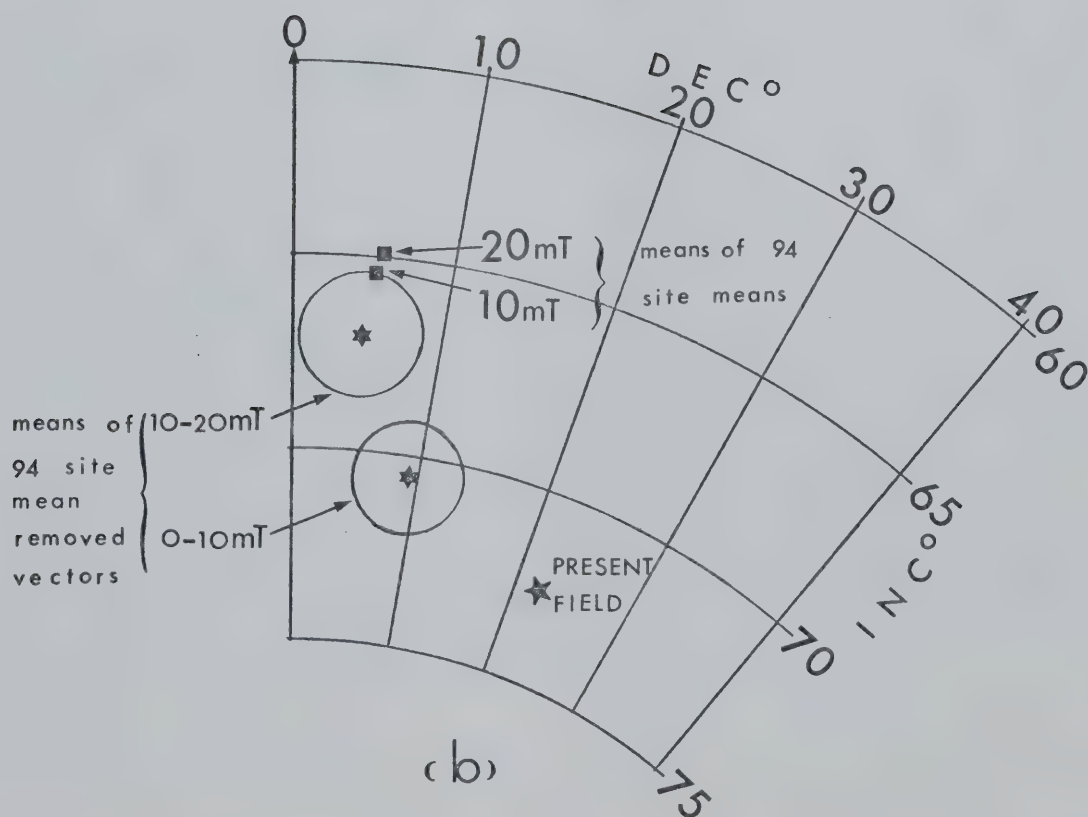
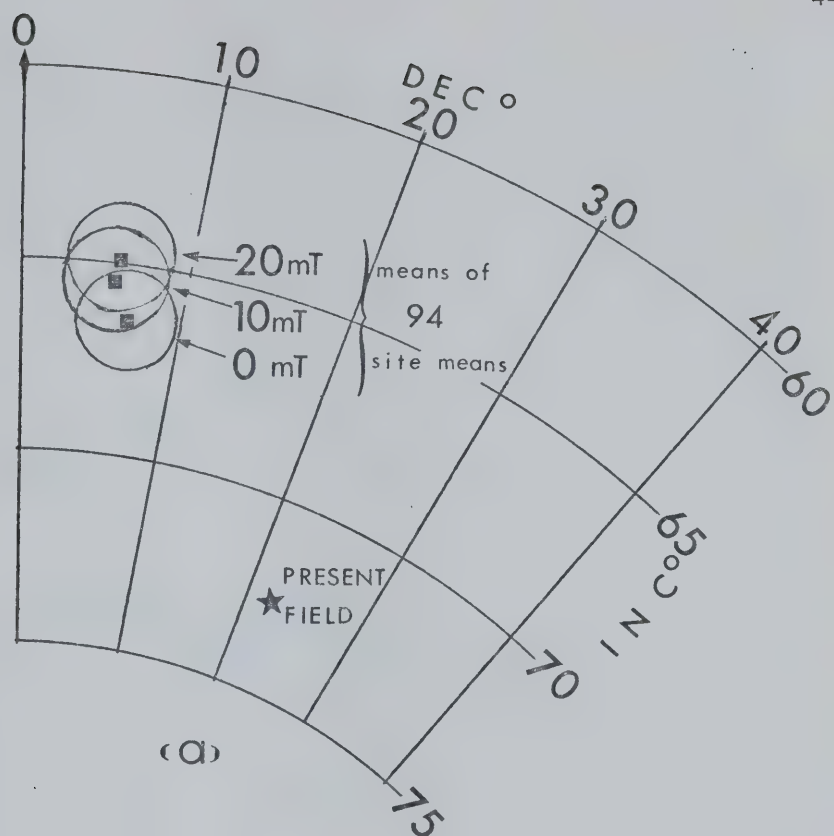
Fig. 3.1(a) Mean of the 94 site means at 0 ,
10 and 20 mT. (Azimuthal equidistant plot)

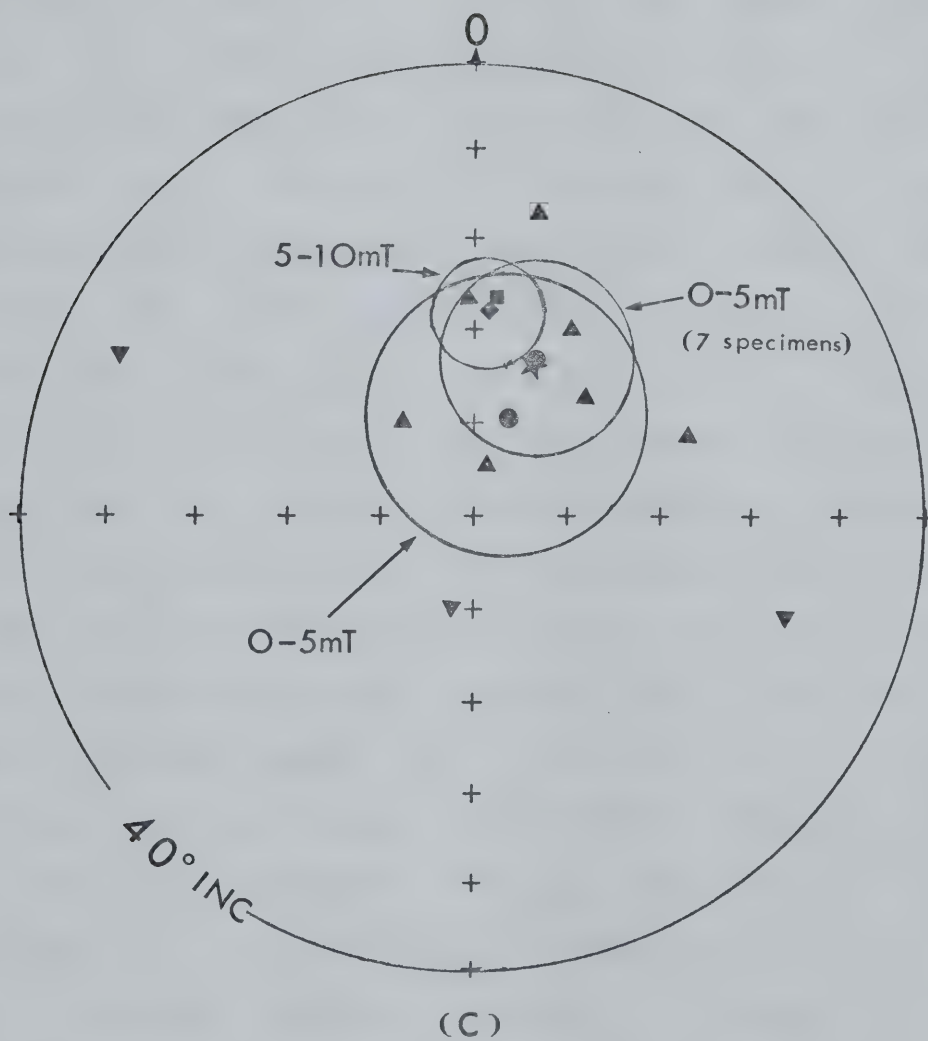
(b) Mean of the 94 site means removed
vectors at 0 - 10 mT and 10 - 20 mT .
(Azimuthal equidistant plot)

(c) Removed vectors for the 10 pilot specimens.
The triangles represent the individual
0 - 5 mT removed vectors ; three of these
(shown as inverted triangles) are rather
divergent . (Equal area plot)

The data plotted are as follows :

			D°	I°	alpha ₉₅ °
Present	Field		022.3	+72.6	-
Site means	0 mT		006.3	+66.4	1.2
	10 mT		005.7	+65.4	1.3
	20 mT		005.9	+64.9	1.3
Removed vectors	0 - 10 mT		009.5	+70.5	1.4
	10 - 20 mT		004.8	+67.0	1.5
Pilot specimens					
removed vectors	0 - 5 mT (10 specimens)		018.7	+77.5	14.7
	5 - 10 mT (10 specimens)		004.4	+67.5	6.4
	0 - 5 mT (7 specimens)		021.2	+72.2	10.4





that a small, recently-acquired, secondary magnetization is present - but the data by no means establish this fact. A clearer picture emerges when the removed vectors are considered: the 10-20 mT data lie close to the final cleaned direction, but the 0-10 mT data are clearly displaced towards the present field vector (Fig. 3.1b). This feature also manifests itself as a small kink in the Zijdeveld diagrams (Fig. 2.4a-j). It appears that a secondary component aligned along the present field is being removed, but that the first demagnetization step (0 to 10 mT) also removes some of the primary remanence. Further scrutiny must rest on the 10 pilot specimens since these provide the only results below 10 mT. The 10 removed vectors at 5-10 mT agree with the previously established 'primary' result but the 0-5 mT data lie much closer to the present field. Three of these removed vectors are quite divergent (Fig. 3.1c), but a more tightly grouped subset of 7 vectors is in excellent agreement with the present field vector. Unfortunately with only 10 pilot specimens involved the circles of 95% confidence are rather large, but there can be little doubt that a recently acquired remanence is present in this material and that peak alternating fields between 5 and 10 mT completely erase this and reveal an earlier, more stable, and presumably primary remanence.

3.2 Viscous Remanent Magnetization

As in many other geophysical and geological problems, time is an important factor. Exposure of magnetic material to magnetic fields over long periods of time can produce serious effects, in particular the gradual acquisition of viscous remanent magnetization (VRM). It has been shown that many magnetic materials exposed to a magnetic field will slowly acquire a magnetization in the direction of that field. The process is temperature-dependent and also depends logarithmically on time. This is attributed to random thermal fluctuations causing irreversible magnetic changes and thus leading to a greater magnetization in the direction of the applied field. The process of VRM is important in the present investigation because it was found that similar specimens from the reconnaissance study (Oberg, 1978) changed their magnetization by small, but detectable, amounts when stored in the laboratory over a period of two years. Consequently it was decided to quantitatively investigate the VRM properties of this material. Four of the pilot specimens (HAA03, HAK02, HBI01 and HCO04) were first demagnetized in a peak alternating field of 180 mT to destroy any remaining NRM. The specimens were then placed in the magnetically shielded room and a field of 1 mT was applied in a known direction. The VRM's were monitored at suitable intervals for 100 hours. The remanent magnetization

of each specimen was observed to increase slowly and its direction approached that of the applied field (Fig. 3.2). The VRM acquired initially interacted with the small magnetic vector remaining after 180 mT treatment but after 4 hours the growing VRM became dominant, and the magnetization (J) increased logarithmically with time (t), which is characteristic of VRM (Shimizu, 1960). Thus, $J = S \cdot \log(t)$, where S is called the magnetic viscosity coefficient. The appropriate value for each specimen was determined from the slope of the corresponding regression line from 4 to 100 hours. These values of S can be used to obtain the value of the VRM that could have been acquired by the sediments in the Earth's ambient field of approximately 0.06 mT (field at lat. 50°N) in about 30,000 years (Table 3.1). These VRM's are not negligible compared to the original NRM. However, the viscous remanence, as expected, is much softer than the NRM, with MDF's between 2.5 and 10 mT compared to values around 20 mT for the NRM (c.f. Figs. 2.2 and 3.3). This means that as AF treatment proceeds the influence of any VRM is continually reduced (see column 6 of table 3.1). The VRM data is given in Appendix 3.

It is of interest to quantitatively compare the magnitude of the predicted VRM acquired over 30,000 years to the magnitude of the secondary magnetic overprint removed from the NRM by AF treatment (section 3.1). Table 3.2 gives

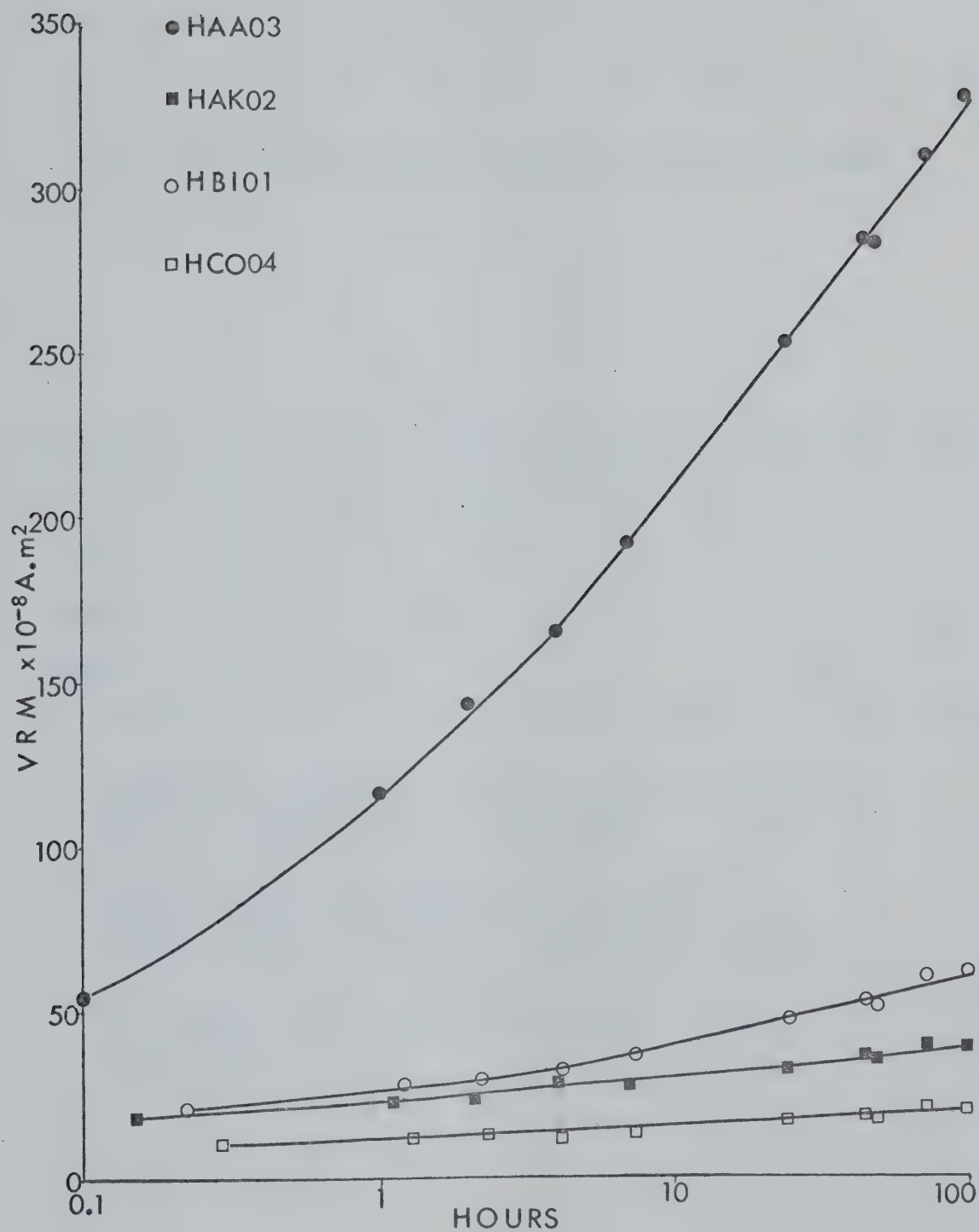


Fig. 3.2 Acquisition of viscous remanent magnetization (VRM).

Table 3.1 Viscous remanent magnetism of four specimens

specimen	r^a	s^b	VRM ^c	(VRM/NRM) %	(VRM ₁₀ /NRM ₁₀) %
HAA03	0.999	7.0	58.8	45	25
HAK02	0.966	0.5	4.5	24	10
HBI01	0.991	1.3	10.7	13	7
HCO04	0.914	0.4	3.1	33	23

^a correlation coefficient obtained from least-squares regression line between magnetization and $\log_{10}(\text{hours})$ (for the interval 4 to 100 hours).

^b Magnetic viscosity coefficient ($\times 10^{-8} \text{ A.m}^2$). Values quoted are those appropriate for an ambient field of 0.06 mT (field at lat. 50°N).

^c VRM ($\times 10^{-8} \text{ A.m}^2$) which would be acquired by exposure to a field of 0.06 mT for 30,000 years.

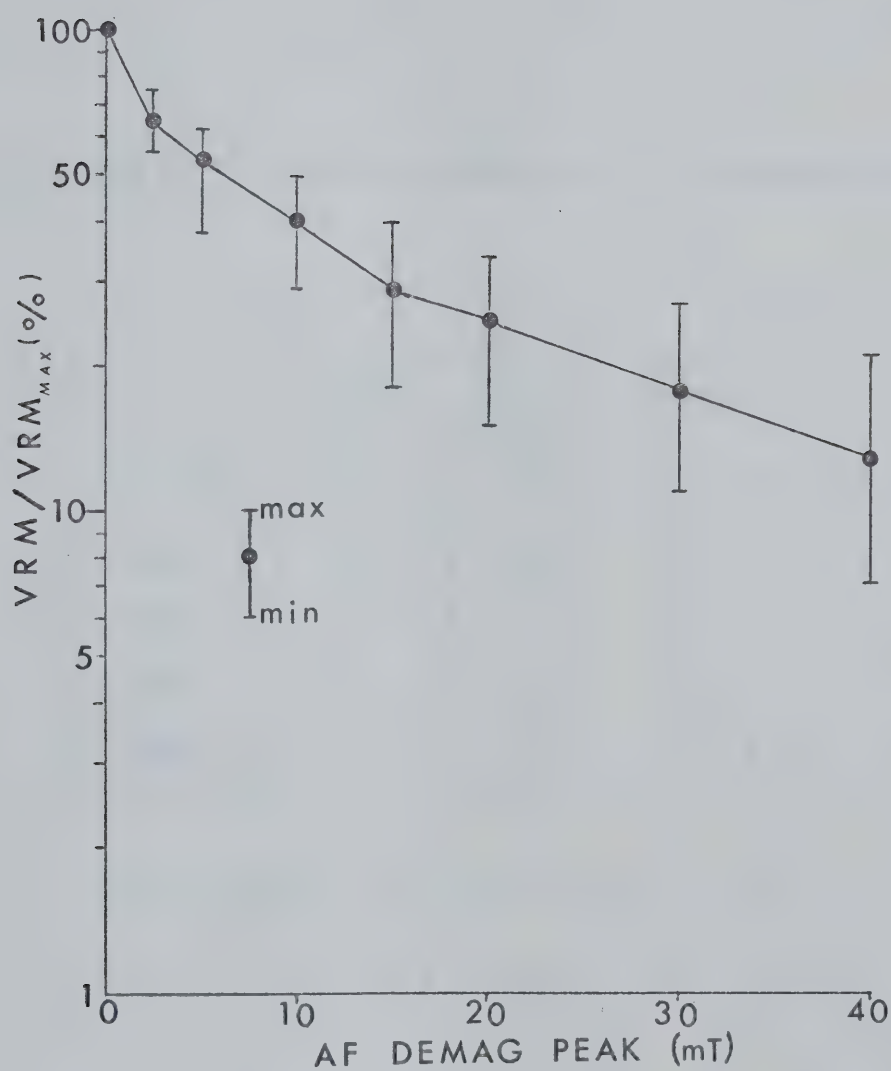


Fig. 3.3 Mean (and range) of the AF demagnetization curves of the 100 hours VRM .

Table 3.2 VRM's and vectors removed by AF demagnetization

specimen	Removed Vectors		Total VRM
	NRM 0 - 10 mT	VRM 0 - 10 mT	
HAA03	22.6	30.5	58.8
HAK02	4.6	3.2	4.5
HBI01	9.3	5.4	10.7
HCO04	4.7	2.0	3.1

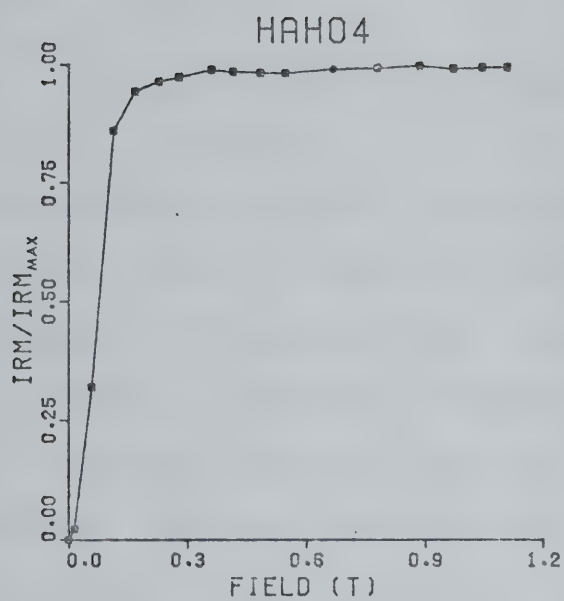
All moments are quoted in $\text{A.m}^2 \times 10^{-8}$.

the appropriate data. Considering the enormous extrapolation involved, from 100 hours in the laboratory to 30,000 years in situ, the agreement is quite encouraging and there is no doubt that the measured VRM characteristics are capable of explaining the observed secondary magnetic components.

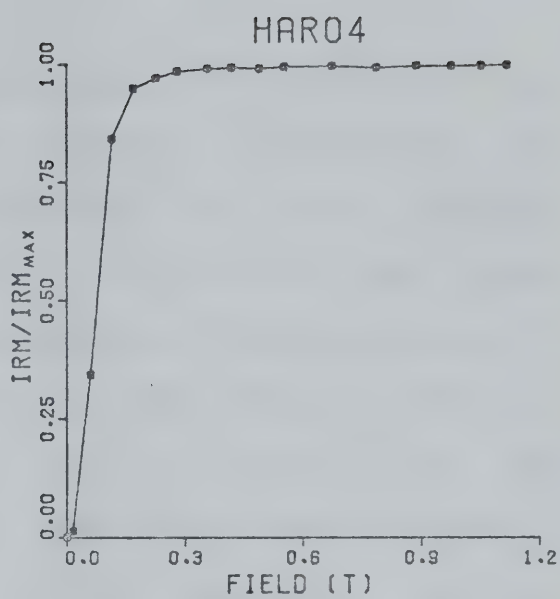
3.3 Magnetic Mineralogy

Any interpretation of the remanent magnetism in a suite of rocks depends on a knowledge of the minerals carrying the remanence. One test to distinguish the primary magnetic mineral is the study of isothermal remanent magnetization (IRM). The IRM of hematite and magnetite of various grain sizes have been studied by Roquet (1954). It was found that hematite and magnetite reach saturation at widely differing magnetic fields; hematite in a field of 3 T and magnetite in a field of 0.3 T. Four specimens (HAH04, HAR04, HAS04 and HBB02) were first demagnetized in a peak alternating field of 180 mT, and then introduced between the poles of an electromagnet and acquired IRM in successively higher fields from 0 to approximately 1 T. The IRM's were measured after each application of field (Appendix 4) and the results are illustrated in Fig. 3.4a-d. It is observed that the specimens saturate in a field of approximately 0.3 T. The IRM test clearly indicates that the magnetic carrier is magnetite, (Roquet, 1954), or a related ferrite (see e.g.

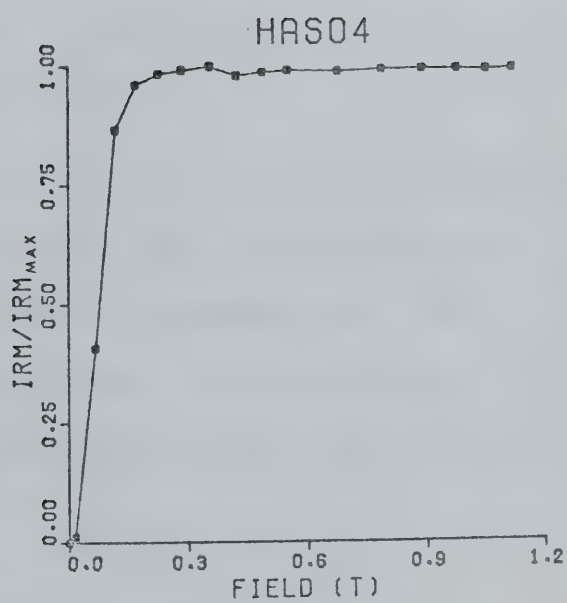
Fig. 3.4a-d IRM build-up curves for specimens
HAH04 , HAR04 , HAS04 and HBB02 .



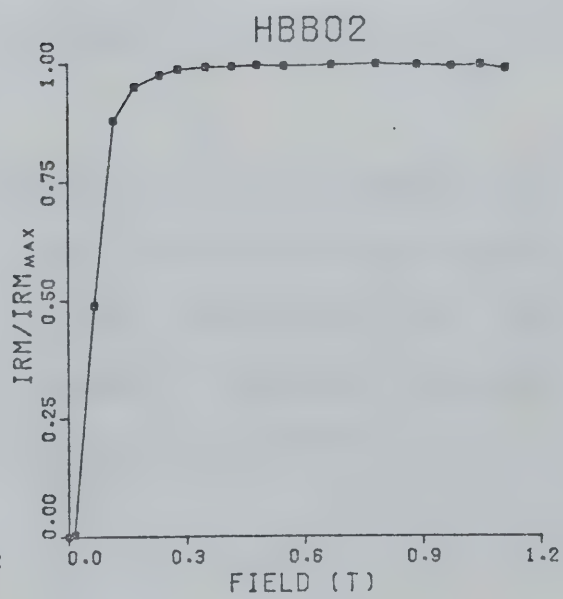
(a)



(b)



(c)



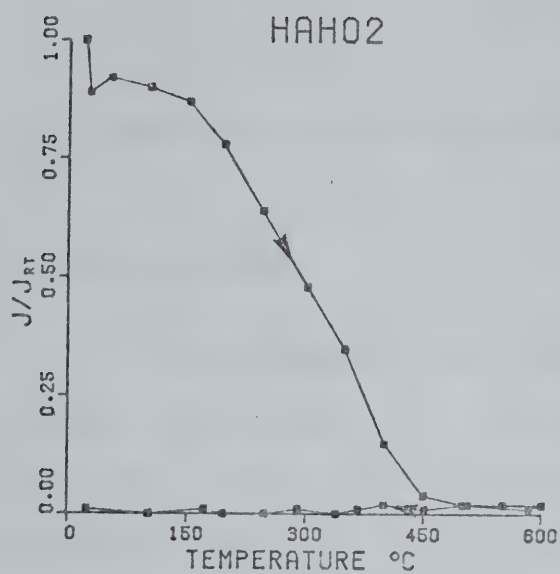
(d)

Day, 1977).

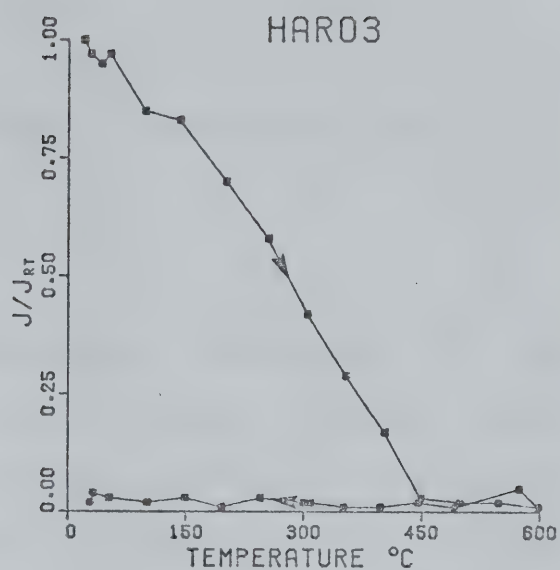
A second method of identification is to determine the Curie temperature of the magnetic constituents. The variation of intensity with temperature of four specimens (HAH02, HAR03, HEG05 and HBB03) was determined with a high temperature Digico spinner magnetometer. The intensity at a particular stabilized temperature was measured over an integrating time of 37 seconds (i.e. 2^8 spins) with the furnace switched off. The high temperature data is given in Appendix 5. The behaviour of the specimens as the temperature was cycled from room temperature to 600°C and back to room temperature is shown in Fig. 3.5a-d. All four blocking temperature spectra are very similar, and imply a Curie temperature of approximately 450°C, which corresponds to a titanomagnetite of composition 80% magnetite and 20% ulvospinel.

It would appear that the remanence in these samples is carried by titanomagnetite grains, hematite being either absent or negligible. This, in turn, suggests that the remanence is depositional and is free of chemical remanence (CRM) overprints which generally reside in hematite.

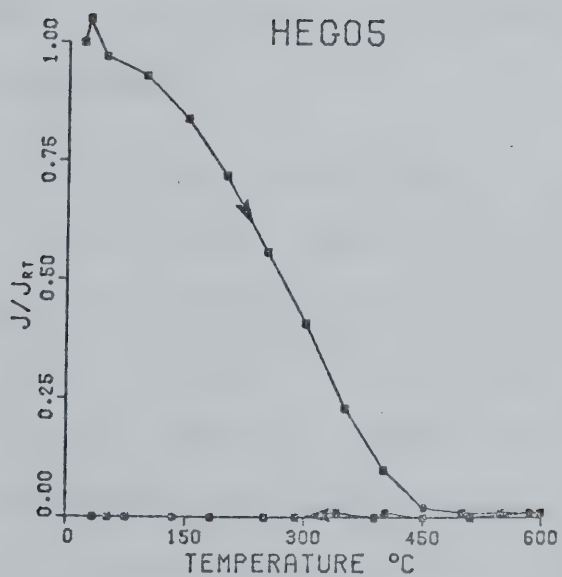
Fig. 3.5a-d Variation of intensity with temperature. The intensity J is normalized to its value, J_{RT} , at room temperature. Specimen HEG05 is carved in the laboratory from the large coherent block (see section 2.4).



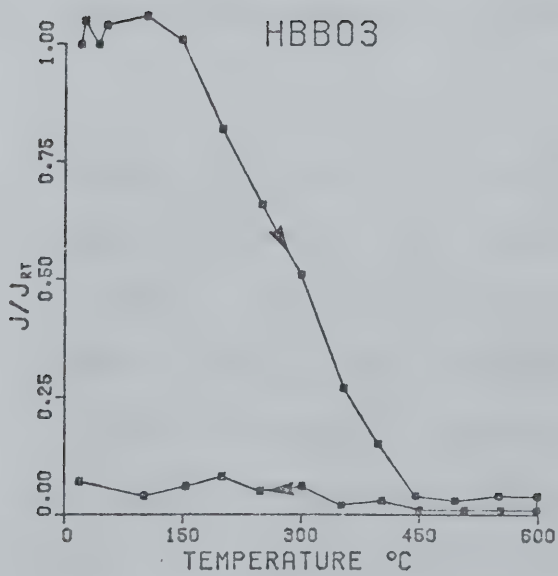
(a)



(b)



(c)



(d)

CHAPTER 4

Analysis of the Riggins Road Paleomagnetic Data

4.1 Introduction

In connection with the basic data illustrated in Fig. 2.5a-c, there are two topics of major importance to be discussed. These are the overall average direction of remanence (and its corresponding paleomagnetic pole) and the smooth declination/inclination oscillations. Both of these are intimately related to the nature of the geomagnetic field and its spectrum of temporal variations but it is convenient to discuss them separately in the first instance.

4.2 Site Means and Overall Mean Paleomagnetic Field Direction

It is common practice to average paleomagnetic data in a hierarchical fashion (Irving, 1964; McElhinny, 1973) using the procedure due originally to Fisher (1953). Specimens from a single site (horizon) are considered to have acquired their primary magnetization simultaneously. Averaging specimen directions to obtain site means reduces the effect of experimental error associated with collection, orientation and measurement. The site means are then

combined to obtain the mean paleomagnetic direction for the entire section. This procedure provides estimates of the magnitude of different types of errors. The within-site scatter reflects experimental error and the recording fidelity of the strata, whereas the between-site scatter obviously includes the effect of real temporal variations.

The site means for the 0, 10 and 20 mT demagnetization data are summarized in Table 4.1 and illustrated in Fig. 4.1a-c. The overall mean direction for the entire sequence at 0 mT is $D=006.3^\circ$, $I=+66.4^\circ$ ($N=94$, $R=93.3895$, $k=152$, $\alpha_{95}=1.2^\circ$); at 10 mT it is $D=005.7^\circ$, $I=+65.4^\circ$ ($N=94$, $R=93.3099$, $k=135$, $\alpha_{95}=1.3^\circ$) and at 20 mT it is $D=005.9^\circ$, $I=+64.9^\circ$ ($N=94$, $R=93.2860$, $k=130$, $\alpha_{95}=1.3^\circ$). All these are significantly different from the present geomagnetic vector at the sampling locality ($D=022.3^\circ$, $I=+72.6^\circ$) (see Fig. 3.1a). Since there is very little difference between the results at 10 and 20 mT, the site means at 10 mT will henceforth be used. On the whole, within-site grouping is good, with values of Fisher's precision parameter (k) greater than 100 in 85% of cases (78 out of 94) (minimum=20, maximum=5,242, arithmetic mean = 342). There is no correlation between k and the lateral spread of the specimens at each site (Fig. 4.2). This implies that the scatter is not due to non-horizontality and/or irregularity of bedding, or to inadequate vertical positioning of

Table 4.1 Site means at 0, 10 and 20 mT.

S	E	0mT				10mT				20 mT			
		D°	I°	R	k	D°	I°	R	k	D°	I°	R	k
HAA	0.0	11.4	59.8	3.9847	196	10.8	58.7	3.9796	147	10.9	56.2	3.9661	88
HAB	0.07	11.9	62.2	3.9887	265	12.1	61.7	3.9878	293	11.5	60.3	3.9906	318
HAC	0.14	16.3	66.2	3.9701	303	15.9	66.0	3.9917	360	16.4	65.2	3.9918	363
HAD	0.21	20.0	64.8	3.9712	340	20.9	63.6	3.9916	357	20.2	62.6	3.9899	297
HAE	0.28	8.5	67.8	3.9926	407	7.8	68.2	3.9935	459	9.0	68.1	3.9933	450
HAF	0.35	359.0	65.9	3.9883	256	357.3	65.8	3.9830	176	357.2	65.4	3.9744	117
HAG	0.42	8.9	67.9	3.9980	1510	9.0	67.9	3.9994	5242	11.1	68.0	3.9996	7748
HAH	0.49	17.7	66.1	3.9909	329	18.2	67.9	3.9900	300	18.5	67.3	3.9917	361
HAI	0.56	8.6	66.7	3.9850	199	8.8	66.4	3.9860	214	10.5	66.8	3.9864	220
HAJ	0.63	5.7	74.1	3.9602	75	6.1	73.6	3.9647	84	9.4	73.2	3.9604	75
HAK	0.75	358.1	70.9	3.9740	115	357.3	72.1	3.9824	170	2.0	69.7	3.9548	66
HAL	0.93	348.4	66.2	3.9858	210	350.0	66.1	3.9881	252	350.7	66.8	3.9752	121
HAM	1.00	0.8	68.9	3.9684	94	359.7	68.5	3.9523	62	0.2	67.8	3.9729	110
HAN	1.07	4.5	68.8	3.9789	142	5.7	68.1	3.9798	148	9.4	69.0	3.9826	172
HAP	1.14	358.2	65.7	3.9759	124	357.7	65.8	3.9750	119	359.2	65.4	3.9695	98
HAQ	1.21	353.2	67.9	3.9977	1306	353.6	67.8	3.9970	1010	355.2	67.0	3.9939	491
HAR	1.28	353.8	60.3	3.9894	283	353.7	59.3	3.9893	279	353.8	58.8	3.9912	341
HAS	1.35	358.9	66.3	3.9946	560	358.9	65.9	3.9941	511	359.3	65.3	3.9930	481
HAT	1.42	353.3	64.3	3.9824	170	353.3	63.7	3.9819	166	353.3	62.9	3.9806	154
HAU	1.49	2.6	72.2	3.9805	153	2.6	71.6	3.9820	166	3.7	71.3	3.9794	145
HAV	1.56	355.5	64.1	3.9917	361	355.4	63.6	3.9926	405	356.7	62.8	3.9929	421
HAW	1.63	353.1	66.4	3.9901	41	352.2	65.6	3.9902	41	352.9	64.8	3.9929	38
HAX	1.70	2.1	70.6	3.9568	69	3.8	70.1	3.9579	71	5.4	70.0	3.9495	59
HAY	1.77	8.9	67.2	3.9861	216	9.2	66.7	3.9850	199	11.1	66.4	3.9846	194
HAZ	1.84	5.3	68.4	3.9934	455	5.0	67.5	3.9924	393	4.0	66.3	3.9914	348
HBA	1.91	6.1	72.5	3.9790	142	9.0	72.7	3.9797	147	8.9	72.1	3.9729	110
HBB	2.00	350.1	72.1	3.9905	316	350.1	70.8	3.9915	351	350.8	69.7	3.9930	429
HBC	2.07	7.7	69.4	3.9961	775	5.0	67.9	3.9951	607	4.3	67.1	3.9962	781
HBD	2.14	0.8	65.7	3.9925	397	0.9	64.7	3.9910	333	359.3	63.9	3.9901	303
HBE	2.21	3.3	63.7	3.9891	275	2.3	63.5	3.9867	226	2.9	63.4	3.9853	204
HBF	2.28	350.8	62.0	3.9789	142	349.2	61.5	3.9788	141	348.3	60.9	3.9750	119
HBG	2.35	357.5	68.9	3.9605	76	356.5	68.8	3.9605	75	356.4	69.1	3.9601	75
HBH	2.42	342.9	74.5	3.9952	620	344.2	73.4	3.9951	606	342.1	72.8	3.9962	789
HBI	2.49	342.8	71.1	3.9917	359	342.5	70.0	3.9900	300	337.2	68.5	3.9862	217
HBJ	2.56	1.0	74.2	3.9966	876	358.7	74.7	3.9961	774	1.4	73.4	3.9932	444
HBK	2.63	3.0	68.9	3.9873	236	2.6	68.2	3.9878	245	3.0	67.0	3.9887	266
HBL	2.70	7.5	73.7	3.9805	153	8.3	73.1	3.9819	165	12.9	73.4	3.9732	111
HBM	2.79	30.2	71.9	3.9782	137	30.8	70.8	3.9805	154	28.2	70.8	3.9790	143
HBN	2.86	8.2	67.3	3.9853	204	8.0	67.4	3.9852	202	8.2	67.8	3.9823	169
HBO	2.93	30.7	63.4	3.9905	316	31.1	63.4	3.9916	359	30.4	65.9	3.9824	170
HBP	3.00	20.3	66.0	3.9800	149	19.6	64.8	3.9796	146	19.3	65.7	3.9806	154
HBQ	3.07	19.7	63.8	3.9860	214	19.0	63.6	3.9821	167	18.6	64.6	3.9805	153
HBR	3.14	20.5	64.5	3.9864	221	20.4	63.6	3.9857	210	19.1	64.9	3.9830	176
HBS	3.21	18.7	63.4	3.9978	1339	15.7	63.2	3.9963	821	13.7	62.3	3.9950	595
HBT	3.28	12.4	61.9	3.9911	338	14.2	61.7	3.9937	479	12.4	61.4	3.9911	338
HBU	3.35	16.0	59.4	3.9910	332	14.4	59.7	3.9933	447	13.8	60.1	3.9940	498
HBV	3.42	12.1	60.1	3.9993	145	9.7	60.0	3.9759	124	10.7	58.9	3.9887	266
HBW	3.49	13.5	66.5	3.9978	1383	12.2	64.5	3.9973	1129	14.8	66.1	3.9935	460
HBX	3.56	7.1	59.6	3.9861	215	6.7	58.8	3.9879	248	6.9	60.8	3.9884	258
HBY	3.63	6.3	56.8	3.9760	125	6.3	55.1	3.9741	116	4.8	55.1	3.9769	130
HBZ	3.70	1.3	52.9	3.9641	83	357.8	50.1	3.9670	91	356.4	43.4	3.9381	48

S	E	0 mT				10 mT				20 mT			
		D°	I°	R	k	D°	I°	R	k	D°	I°	R	k
HCA	3.77	353.4	58.9	3.9446	54	351.9	56.6	3.9378	48	351.5	57.2	3.9514	61
HCB	3.84	359.9	60.5	3.9535	64	356.3	58.9	3.9416	51	348.6	61.4	3.8875	26
HCC	3.91	4.9	62.2	3.9199	37	2.7	60.2	3.8506	20	359.4	59.5	3.8453	19
HCD	3.98	2.2	63.2	3.9289	42	355.2	60.3	3.8673	22	355.1	58.3	3.8718	23
HCE	4.05	3.3	54.7	3.9834	180	3.0	52.5	3.9863	218	2.2	50.1	3.9768	129
HCF	4.12	354.7	68.9	3.9746	118	356.9	65.8	3.9616	78	359.9	64.7	3.9659	87
HCG	4.19	0.8	54.2	3.9761	125	0.4	52.4	3.9811	159	0.2	52.7	3.9795	146
HCH	4.26	6.7	58.0	3.9916	163	5.8	56.8	3.9812	159	8.4	56.7	3.9886	262
HCI	4.33	358.6	56.7	3.9640	83	358.0	53.5	3.9495	59	358.0	52.5	3.9408	50
H CJ	4.40	11.2	58.7	3.9808	156	12.8	55.3	3.9787	140	12.3	55.5	3.9809	157
HCK	4.47	19.0	59.4	3.9831	251	16.7	58.6	3.9848	197	18.9	56.8	3.9839	186
HCL	4.54	7.8	52.5	3.9950	600	7.9	50.3	3.9945	544	10.1	50.3	3.9941	510
HCM	4.61	4.6	52.8	3.9778	135	2.3	49.0	3.9815	162	2.1	51.2	3.9885	260
H CN	4.68	11.7	60.9	3.9825	171	11.1	59.7	3.9847	195	12.8	59.5	3.9725	109
HCO	4.75	13.5	59.7	3.9975	1204	14.7	59.4	3.9843	190	11.9	63.4	3.9948	579
HCP	4.82	13.3	64.9	3.9918	367	14.4	61.7	3.9846	194	18.4	62.9	3.9904	311
HCR	4.89	18.9	63.9	3.9889	2621	19.0	61.9	3.9947	568	20.1	60.4	3.9778	135
HCR	4.96	15.4	66.8	3.9917	363	12.9	65.6	3.9932	441	9.7	65.7	3.9907	322
HCS	5.03	15.5	66.0	3.9878	245	19.3	65.9	3.9627	80	16.1	65.4	3.9750	119
HCT	5.10	16.2	67.8	3.9802	151	14.3	66.7	3.9821	168	14.4	65.0	3.9903	308
HCU	5.17	13.8	65.9	3.9938	480	15.0	65.3	3.9911	336	13.2	64.2	3.9946	556
HCV	5.24	10.7	67.9	3.9817	163	10.1	66.4	3.9908	325	9.8	65.9	3.9962	794
HCW	5.31	11.0	65.2	3.9831	177	10.6	64.8	3.9748	119	12.7	63.6	3.9810	158
H CX	5.38	14.7	66.4	3.9533	64	13.7	65.5	3.9537	64	13.1	64.9	3.9511	61
HCY	5.45	354.0	73.2	3.9283	41	353.3	73.8	3.9054	31	355.4	74.3	3.8937	28
HCZ	5.52	2.3	70.8	3.9829	175	3.5	68.5	3.9799	149	0.2	68.3	3.9771	130
HDA	5.59	8.0	72.8	3.9275	41	11.6	72.3	3.9016	30	13.4	71.1	3.9254	40
HDB	5.66	359.1	74.7	3.9782	137	359.8	72.1	3.9760	125	0.6	71.2	3.9739	114
HDC	5.73	358.9	70.3	3.9967	923	359.7	67.7	3.9966	891	1.0	67.4	3.9935	462
HDD	5.80	1.3	68.1	3.9963	810	2.6	66.5	3.9940	504	0.1	64.1	3.9953	644
HDE	5.87	0.0	72.1	3.9940	500	353.7	70.1	3.9949	591	5.5	68.5	3.9912	341
HDF	5.94	10.2	72.8	3.9954	645	10.5	69.9	3.9944	534	14.9	69.6	3.9912	339
H DG	6.01	4.5	69.5	3.9877	244	2.4	67.5	3.9896	239	3.9	67.1	3.9898	294
H DH	6.08	3.8	71.2	3.9967	907	3.3	69.9	3.9962	799	1.2	68.7	3.9945	547
HDI	6.15	6.3	71.5	3.9893	280	6.5	69.8	3.9849	198	359.9	65.7	3.9636	82
H DJ	6.22	4.2	74.8	3.9957	701	1.9	72.9	3.9964	837	4.4	72.1	3.9967	911
HDK	6.29	6.4	69.7	3.9929	424	7.8	67.4	3.9869	228	5.6	65.8	3.9853	203
HDL	6.36	6.5	69.8	3.9773	131	7.3	66.4	3.9795	146	10.2	65.2	3.9705	101
H DM	6.43	10.1	69.7	3.9900	301	10.4	69.1	3.9914	347	12.4	68.3	3.9895	286
H DN	6.50	11.7	73.6	3.9939	494	12.1	73.3	3.9949	592	12.9	72.8	3.9923	390
H DO	6.57	11.6	73.2	3.9916	357	10.8	72.6	3.9891	274	12.5	72.7	3.9846	194
H DP	6.64	10.4	72.8	3.9958	720	7.7	72.1	3.9948	579	7.5	70.4	3.9951	616
H DQ	6.71	357.2	69.1	3.9901	304	356.6	66.1	3.9765	127	359.5	63.2	3.9661	88

S site

E elevation (metres)

D declination

I inclination

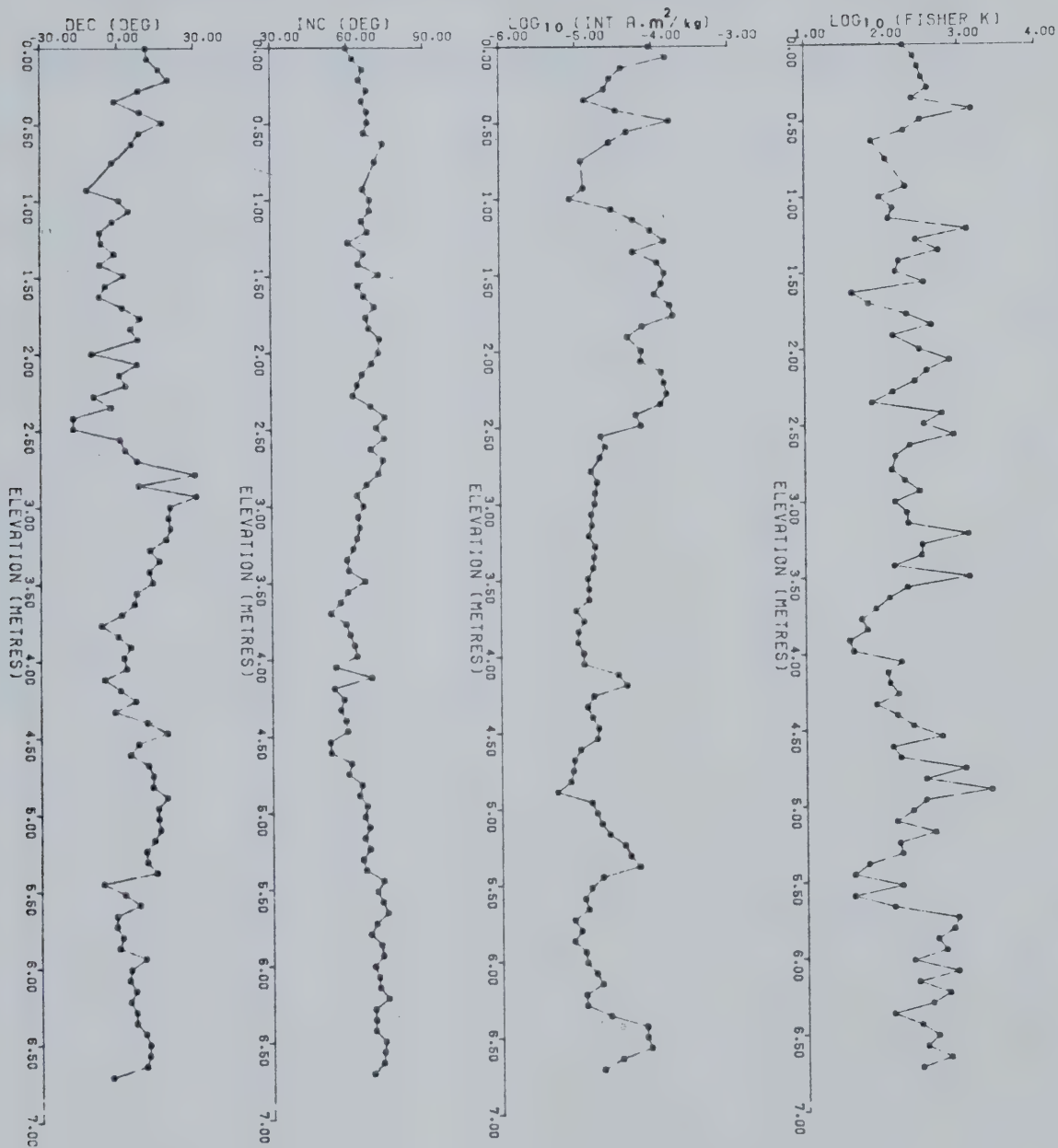
R vector resultant

k Fisher's precision parameter

Fig. 4.1a-c Site means ; declination , inclination , intensity
and Fisher's precision parameter (k) at 0, 10
and 20 mT.

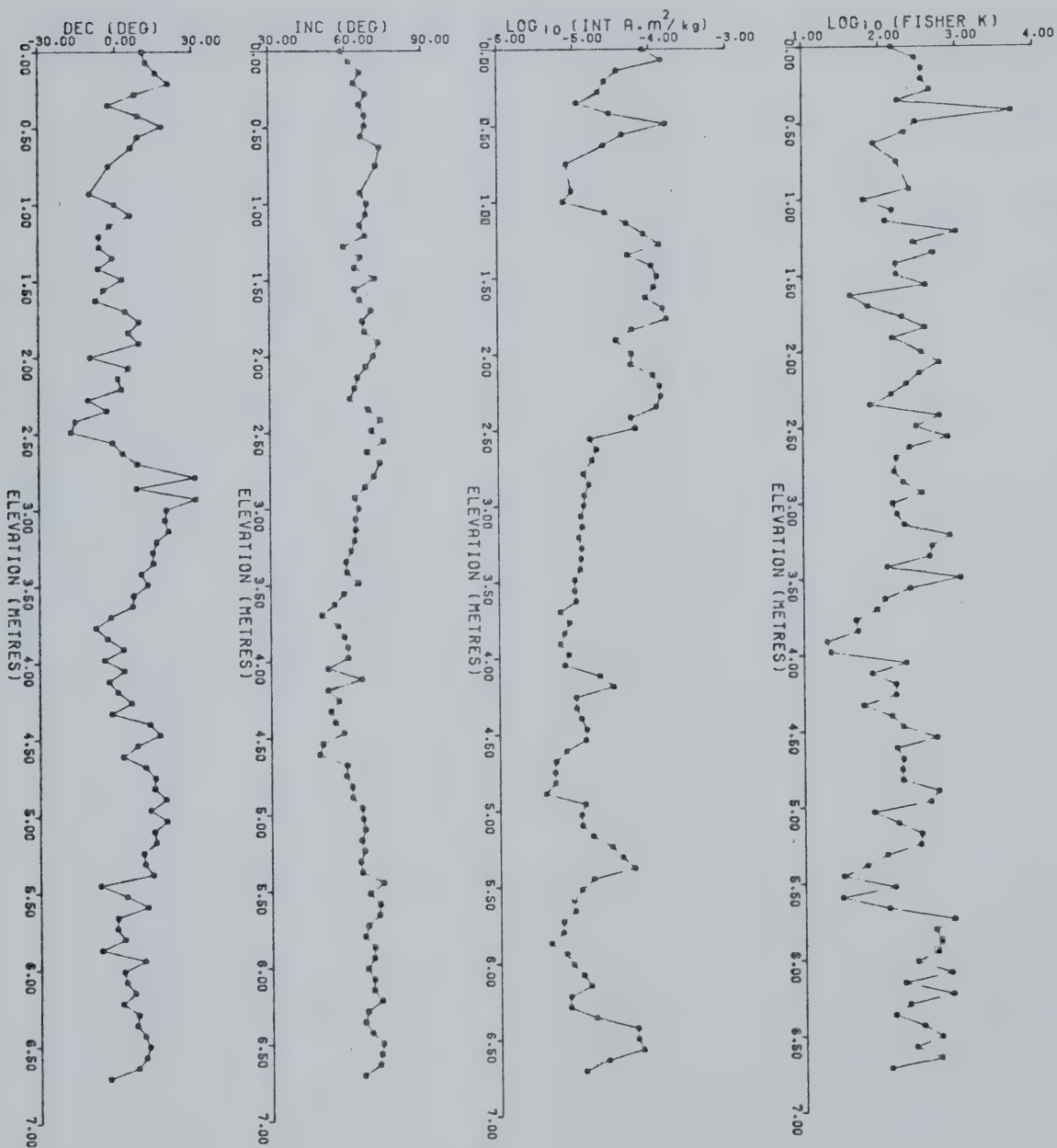
(a)

RIGGINS ROAD SITE MEANS (0 mT)



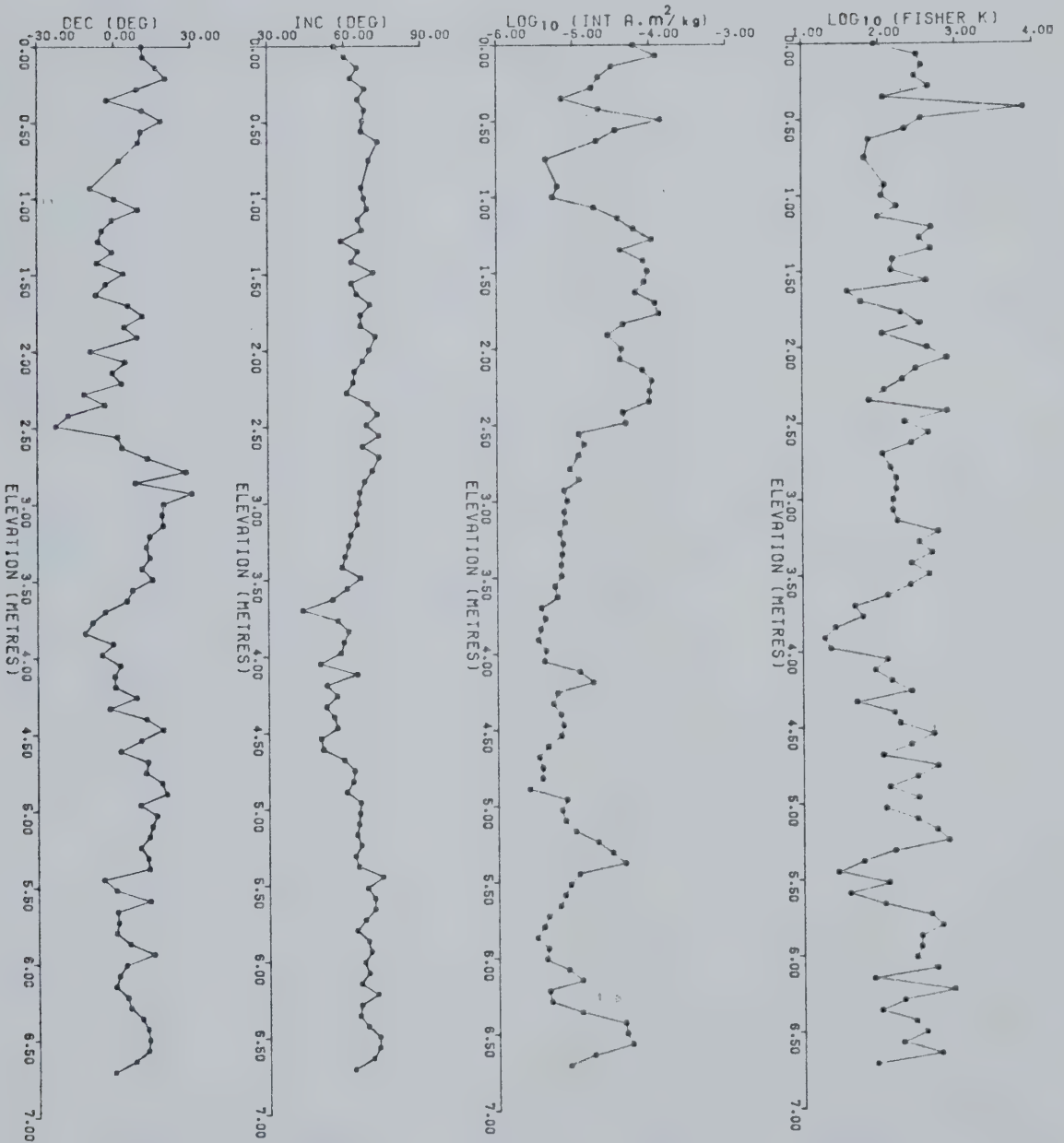
(b)

RIGGINS ROAD SITE MEANS (10mT)



(C)

RIGGINS ROAD SITE MEANS (20mT)



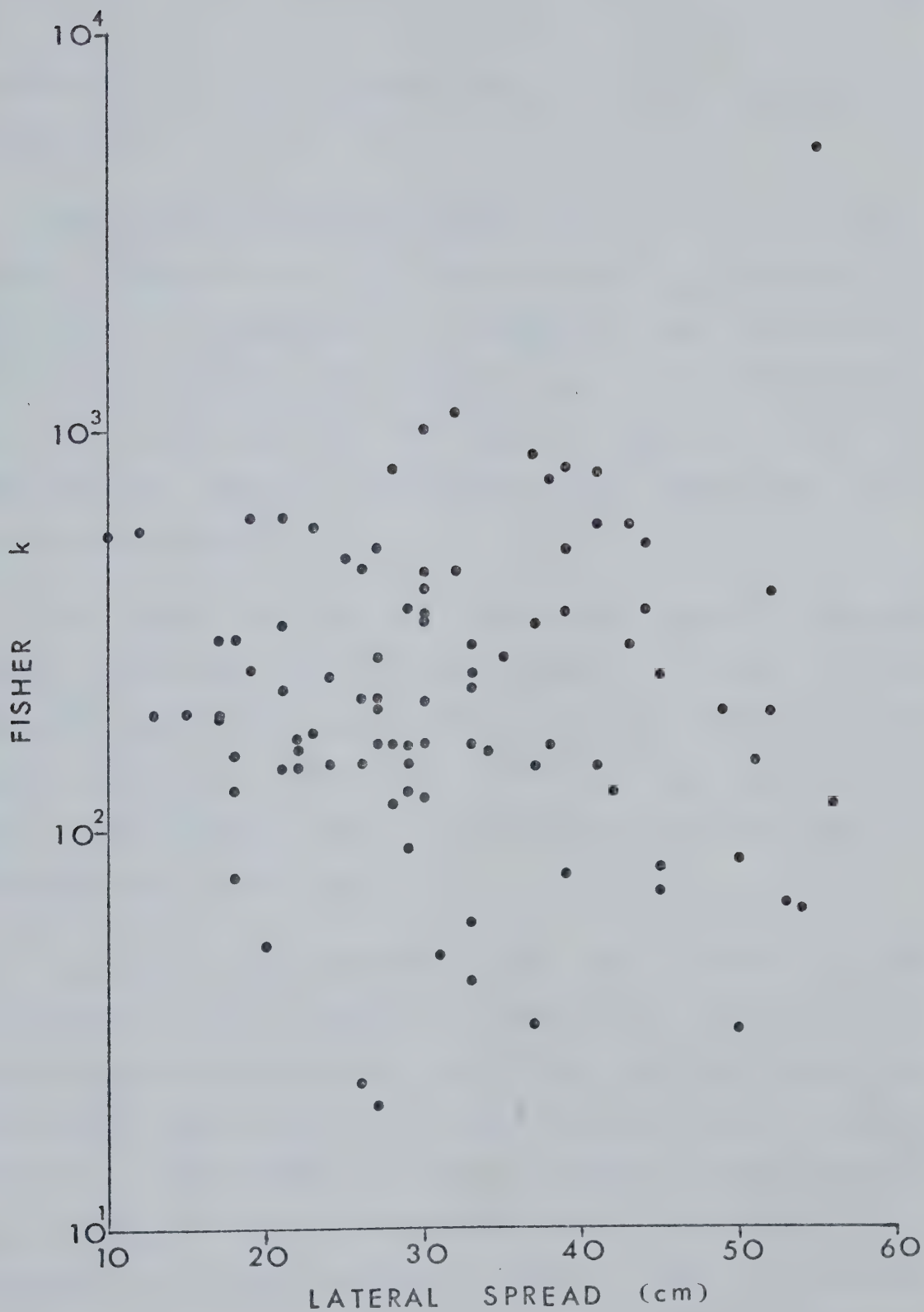


Fig. 4.2 A plot of Fisher k versus the lateral spread of specimens at each site.

specimens; it is probably due to minor lithological variations.

The standard two-tier analysis (Watson & Irving, 1957) yields within-site (k_W) and between-site (k_B) precisions of 140 and 178 respectively. As expected, the between-site precision increases when freed of the effect of within-site scatter. Completion of the two-tier analysis leads to $k_0=12,716$ and $\alpha_{95}=1.2^\circ$, but the slight improvement is of no real significance.

The pole obtained from the mean direction lies at 3.4°E , 85.4°N ($dp=1.7^\circ$, $dm=1.2^\circ$), whilst the mean of the virtual geomagnetic poles (VGP's) (Fig.4.3) lies at 0.0°E , 85.6°N ($N=94$, $R=92.7032$, $K=72$, $A_{95}=1.7^\circ$). Thus the overall mean paleomagnetic pole is statistically distinct from the rotation axis of the earth.

In early paleomagnetic work this small (4.4°) difference would probably have been attributed to methodological inadequacies, but a great deal of interest is currently being directed towards these 'second order' features, and further scrutiny is therefore warranted. The pole obtained is 'right-handed' and 'far-sided', in agreement with global analyses of Wilson (1970, 1971, 1972). Merrill & McElhinny (1977) have updated these studies and provide a comprehensive compilation of 266 high-quality

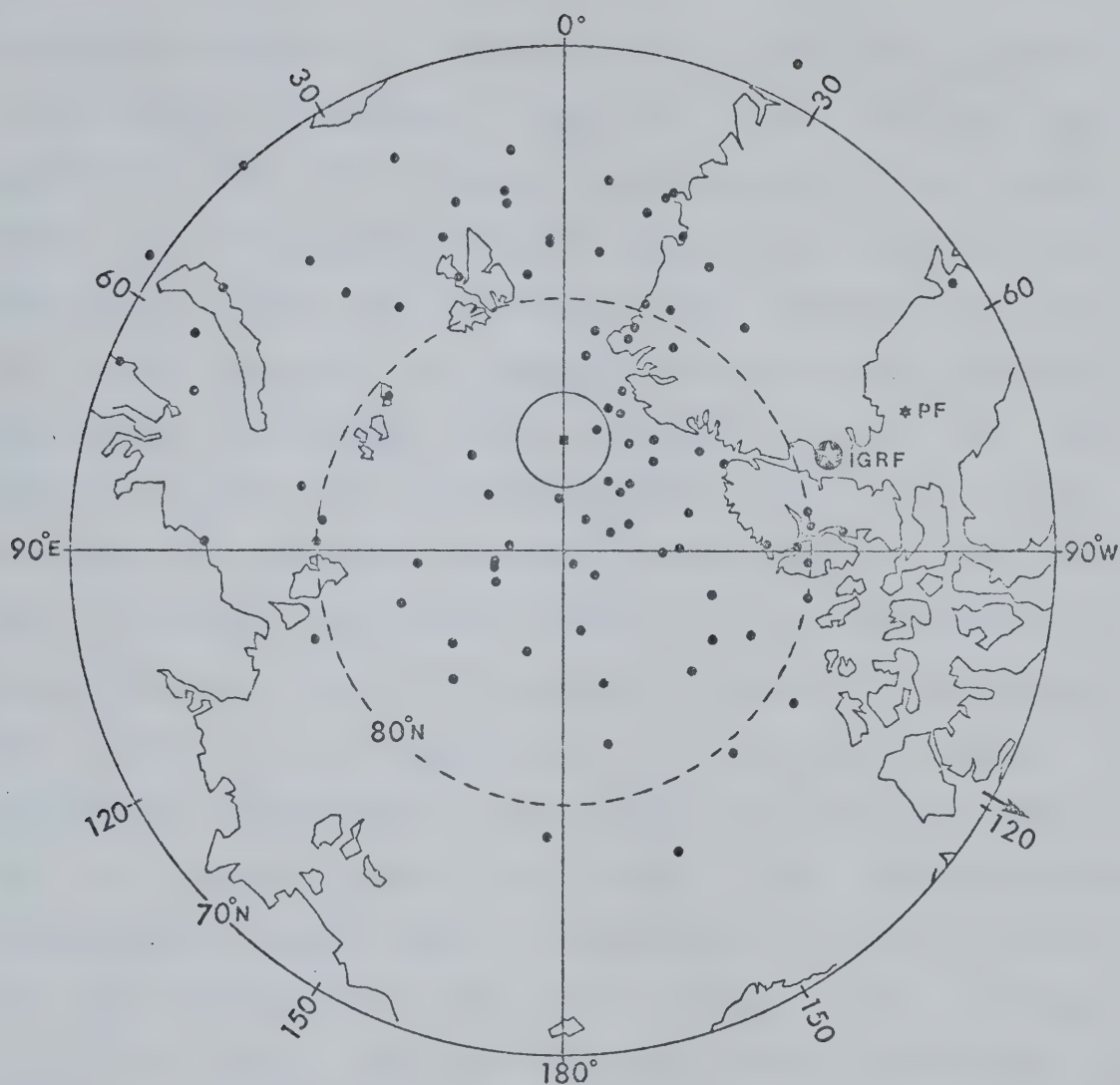


Fig. 4.3 Virtual geomagnetic poles (VGP's) for all 94 horizons with their mean and its circle of 95% confidence. The dipole axis for the 1965 International Geomagnetic Reference Field and the pole corresponding to the present field vector at the sampling site are indicated by IGRF and PF respectively. The longitude of the sampling site is shown by an arrow at the perimeter. (Equal area projection)

published results. Of these 101 are of particular interest to the present discussion, being of normal polarity and Quaternary age (0 - 2 m.y.). For discussion of the 'right-handed' and 'far-sided' effects Wilson (1972) introduced the convenient 'common site longitude' (CSL) concept in which each sampling site is imagined to be at zero longitude. Merrill and McElhinny (1977) obtained a mean CSL pole position of 87.72°N , 166.14°E ($N=101$, $R=100.03221$, $K=103.3$, $A95=1.39$). By this same convention, the Riggins Road pole lies at 85.6°N , 118.9°E with $A95=1.7^{\circ}$ (Fig. 4.4). These two poles differ by only 3.3° ; assuming a Fisherian distribution with $K=103.3$, the probability of observing such an individual divergence is quite high (84%). It thus appears that the Riggins Road data typify the time-averaged paleomagnetic field, which is dominated by the axial dipole, but has detectable higher order terms. This, in turn, implies that under suitable sedimentological conditions a time span of 9,000 years is sufficient to yield an acceptable estimate of the local paleofield. However, poles deduced from such data using the usual dipole mapping function will obviously not yield a precise estimate of the spin axis (geographic pole), because of the persistent non-dipole terms. Merrill & McElhinny propose a slightly modified procedure for calculating poles which allows for these effects.

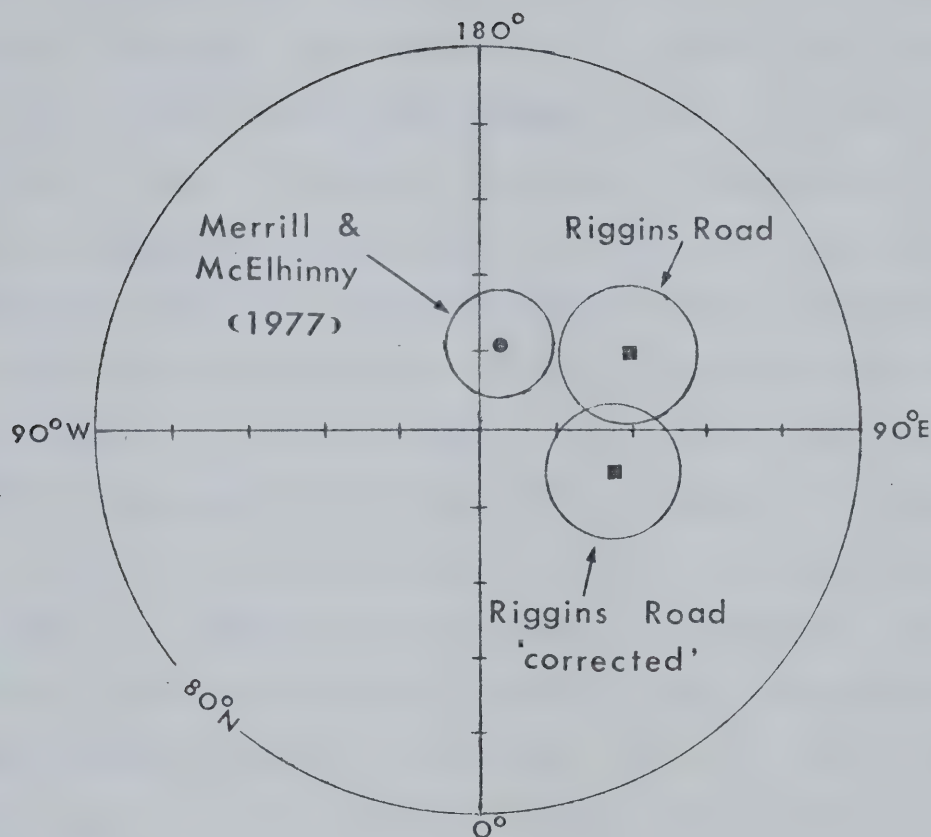


Fig. 4.4 Mean common site longitude (CSL) pole position for the Quaternary (Merrill & McElhinny, 1977) and for the Riggins Road data with their respective circles of 95% confidence (see text). (Equal area projection)

Cox (1975) has summarized a large body of excellent paleomagnetic data from basaltic flows exposed on the Hawaiian Islands. He concludes that the time-averaged paleofield diverges from that of a geocentric axial dipole field by $7.7^\circ \pm 2^\circ$, the discrepancy being entirely in inclination. The smallest long-term 'anomalous' field capable of explaining this offset is 5,400 nT ($\Delta X = 3,300$ nT, $\Delta Z = -4,400$ nT), which is definitely appreciable compared to typical IGRF non-dipole values. As possible explanations Cox rejects Wilson's (1971) offset dipole model, and also the 'standing' non-dipole field model of Yukutake & Tachinaka (1969). His favoured explanation involves biased drifting fields and is discussed more fully in section 4.3 in connection with the present data. For the moment we note that the Riggins Road pole lies 4.4° from the spin axis, corresponding to a directional divergence at the site of 3.1° . The minimum long term anomalous field capable of explaining this offset is 2,800 nT, (assuming an axial dipole field of 52,000 nT at 50.3°N) with components $\Delta X = 1,700$ nT, $\Delta Y = 2,100$ nT, and $\Delta Z = -700$ nT. It is seen that, unlike the Hawaiian case, the eastward (i.e. ΔY) component is very appreciable.

Merrill & McElhinny (1977) feel that the permanent quadrupole is now sufficiently well established (at least for the last 5 m.y.) to warrant a modification such that the

usual 'dipole equation' $\tan I = 2 \cot P$ is replaced by :

$$\tan I = [4 \cos P + 3R(\cos^2 P - 1)] / [2 \sin P + 3R \sin 2P]$$

where I is inclination, P is colatitude and $R = g_2^0 / g_1^0$: g_2^0 and g_1^0 being the geocentric axial quadrupole and dipole Gaussian coefficients respectively. This modification refers to the far-sided effect, the proposed field being entirely zonal. They obtain $R = +0.050$ for normal polarity data spanning the last 5 m.y.; this compares favourably with the 1975 IGRF value of $+0.063$. Taking $R = +0.050$ the corrected Riggins Road pole lies at $45.1^\circ W$, $86.3^\circ N$ (Fig. 4.4), still 3.7° from the spin axis and now requiring a 'permanent' anomalous field of 2,200 nT ($\Delta X = 400$ nT, $\Delta Y = 2,100$ nT, $\Delta Z = -200$ nT). The eastward component now dominates of course, since the meridional components have been essentially removed by the quadrupole correction.

Merrill & McElhinny also analyse the right-handed effect first noted by Wilson (1972). They conclude that Wilson was misled by unevenly distributed data, there being a paucity of data from the Pacific region. They propose both right-handed and left-handed anomalies constituting a symmetrical sinusoidal variation of peak amplitude $\pm 2^\circ$ (Fig. 4.5). At the longitude and latitude of Riggins Road they predict a left-handed divergence of 2.8° whereas we find a right-handed value of $\Delta D = 5.7^\circ$. Obviously a single datum such as this cannot rule out their model, but our data, which

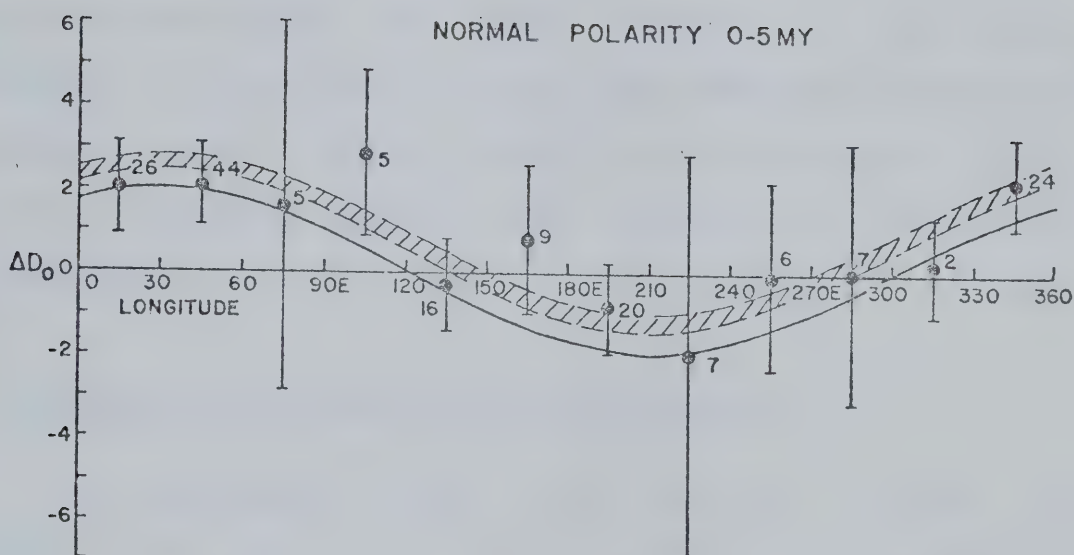


Fig. 4.5 ΔD_0 anomaly averaged by 30° longitude sectors. $\Delta D_0 = \tan^{-1} (\tan \Delta D \cos \lambda)$ where ΔD is the declination anomaly (departure of D from zero) and λ is the latitude. Thus ΔD_0 is the equator-normalized value of ΔD . Simple sinusoidal curves that best fit the normal data lie within the hatched region. Bars indicate the standard error (after Merrill & McElhinny, 1977).

seem to represent a high quality recording, clearly conflict with it.

These differences are small and further work is necessary to fully establish their validity. At the present time the observations and their implications are simply presented at face value. However, the detailed analysis and discussion of the temporal sequence of field vectors given in the following section lends credence to the above inferences.

4.3 Declination and Inclination Oscillations

The geomagnetic record (Fig. 4.1a-c) reveals no evidence of any large angular shifts which could be correlated with the geomagnetic excursions reported from Mono Lake, California (25,000-24,000 yrs.B.P.; Denham, 1974; Liddicoat & Coe, 1975) or that from Lake Mungo, Australia (30,780-28,140 yrs.B.P.; Barbetti & McElhinny, 1972) even though the sampling interval is approximately 100 years. This implies that such excursions are not global events, but result from the spatially restricted effects of specific non-dipole sources (Harrison & Ramirez, 1975; Coe, 1977). No large excursions are recorded, but smooth declination and inclination oscillations are observed. These presumably result from 'regular' secular variation and thus provide an

opportunity to study temporal geomagnetic variations.

Beran & Watson (1967) have devised a test for serial correlation of a sequence of unit vectors. If N successive points are represented by directions of magnetization X_1, \dots, X_N and if there is a strong nearest neighbour correlation, then the angle between successive vectors will be much smaller than the angle between vectors with very different serial numbers. Thus the cosines of the angles between successive vectors are expected to be large. Therefore a large L , where $L(I) = \sum X_i \cdot X_{i+1}$, signifies serial correlation. The significance level is given by :

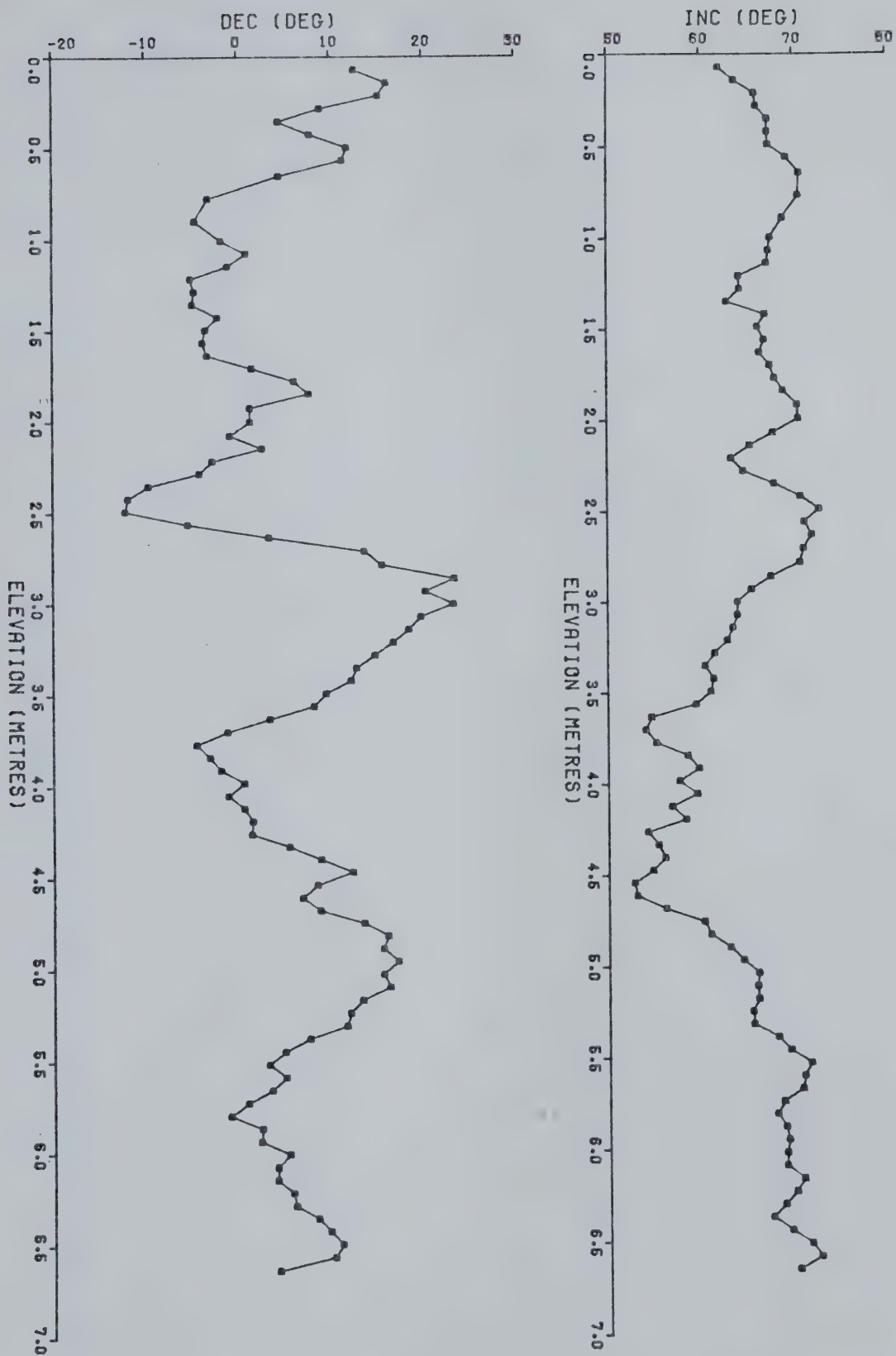
$$s = [L(I) - E(L)] / [\text{Var}(L)]^{1/2}$$

where $E(L)$ is the theoretical mean of $L(P) = \sum X_i \cdot X_j$ for a completely randomized sequence of vectors and $\text{Var}(L) = E(L) - E(L^2)$. For the 1% significance level the value of s is 2.326. For our data this test yields a value of $s=8.860$ indicating that the probability of sequential ordering is very much greater than 99%. This implies that the apparent oscillations in declination and inclination magnetograms (Fig. 4.1b) represent real temporal fluctuations in the paleofield. Similar oscillations were reported many years ago by Johnson et al. (1948), but only in this decade has there been a revival of interest in the study of secular variation obtained from recent sediments (Opdyke et al., 1971; Thompson, 1975; Creer et al., 1976; Creer, 1977).

The oscillations are very clearly revealed when the data of Fig. 4.1b are smoothed by a moving average (Fig. 4.6a,b). Fluctuations up to about 40° in declination and about 20° in inclination are observed, and visual inspection suggests periodicities of a few thousand years. Spectral analysis results will be more fully discussed in the following section; at this stage it is both convenient and worthwhile to scrutinize the actual pattern of paleofield vectors. In Fig. 4.7a the sequence of 94 site mean directions are illustrated. A coherent pattern is discernible, but smoothing by a moving average emphasizes the underlying pattern (Fig. 4.7b,c). A series of open loops emerge, reminiscent of historical observatory records. The amplitude of these loops is similar to the historical records for London and Paris (see Fig. 1.2), but the periodicities involved are considerably larger. Perhaps the most remarkable feature is the fact that the same 'three-quarter loop' path is traversed repeatedly, first in a counter clockwise sense, then clockwise, and finally half of it is traversed counterclockwise again. We return to the implications of this pattern below, but first it is instructive to compare these results with Cox's suggestion of biased drifting fields introduced in section 4.2. The inset in Fig. 4.7a (from Cox, 1975) indicates how he envisages spatially non-isotropic disturbances leading to a

Fig. 4.6a,b Magnetograms of three-point and five-point moving averages .

(a)



(b)

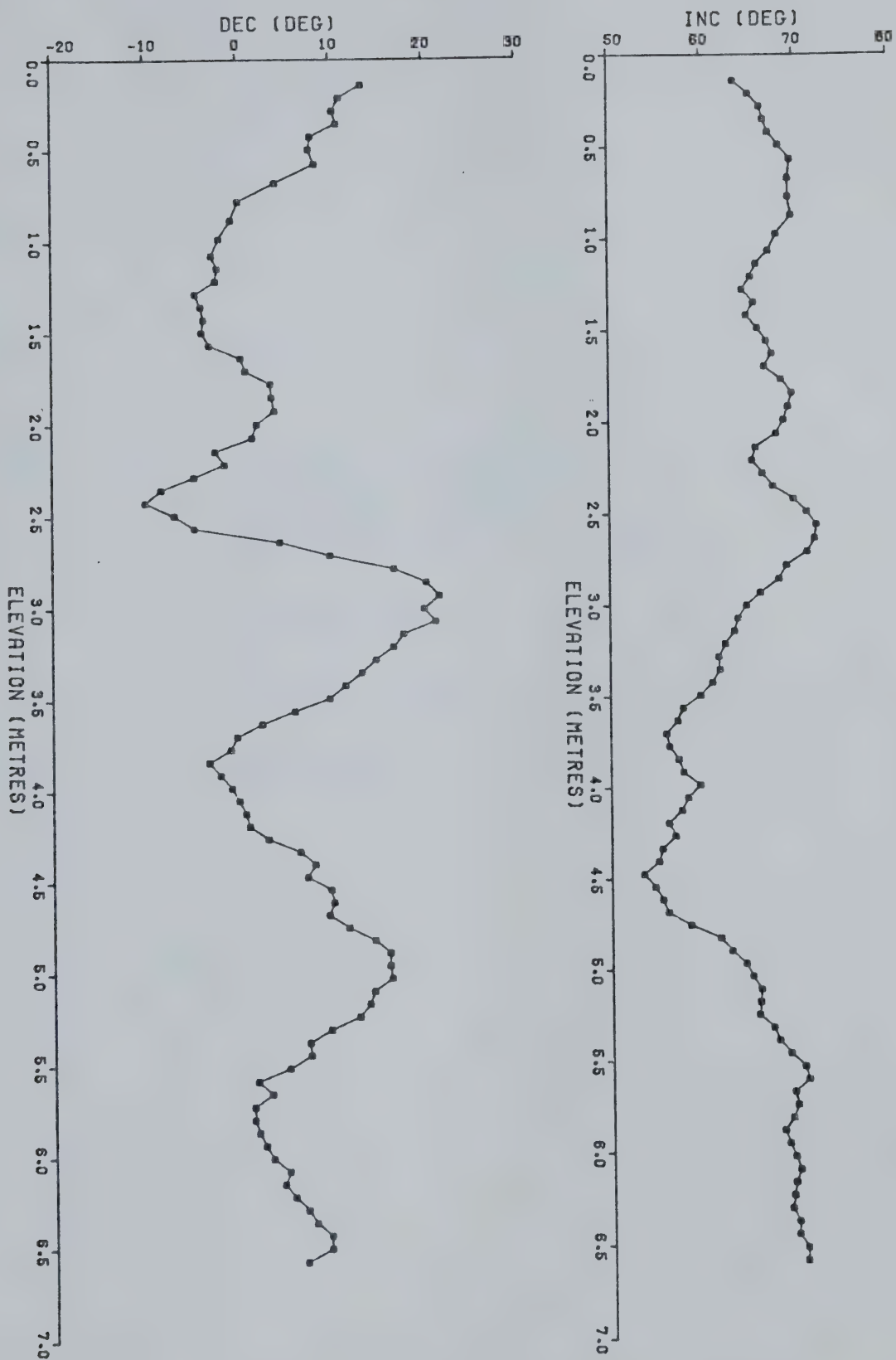
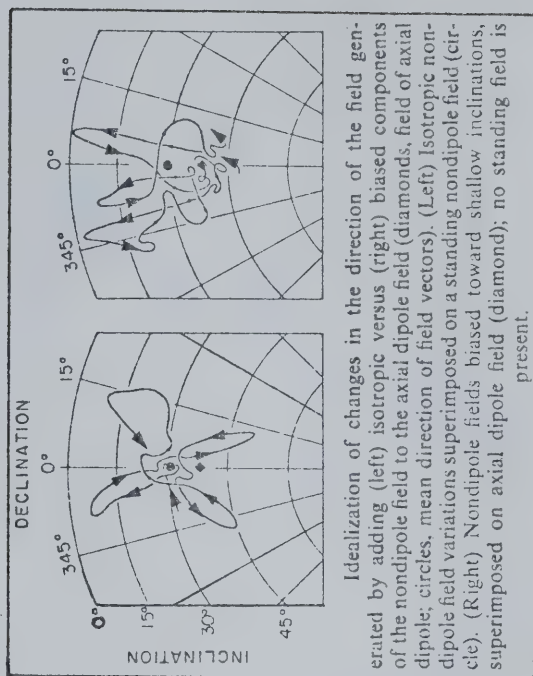
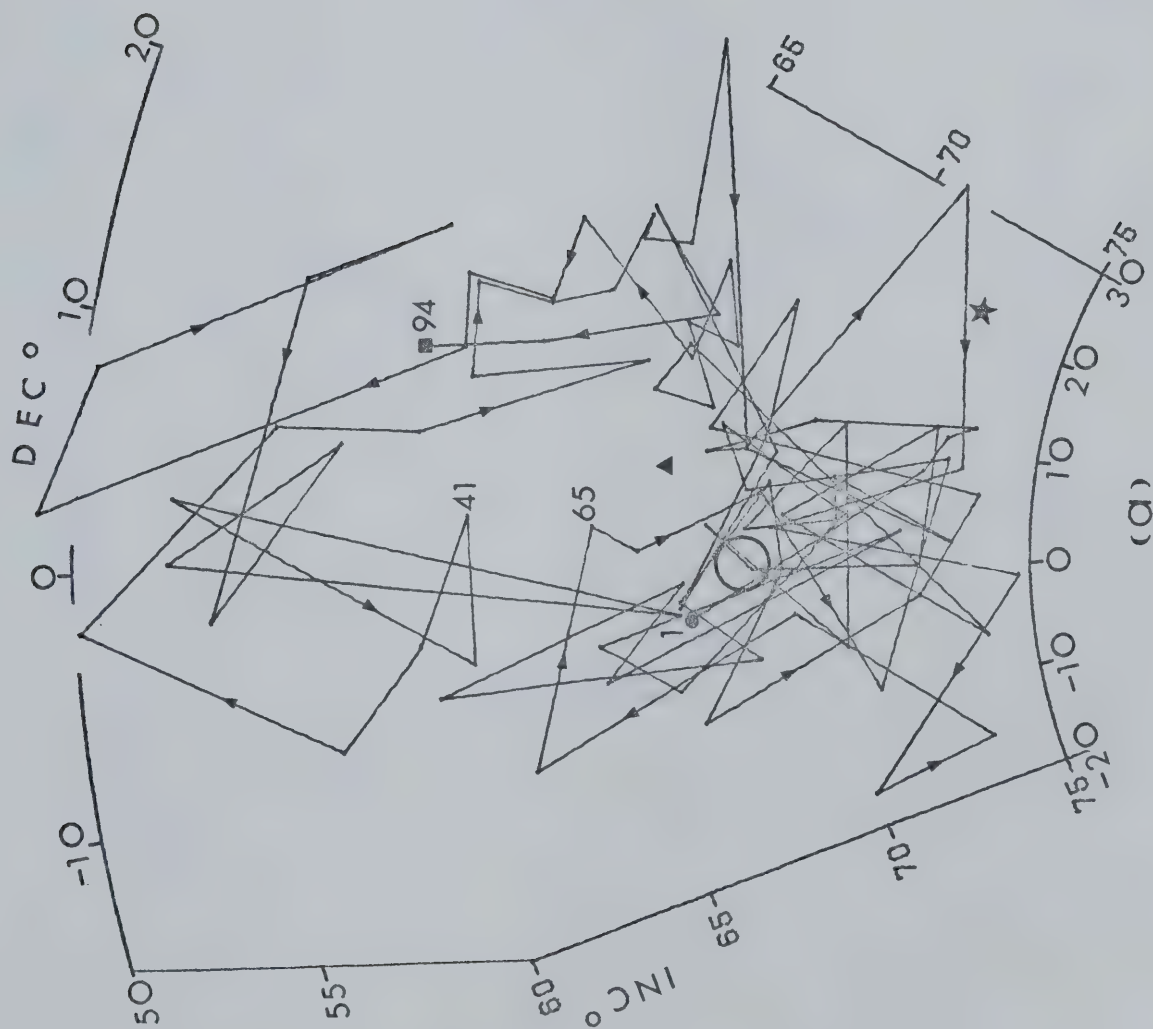


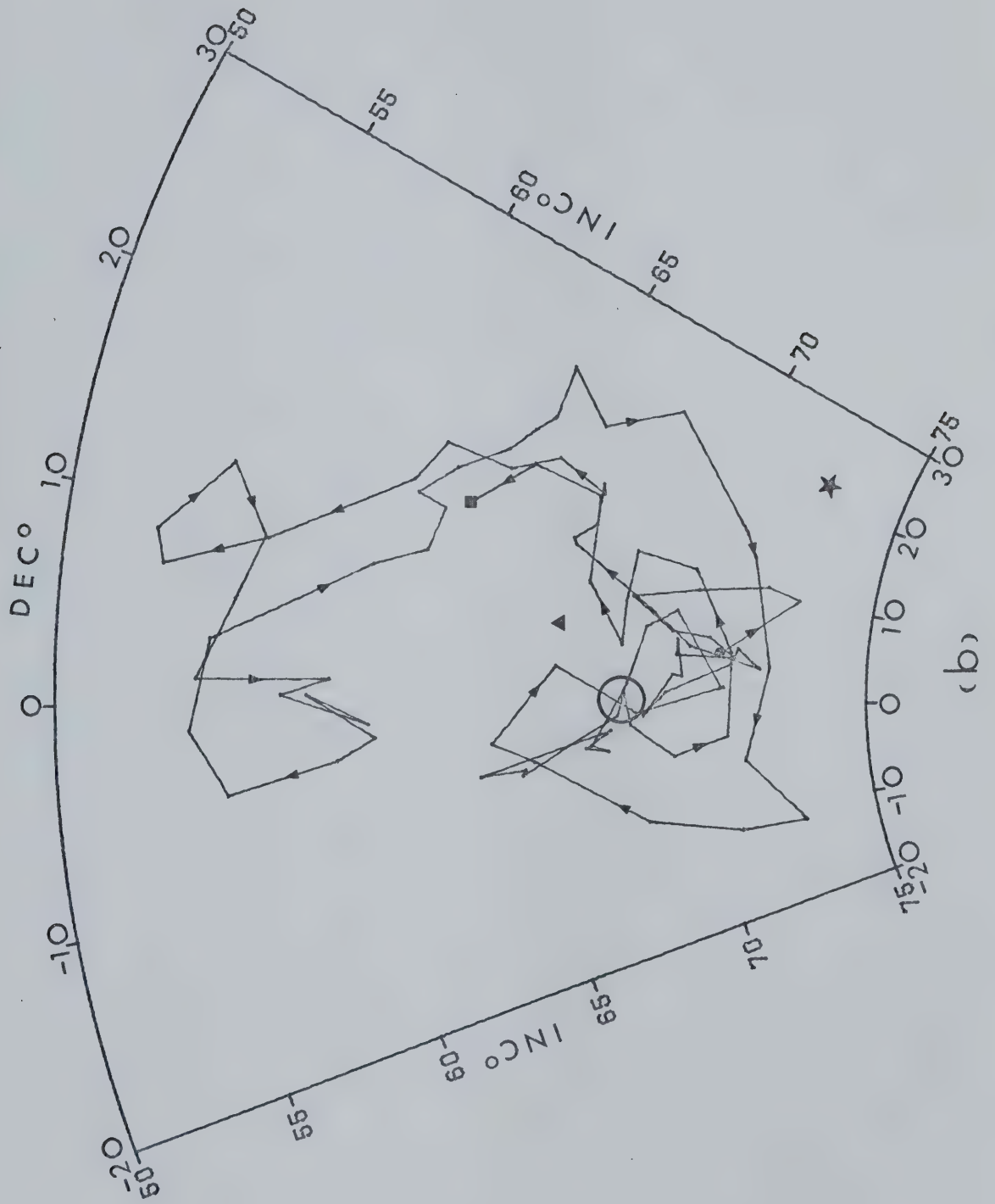
Fig. 4.7 (a) Azimuthal equidistant plot of the 94 site means.

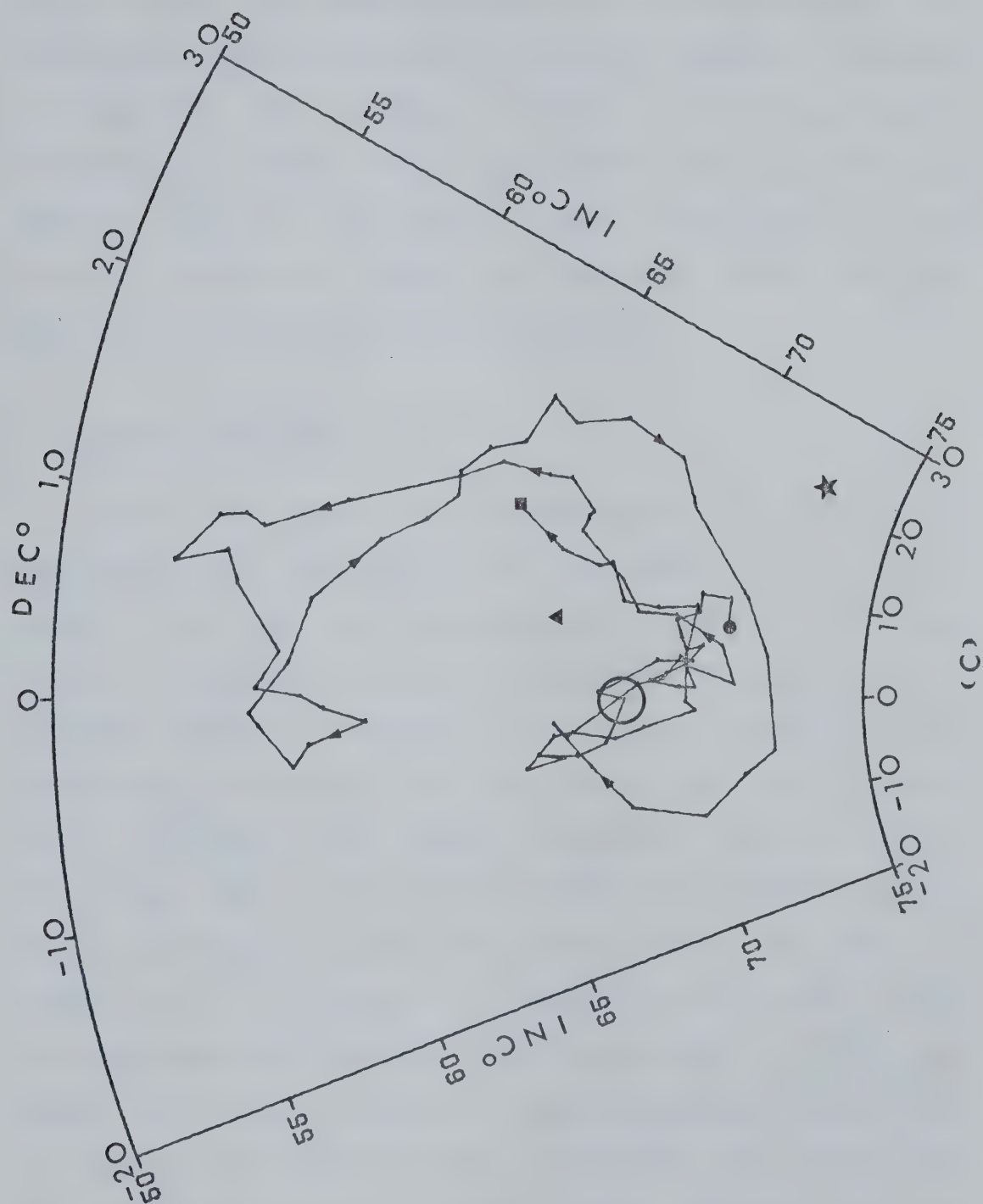
- oldest horizon
- youngest horizon
- ▲ vectorial mean of 94 sites
- ★ present field at sampling site
- geocentric axial dipole direction

The inset diagram (after Cox, 1975) illustrates idealized secular variation patterns (see text) .

(b),(c) Three-point and five-point moving averages of the data shown in (a) .







small offset in the time averaged paleofield vector. The Riggins Road data conform rather well to this concept, but the bias is strongly eastward as well as towards shallower inclinations. The overall picture is therefore quite satisfying, in terms of the final effect, but the underlying cause is not at all clear. Further discussion of the possible cause, or causes, is postponed until after the spectral analysis results are described.

4.4 Spectral Analysis

Fourier analysis of the declination and inclination magnetograms has been carried out. The results (Fig. 4.8a,b) confirm that the main periodicities are a few thousand years, as suggested by visual inspection. The power spectra obtained compare favourably with those of Yukutake (1962) who analysed Quaternary data from Japan and New England. Fourier analysis has several drawbacks for this type of short noisy data. An alternative method of spectral analysis whereby information concerning the degree and sense of looping can be obtained in addition to the power at any given frequency has been put forward by Denham (1975). The method essentially involves treating both the declination and inclination simultaneously as a complex time series, and uses the maximum entropy method (MEM) developed by Burg (1967). The spectra produced by complex series are often

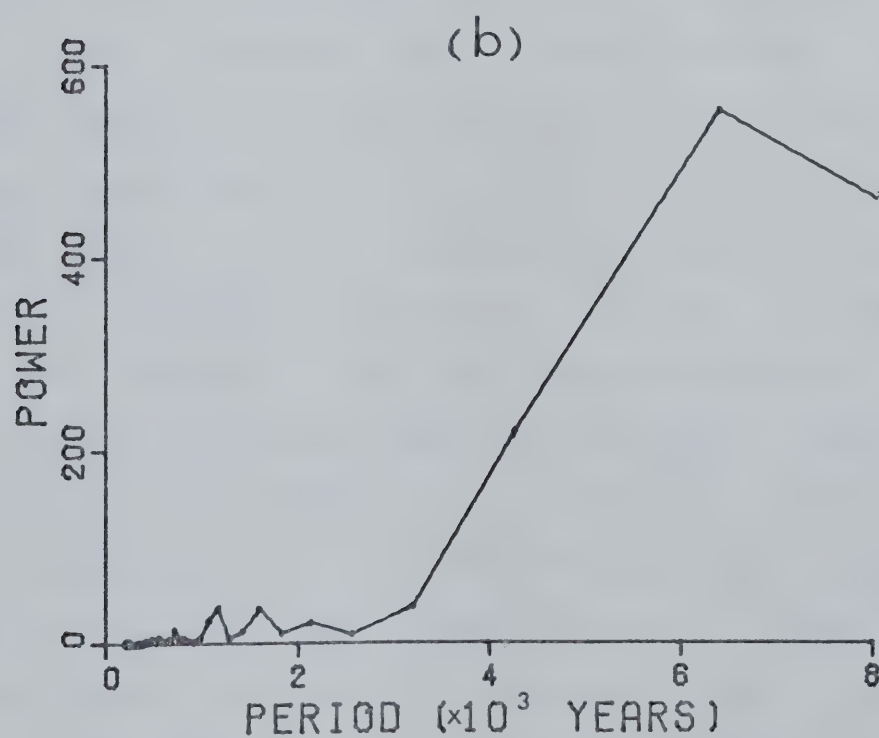
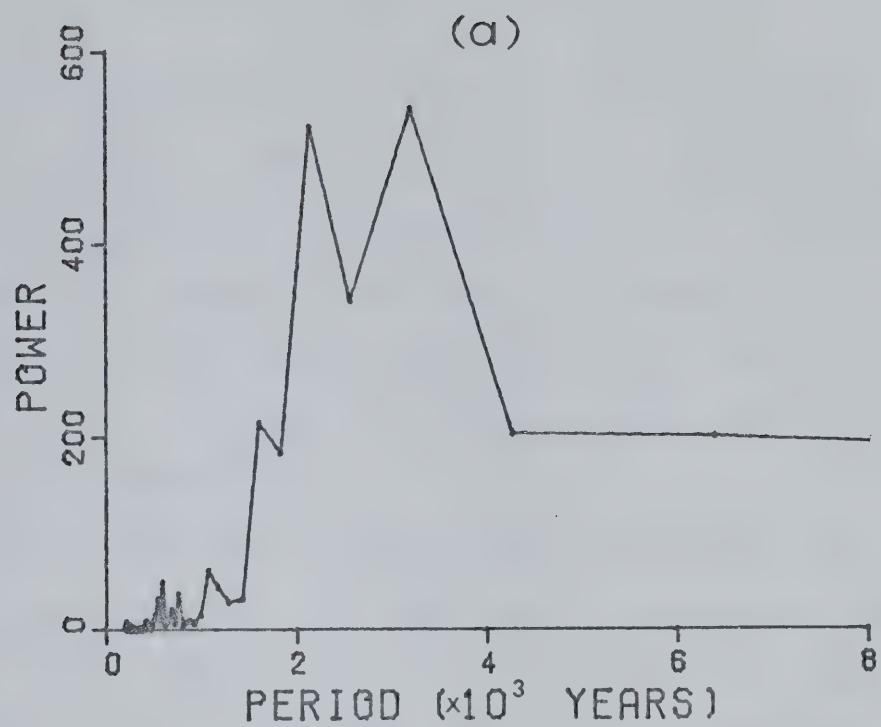


Fig. 4.8a,b Declination and inclination power spectra obtained by Fourier analysis.

asymmetrical i.e. a peak in the 'positive' half of the spectrum is not the same size as its corresponding peak in the 'negative' half of the frequency spectrum. At any given frequency, the greater the degree of asymmetry, the more circular will be the looping. The looping at any arbitrary frequency, f , is generally elliptical with semi-major and semi-minor axes given by :

$$|[P(f)]^{1/2} + [P(-f)]^{1/2}| \text{ and } |[P(f)]^{1/2} - [P(-f)]^{1/2}|$$

respectively where $P(f)$ is the power associated with a spectral peak centred on f . The sense of the looping is determined by the sign of $P(f) - P(-f)$, (positive for clockwise and negative for counterclockwise). The appropriate complex series is generated by first mapping the directional information onto an azimuthal equidistant polar projection centred on the vectorial mean of the data. The MEM algorithm employed was originally designed to analyse real data only (Anderson, 1974) and minor modifications were necessary for analysing the complex time series; these were accomplished by Oberg (1978). Oberg carried out a series of numerical experiments to test the method. He used a variety of synthetic data sets with known frequency content and noise. He found that the MEM technique is able to recover the input signal even in the presence of noise almost twice its amplitude. It was therefore decided to apply the technique to the present data, using programs kindly

provided by C.J.Oberg.

The ability of the maximum entropy technique to provide a good spectral estimate depends on the proper choice of prediction error filter (PEF) length. Ulrych and Bishop (1975) suggest that the optimum filter length is that which minimizes the so-called 'final prediction error' (FPE). Fig. 4.9 illustrates the FPE versus the filter length for the present data set. The position of the first minimum is rather surprising since a filter length of 3 would be far too short to resolve any appreciable detail in the spectrum. By using a filter length of 8, which is the second FPE minimum, a rather poor resolution of the spectrum is obtained (Fig. 4.10a). In order to obtain better resolution, filter lengths of 14 and 30 were also used (Fig. 4.10b,c). In all cases periods of about 6,000 and 2,000 years emerge (Table 4.2). These periods are similar to those found in the reconnaissance study by Oberg (1978), but there are some important differences. In particular, Oberg found a clockwise circular looping with a 2,000 year period, whereas the more complete data now available indicate both clockwise and counterclockwise looping at periods near 2,000 years.

An attempt has been made to assess the frequency content as a function of time by subdividing the present data set. Fig. 4.7a-c offers guidance as to the most

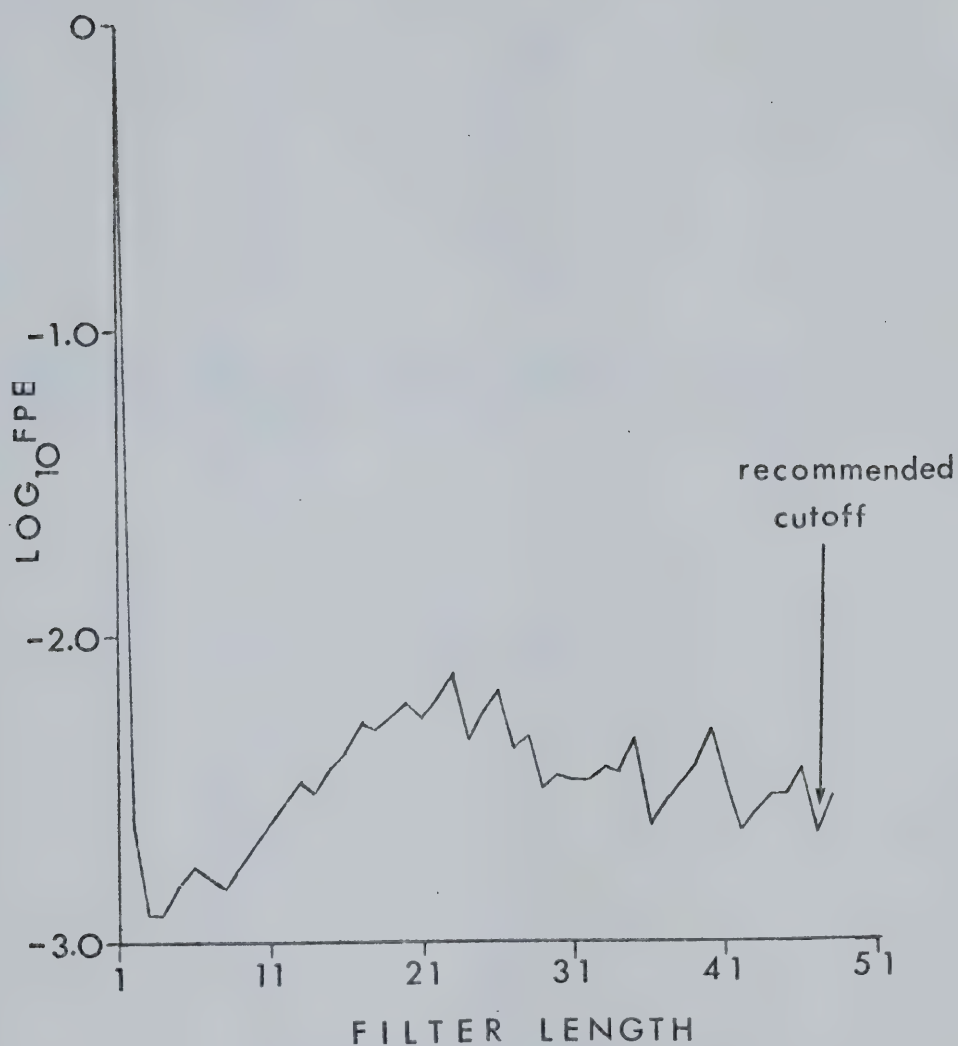


Fig. 4.9 Plot of FPE versus prediction error filter length. Ulrych & Bishop (1975) have suggested that a cutoff of $N/2$ (N = number of data points) in the filter length be imposed when using the criterion.

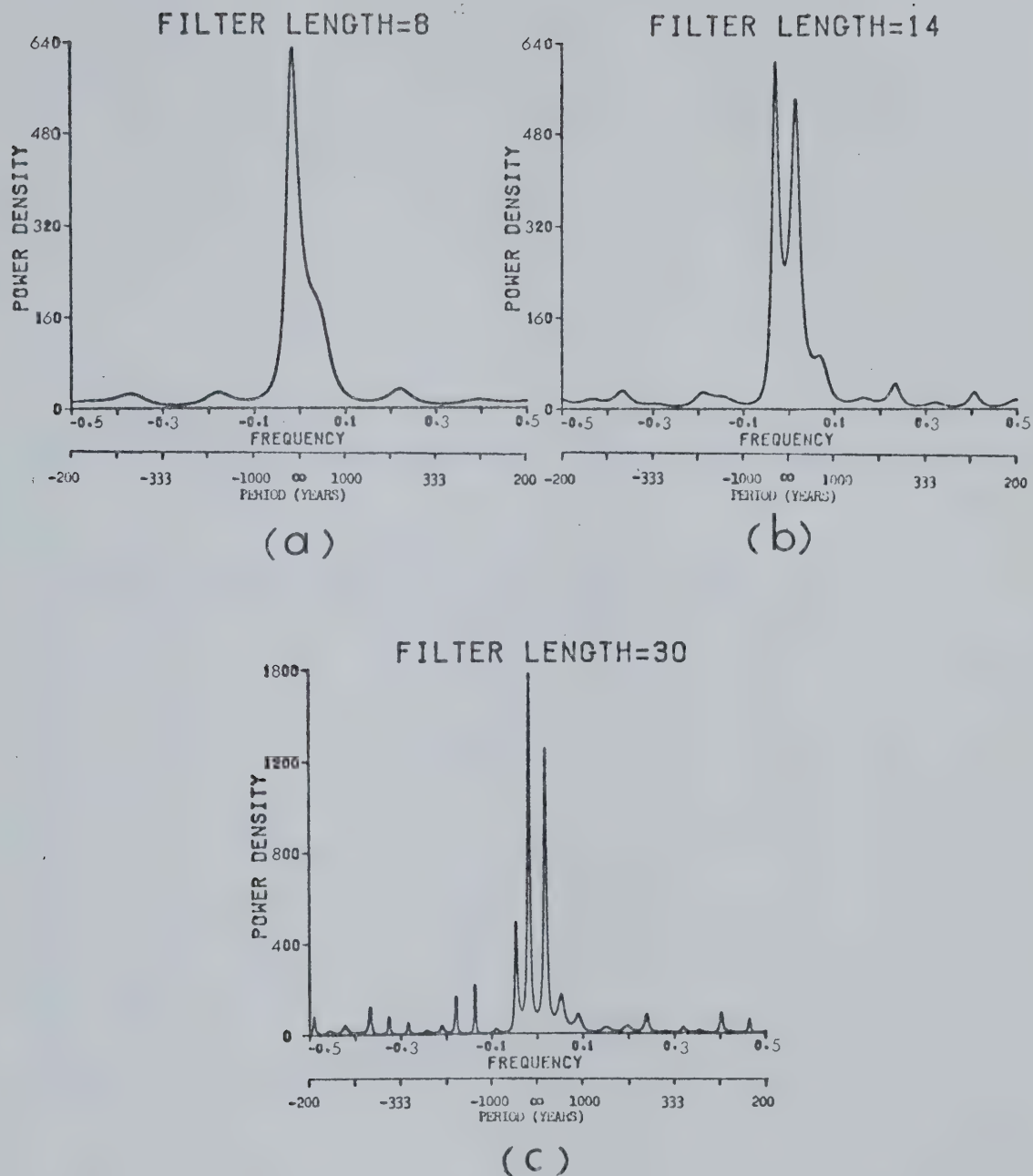


Fig. 4.10a-c MEM power spectra of the complex time series. The units associated with the ordinate can be thought of as (degrees)/unit frequency since the amplitude of oscillation (in degrees) associated with a given peak is equal to the square root of the area under the peak. Power in the positive frequency of the spectrum is indicative of clockwise looping whereas counterclockwise power resides in the negative frequency half of the spectrum.

Table 4.2 Periods and sense of looping with different filter lengths

data	filter length	sense of loop	period (years)
1-94	8	counterclockwise	5,880
		clockwise	1,980
1-94	14	clockwise	6,520
		clockwise	1,330
		counterclockwise	3,150
1-94	30	counterclockwise	5,500
		clockwise	1,880
		counterclockwise	2,150

appropriate manner in which to do this. A subdivision into three sections is suggested, i.e. horizons 1 (elevation 6.71 m) to 41 (elevation 3.91 m), 41 to 65 (elevation 2.21 m), and 65 to 94 (elevation 0 m). MEM analysis of these three sub-sets yields the results illustrated in Fig. 4.11a-c and summarized in Table 4.3. These confirm expectations based on visual inspection of Fig. 4.7a-c. The earlier part of the sequence is dominated by periods around 5,000-6,000 years, but the upper half is dominated by shorter periods of 2,000-3,000 years. This kind of variation in spectral content renders the use of spectral estimators quite hazardous unless very long data sequences capable of meaningful subdivision are available. This is not usually the case in paleomagnetic investigations. Nevertheless the existence of major periodicities at 5,000-6,000 years and 2,000-3,000 years seem to be well founded. Furthermore, it is worthwhile to note that despite the closer sampling used in this study compared to Oberg's reconnaissance work, no strong high frequency spectral peaks emerge. Reference to historical data (see Fig. 1.2) would suggest periodicities of several centuries. Although small peaks do appear in the MEM power spectra at these frequencies, they are too small to be regarded as real. This suggests that either such signals were absent, or that the deposition and dewatering involved in the natural recoding process somehow acts as a high-cut

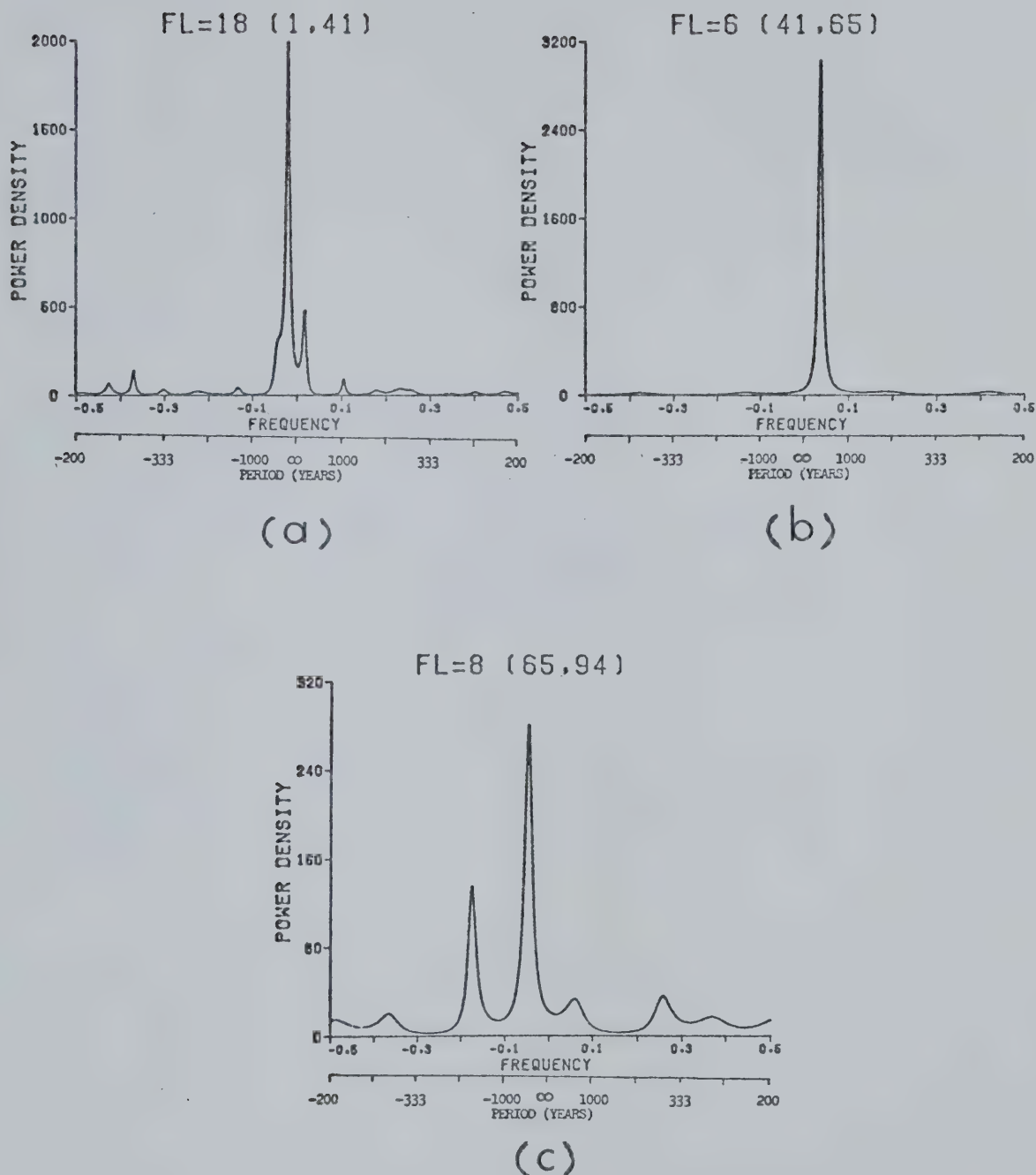


Fig. 4.11a-c MEM power spectra of the divided data set. The filter lengths are chosen according to the Urych & Bishop (1975) criterion.

Table 4.3 Periods and sense of looping of the divided data set

data	filter length	sense of loop	period (years)
1-41	18	counterclockwise	5,300
		counterclockwise	2,200
41-65	6	clockwise	2,700
65-94	8	counterclockwise	2,100

filter and suppresses such signals. This lack of high-frequency content is supported by the results of the finer-scale carving experiment illustrated in Fig. 2.6.

4.5 Discussion

Some simple preliminary modelling is attempted in order to investigate the possible underlying cause(s) of the secular variation pattern observed. The non-dipole has been observed to undergo westward drift during the last few decades (Bullard et al., 1950). At latitude 50°N this drift would produce the secular variation pattern of Fig. 4.12. Some features are similar to those observed in our data but the correspondence is not compelling. Furthermore, the periodicities would almost certainly be too short, unless the 'usual' westward drift rate of about $0.2^{\circ}/\text{yr}$ was a factor of two or three slower in the past. Periods of about 5,000 years are more likely associated with the main axial dipole (Table 1.1). The model of Opdyke et al. (1972) involving a 6,000 year dipole precession is attractive. At latitude 50°N such a model would produce elliptical secular variation patterns (Fig. 4.13) which are similar but not identical to those shown in Fig. 4.7a-c. A model whereby the pole is allowed to 'nod' back and forth along a given meridian yields the temporal variations shown in Figs. 4.14a-e. These simple models show some of the required

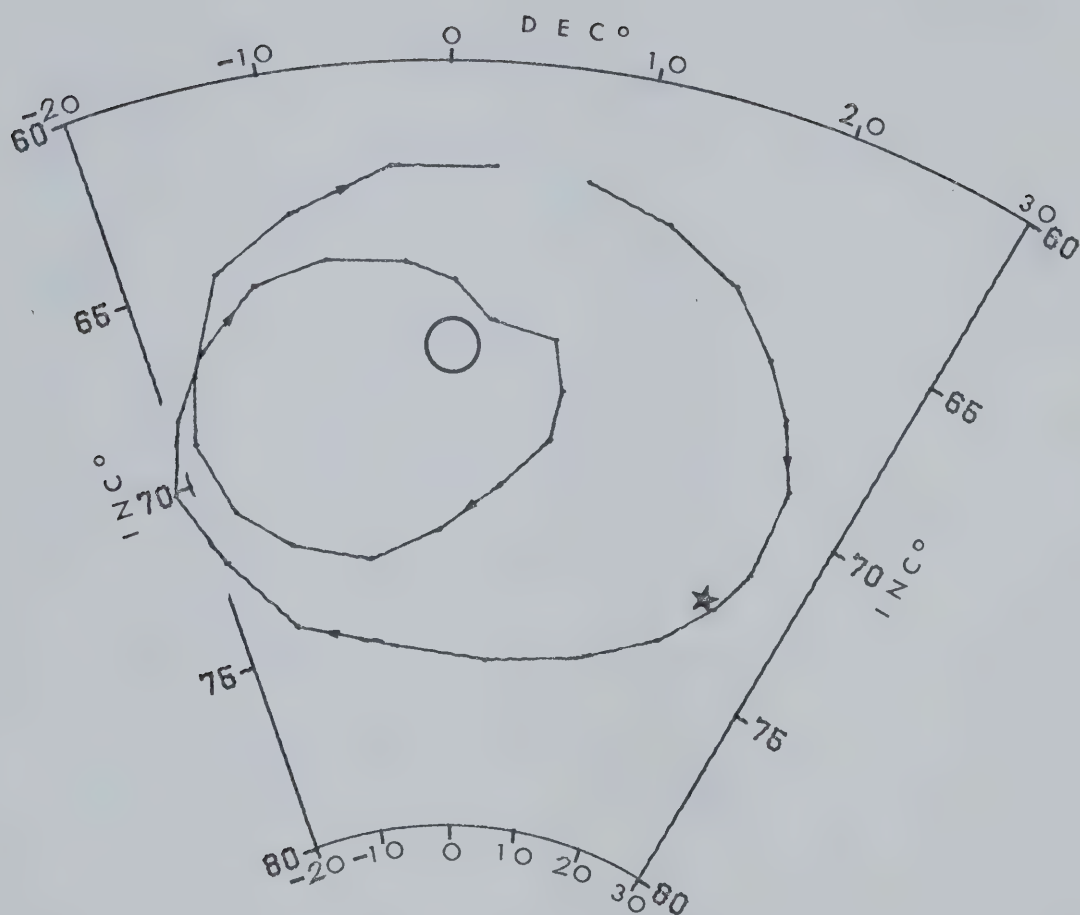


Fig. 4.12 Secular variations pattern obtained at latitude 50°N by letting the 1945 non-dipole field drifts westward (data from Bullard et al., 1950).

★ present field at sampling site

○ geocentric axial dipole direction

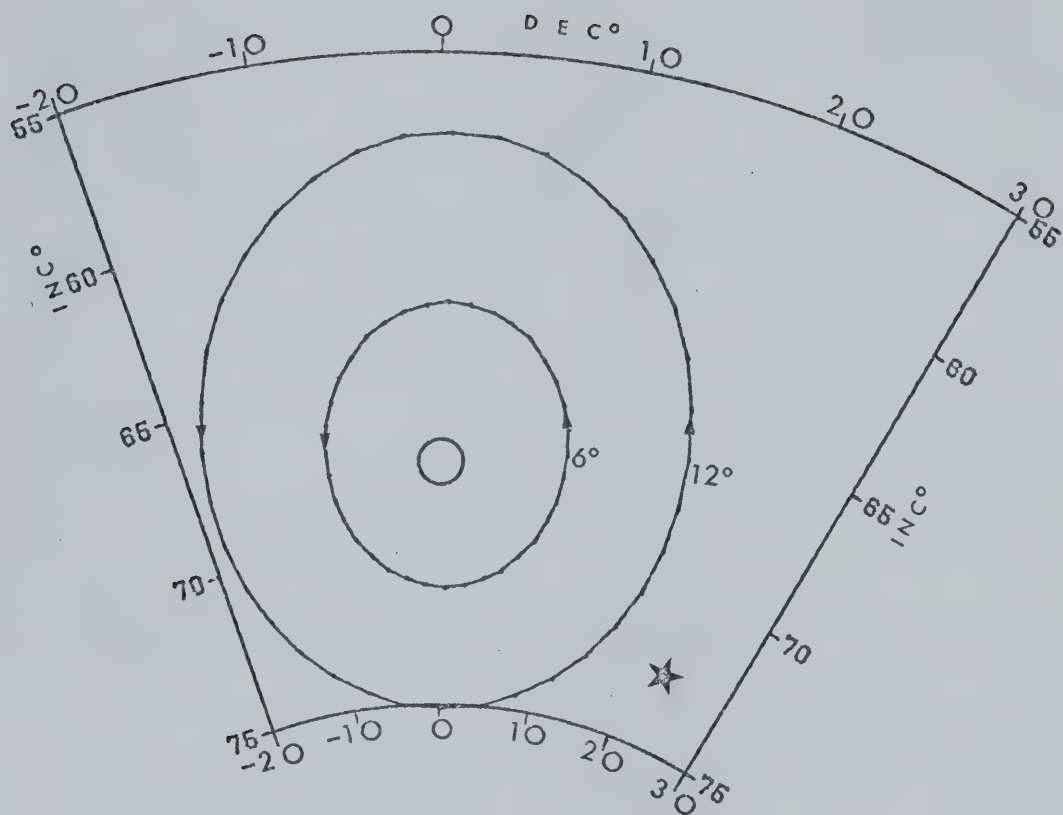


Fig. 4.13 Secular variations pattern when the dipole is allowed to precess counterclockwise around the spin axis at distances of 6° and 12° .

★ present field at sampling site

○ geocentric axial dipole direction

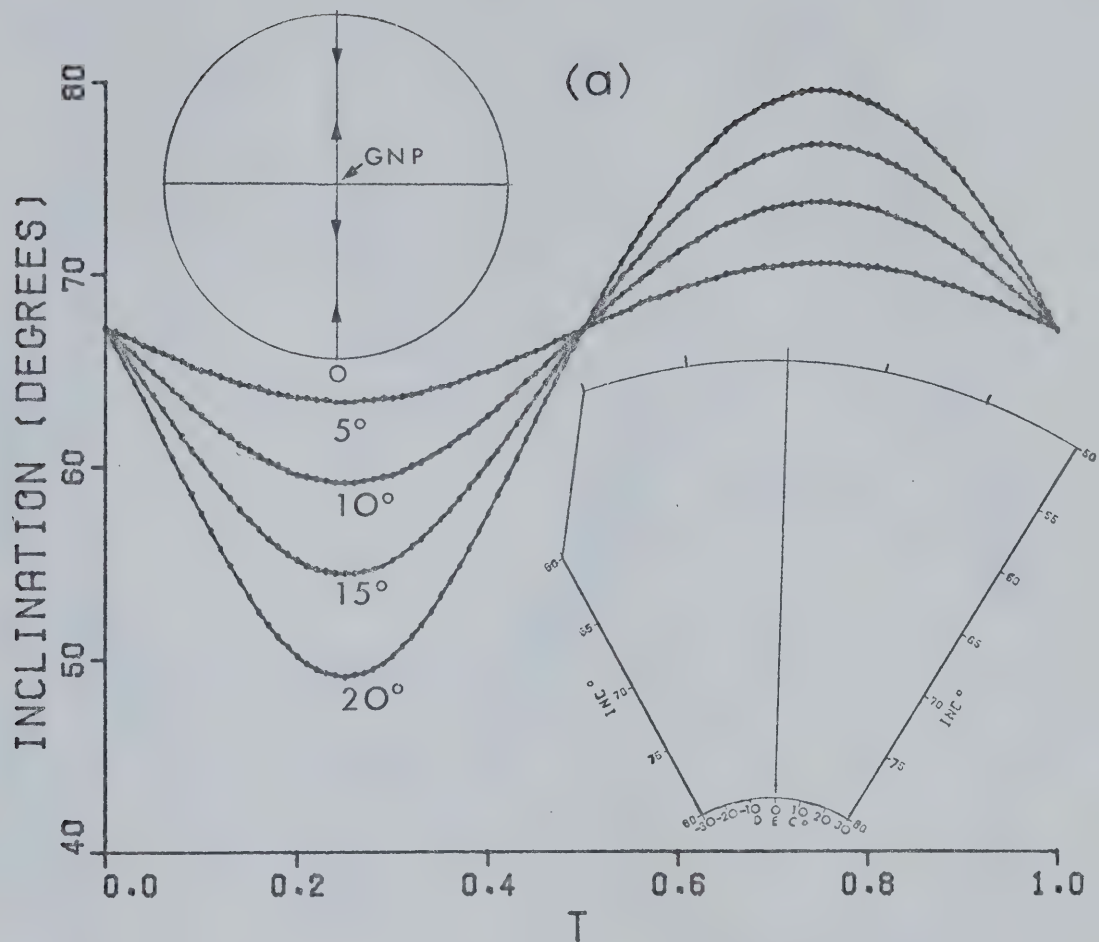
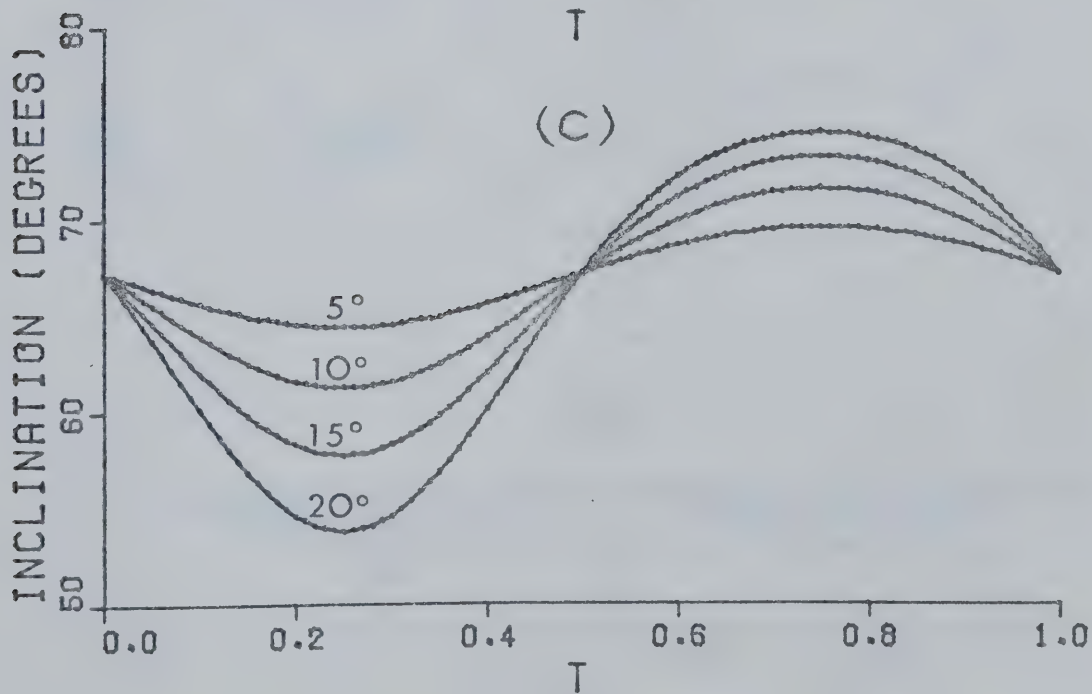
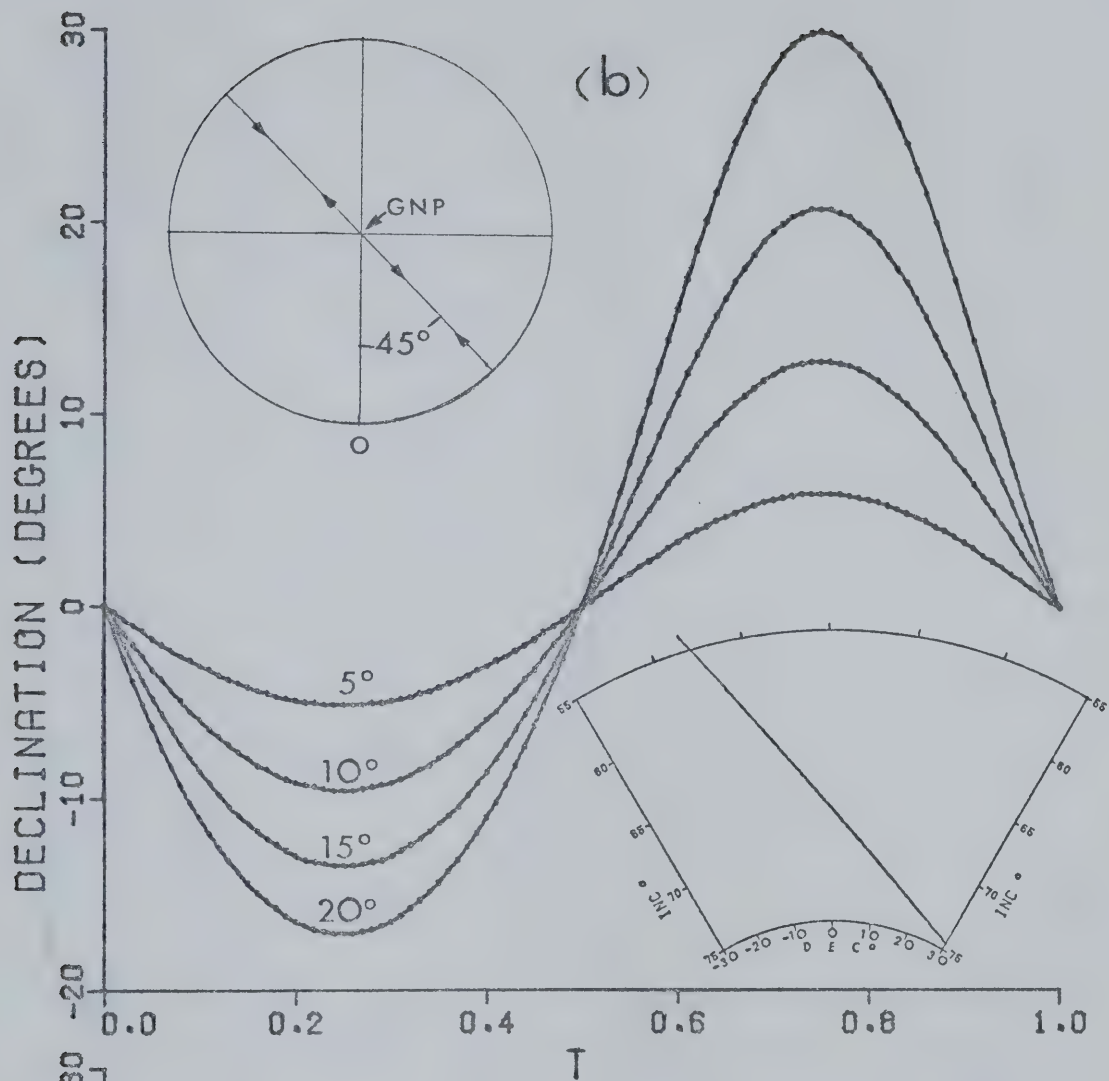
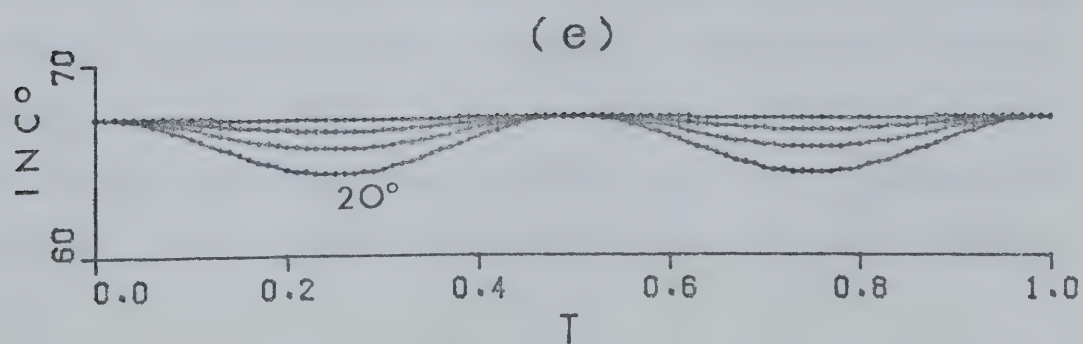
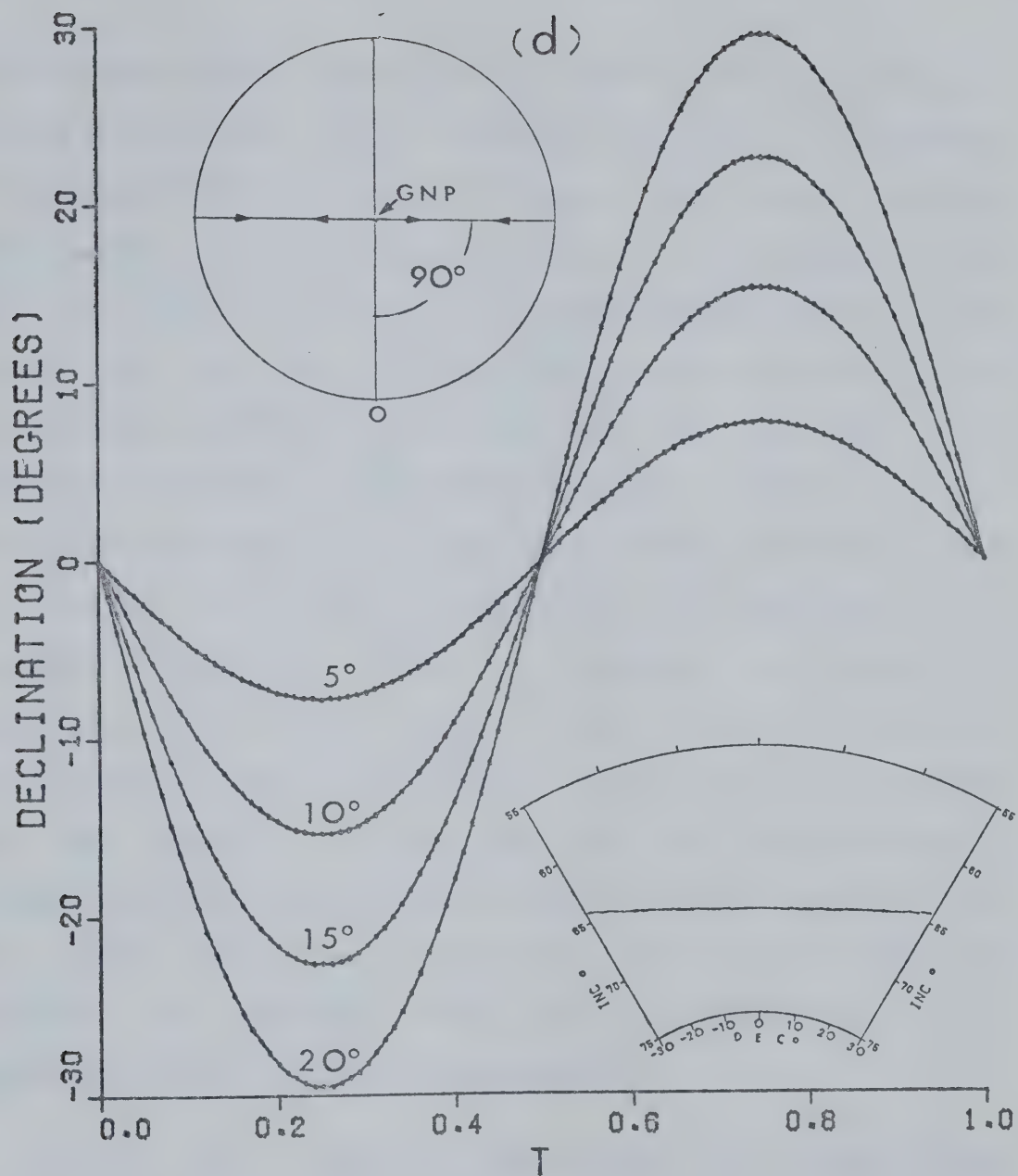


Fig. 4.14 (a) Temporal variations of inclination when the pole is allowed to 'nod' back and forth along the meridian of the observer (declination will always be zero). (Numbers denote maximum displacement from the spin axis in degrees)

(b),(c) Temporal variations of declination and inclination when the pole is allowed to 'nod' back and forth along a meridian at 45° to the meridian of the observer.

(d),(e) Temporal variations of declination and inclination when the pole is allowed to 'nod' back and forth along a meridian at 90° to the meridian of the observer.





features but none of them fit the observed secular variation pattern at all well. We are therefore compelled to consider more sophisticated models. A variety of such models has been investigated and an example of these is illustrated in Fig. 4.15. This model involves dipole oscillations (period 8,250 years; see Fig. 1.3), dipole nodding along the meridian of the observer (at 50°N) with amplitude 10° (period 5,500 years) and non-dipole oscillations (period 2,350 years). The non-dipole is assumed to be biased eastward (maximum +5,000 nT, minimum -1,000 nT). Such a bias is reminiscent of a 'standing' non-dipole field as suggested by Yukutake & Tachinaka (1969) (Fig. 4.16). In this context it is worth noting that the present non-dipole field at the sampling site also points eastwards (see Fig. 1.1). The similarity between the observed smoothed secular variation pattern and the model above is satisfactory for the preliminary purposes, and indicates that minor modifications could reproduce the observations very closely.

Finally it is perhaps worth noting that Weyes (1978) has recently proposed that the spin axis 'nods' with a period of 5,600 years. He bases his conclusion on analysis of ancient shorelines and proposes a link with glacial periods; the geographic pole movement amounts to only a degree or so. Although the connection with our geomagnetic period at 5,000-6,000 years is obscure, the similarity of

Fig. 4.15 Azimuthal equidistant plot of secular variations pattern obtained from a model whereby the observer is situated at latitude 50°N and

(i) the dipole oscillates with a period $T_{\text{DO}} = 8,250$ years.

(ii) the dipole nods along the meridian of the observer with a period $T_{\text{DN}} = 5,500$ years. The nodding is assumed to be a simple harmonic motion centred at the rotation axis and amplitude of 10° . The displacement from the rotation axis along the given meridian is given by :

$$X = 10 \sin(2\pi t / T_{\text{DN}})^{\circ}$$

Thus the dipole intensity is given by :

$$F_{\text{D}} = (M/R^3)(1 + 3\cos^2 p)^{1/2} T.$$

where M (dipole moment) = $(8 + 4\cos^2 p / T_{\text{DO}}) \times 10^{22} \text{ A.m}^2$

R (Earth's radius) = $6.356 \times 10^6 \text{ m}$.

p paleomagnetic colatitude

t time (years)

(iii) the non-dipole is biased eastwards and oscillates with a period $T_{\text{NDO}} = 2,350$ years. The non-dipole intensity is given by :

$$F_{\text{ND}} = 3,000 \sin(2\pi t / T_{\text{NDO}}) + 2,000 \text{ nT}.$$

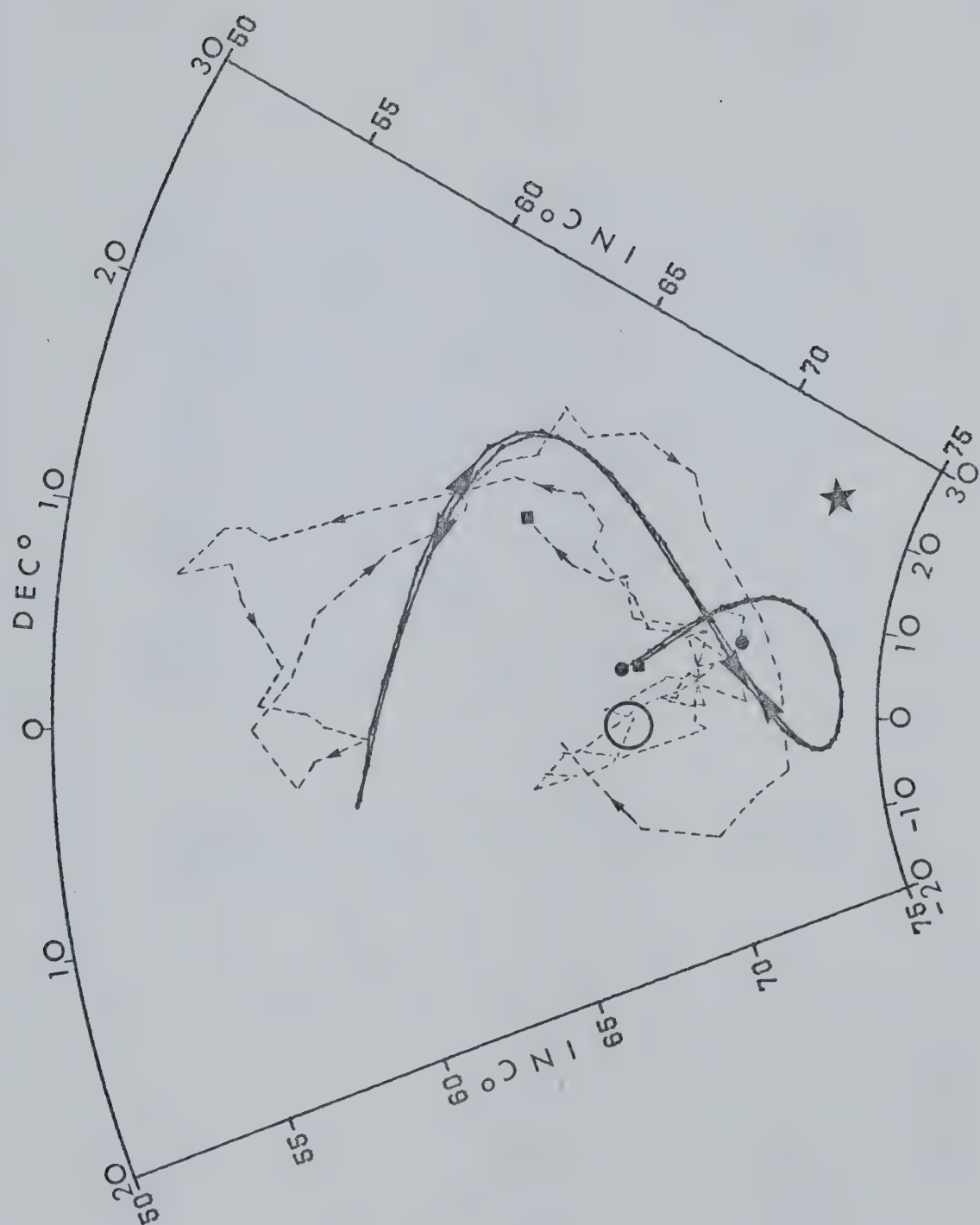
Dashed lines represent the observed secular variations pattern (smoothed by five-point moving average) (see Fig. 4.7c) .

● oldest horizon

■ youngest horizon

★ present field at sampling site

○ geocentric axial dipole direction



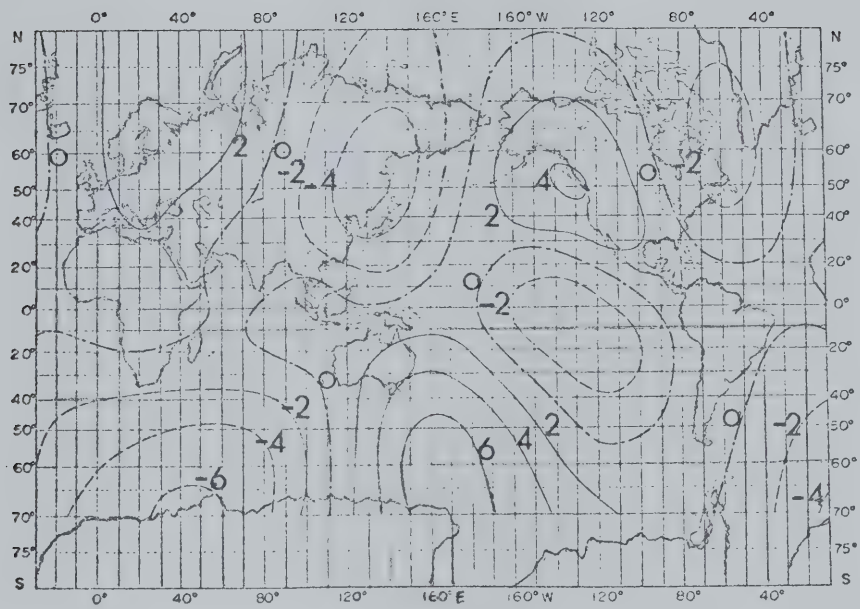


Fig. 4.16 Standing part of the non-dipole east component, contour interval 2,000 nT (after Yukutake & Tachinaka, 1969).

periods is rather intriguing.

CHAPTER 5

Summary and Conclusions

Nagata et al. (1943, 1945, 1949) studied the magnetization of the upper 7 metres of the Narita bed which consists chiefly of fine sands spanning from 70,000-42,000 yrs.B.P. Yukutake (1962) smoothed the declination and inclination variations observed. Skiles (1970) observed that the smoothed data clearly define three clockwise loops with periods of 1,800 years, but the dating information is rather uncertain. Following a comprehensive discussion, Skiles concludes that this implies a westward drift of the perturbing magnetic sources; he thus infers that westward drift of the non-dipole field was in existence some 50,000 years ago.

Opdyke et al. (1972) studied the paleomagnetism of two Aegean deep-sea cores together spanning from 27,000-0 yrs.B.P. The cores have average magnetic inclinations of $55^{\circ} \pm 14^{\circ}$ s.d. and $46^{\circ} \pm 13^{\circ}$ s.d. which are similar to the inclination of the geocentric axial dipole model at the sampling locality ($I=+55^{\circ}$). No declination information is available, but the inclination variations reveal the presence of a 6,000 year periodicity. They interpret this

pattern in terms of 'dipole wobble' in which the axis of the geomagnetic dipole precesses uniformly around the spin axis along a counterclockwise circular path of radius 12° .

Mackereth (1971) describes long-period declination oscillations in cores taken from post-glacial organic sediments deposited at the bottom of Lake Windermere, England. Subsequent analysis by Creer et al. (1972) indicates that the corresponding inclination variations were of irregular period and amplitude. Thompson (1975) after extending these studies to other UK and Swedish lakes argued that the main characteristics of declination and inclination variations of Lake Windermere are recognizable elsewhere in north-western Europe throughout the Holocene. It thus appears that paleomagnetic studies of Late Quaternary lacustrine sediments may have some potential for application to regional geological correlation, as well as providing essential data for geomagnetic studies.

Creer (1974) obtained a paleomagnetic record from a core at station 1474 during the Black Sea cruise of AtlantisII of the Woods Hole Oceanographic Institution. Five radiocarbon ages were determined from samples taken at intervals along the 11 metre long core, which spans from 25,000-7,000 yrs.B.P. The magnetic record exhibits inclination variations with clearly defined maxima and

minima, and a period of about 2,800 years. Similar inclination oscillations were measured in a section of sediments from the Upper Dry Cave at Jeita, Lebanon spanning approximately 16,000-0 yrs.B.P. Creer & Kopper (1976) have correlated these records for the overlapping time interval. Thus the inclination oscillation appears to have continued from 25,000-0 yrs.B.P. The Jeita declination record yields evidence of a 1,700 year periodicity. The geomagnetic record from sediments of Lake Michigan (core stations 895 and 937) and Lake Eire (core station 13194) (Creer et al., 1976) are superficially similar to those obtained at Lake Windermere with distinct declination oscillations, but there are no strong periodicities in inclination. However at Lake Michigan, the declination is observed to have oscillated back to 11,500 yrs.B.P. with a period of about 2,000 years which is somewhat less than the 2,700 year period observed at Lake Windermere.

It thus appears that regular declination oscillations are present at some sites whilst at other sites inclination oscillations are more prominent. In both cases periods of a few thousands years are characteristic. The absence of a steady inclination period related to the declination period will mean that the declination oscillations cannot be accounted for simply by supposing that the geomagnetic axis precessed about the spin axis. Furthermore, when the path of

the time sequence of paleomagnetic field vectors is plotted on the 'D-I' plane, both clockwise and counterclockwise loops are observed (Creer et al., 1972). Thus the observed variation may originate from westward and sometimes from eastward drifting sources (Skiles, 1970). A model whereby the geomagnetic sources drift either westward or eastward around the geographic axis would produce similar secular variation patterns for sites occupying approximately the same latitude, with a time lag due to the longitudinal difference. The observations, however, indicate periods which remain constant over many oscillations at a given site, and different dominant periods at different sites. Thus Creer (1977) favours a model in which the non-dipole field originates from stationary oscillating or pulsating sources situated in the outer core. The corresponding perturbing fields therefore have a regional rather than a global influence.

The present work is a follow up detailed study of the reconnaissance investigation by Oberg (1978). A 7 metres thick section spanning some 9,000 years which is part of a much thicker sequences laid down during the Olympia Interglaciation (43,000-20,000 yrs.B.P.) was sampled at 7 cm intervals. Magnetic measurements reveal the presence of a small viscous remanent magnetization which is removed by AF demagnetization in 10 mT, leaving a stable remanent

magnetization. IRM curves and thermal demagnetization indicate that the magnetic carrier is titanomagnetite, and this suggests that the paleomagnetic directions represent a DRM rather than a later CRM which would normally be expected to reside in hematite. The overall mean direction for the entire sequence is $D=005.7^\circ$, $I=+65.4^\circ$ ($N=94$, $R=93.3099$, $k=135$, $\alpha_{95}=1.3^\circ$), which is significantly different from the geomagnetic field vector at the sampling site ($D=022.3^\circ$, $I=+72.6^\circ$). The mean of the virtual geomagnetic poles lies at $0.0^\circ E$ and $85.6^\circ N$ ($N=94$, $R=92.7032$, $K=72$, $A_{95}=1.7^\circ$) being both 'right-handed' and 'far-sided', and is statistically distinct from the spin axis of the Earth. The application of the small quadrupole correction suggested by Merrill & McElhinny (1977) moves the pole in such a way that it is no longer 'far-sided', but it is still right-handed. This conflicts with Merrill & McElhinny (1977) who suggest a left-handed (negative ΔD) anomaly at the sampling locality.

The Beran-Watson test indicates that the serial correlation of the geomagnetic vectors is much greater than 99%, and this implies that the oscillations observed are real temporal variations of the paleofield. Periods of a few thousand years are observed; but no periods of around 500 years (as would be expected from historical records) are present even though the sampling density has a Nyquist cut-off of approximately 200 years. The absence of these high

frequency signals in the geomagnetic record is probably due to the deposition and dewatering involved in the natural recording process which somehow acts as a high-cut filter and suppresses such signals.

The secular variation pattern agrees very well with Cox's (1975) model of biased drifting fields, but the bias is strongly eastward as well as towards lower inclinations. This is consistent with Wilson's 'right-handed' effect, but the origin of such a global feature remains obscure.

BIBLIOGRAPHY

- Allbridge, L.D. & Hurwitz, L. (1964) Radial dipoles as sources of the Earth's main magnetic field. *J. Geophys. Res.* 69, p2631-2640
- Andersen, N. (1974) On the calculation of filter coefficients for maximum entropy spectral analysis. *Geophys.*, 39, p69-72
- Barbetti, M. & McElhinny, M. (1972) Evidence of geomagnetic excursion 30,000yr.B.P. *Nature*, 239, p327-330
- Beran, R.J. & Watson, G.S. (1967) Testing a sequence of unit vectors for serial correlation. *J. geophys. Res.*, 72, p5655-5659
- Blow, R.A. & Hamilton, N. (1978) Effect of compaction on the the acquisition of a detrital remanent magnetization in fine-grained sediments. *Geophys. J. R. astro. Soc.* 52 p13-23
- Briden, J.C. (1972) A stability index of remanent magnetism *J. Geophys. Res.* Vol 77. No.8, p1401-1405
- Bullard, E.C. (1949) The magnetic field within the Earth. *Proc. Roy. Soc. London*, A197, p433-453
- Bullard, E.C., Freedman, C., Gellman, H. & Nixon, J. (1950) The westward drift of the Earth's magnetic field. *Phil. Trans. Roy. Soc. (London)*, A, 243, p67-92
- Burg, J.P. (1967) Maximum entropy spectral analysis, paper presented at the 37th Annual Meeting, Soc. explor. Geophys., Oklahoma City, October 31
- Cox, A. (1968) Length of geomagnetic polarity intervals. *J. geophys. Res.* v.73, p3247-3260
- Cox, A. (1975) The frequency of geomagnetic reversals and the symmetry of the non-dipole field. *Reviews of Geophysics and Space Physics* Vol15 No.3, p35-51
- Creer, K.M., Thompson, R., Molyneux, L. & Mackereth, F.J.H. (1972) Variation recorded in the stable magnetic remanence of recent sediments. *Earth Planet. Sci. Lett.* 14, p115-127
- Creer, K.M. (1974) Geomagnetic variations for the interval 7,000-25,000 yr.B.P. as recorded in a core of sediments from station 1474 of the Black Sea cruise of 'AtlantisII'. *Earth planet. Sci. Lett.*, 23, p34-42

- Creer, K.M. & Kopper, J.S. (1976) Secular oscillations of the geomagnetic field recorded by sediments deposited in the Mediterranean region. *Geophys. J. R. astr. Soc.*, 45, p35-58
- Creer, K.M. Gross, D.L. & Lineback, J.A. (1976) Origin of regional geomagnetic variations, recorded by Wisconsinan and Holocene sediments from Lake Michigan U.S.A., and Lake Windermere, England. *Geol. Soc. Am. Bull.*, 87, p531-540
- Creer, K.M. (1977) Geomagnetic secular variation during the last 25,000 years: an interpretation of data obtained from rapidly deposited sediments. *Geophys. J. R. astr. Soc.*, 48, p91-109
- Denham, C.R. (1974) Counter-clockwise motion of paleomagnetic directions 24,000 years ago at Mono Lake, California. *J. Geomagn. Geoelect.* 26, p487
- Denham, C.R. (1975) Spectral analysis of paleomagnetic time series. *J. geophys. Res.* 80, p1897-1901
- Elasser, W.M. (1946) Induction effects in terrestrial magnetism: Part I. Theory. *Phys. Rev.*, 69, p106-116
- Fisher, R.A. (1953) Dispersion on a sphere. *Proc. Roy. Soc. London*, A217, p295-305
- Griffiths, D.H., King, R.F., Rees, A.I. & Wright, A.E. (1960) The remanent magnetization of some recent varved sediments. *Proc. Roy. Soc. London* A256, p359-383
- Gubbins, D. (1974) Theories of the geomagnetic and solar dynamos. *Rev. Geophys. Space Phys.* 12, p137-154
- Harrison, C.G.A. & Ramirez, E. (1975) Areal coverage of spurious reversals of the Earth's magnetic field. *J. Geomagn. Geoelec.* 27, p139
- Irving, E. and Major, A. (1964) Post-depositional detrital remanent magnetization in a synthetic sediment. *Sedimentology*, 3, p135-143
- Irving, E. (1957) The origin of the paleomagnetism of the Torridonian sandstone series of Northwest Scotland. *Phil. Trans. Roy. Soc. London* A250 p100-110
- Irving, E. (1967) Evidence for paleomagnetic inclination error in sediment. *Nature*, 213, p483-484
- Jacobs, J.A. (1975) The Earth's core. Academic Press (London)

Johnson, E.A., Murphy, T. & Torrenson, O.W. (1948) Prehistory of the Earth's magnetic field. *Terr. Magn. Atmos. Elec.* 53 349-372

King, R.F. (1955) The remanent magnetism of artificially deposited sediments. *Mon. Not. Roy. Astr. Soc. Geophys. Supp.*, 7, p115-134

Liddicoat, J.C. & Coe, R.A. (1975) Mono Lake 24,000 yrs.B.P. geomagnetic excursions: additional data. *EOS Trans. Am. geophys. Un.*, 56, p978

Lowes, F.J. (1955) Secular variation and the non-dipole field. *Ann. Geophys.*, 11, p91-94

Lowrie, W. & Alvarez, W. (1977) Late Cretaceous geomagnetic polarity sequences: detailed rocks and paleomagnetic studies of the Scaglia Rossa limestone at Gubbio, Italy. *Geophys. J. R. astr. Soc.*, 51, p561-582

Mackereth, F.H. (1971) On the variation in directions of the horizontal component of the remanent magnetization in lake sediments. *Earth planet. Sci. Lett.*, 12, p332-338

McElhinny, M.W. (1973) *Paleomagnetism and plate tectonics.* Cambridge Univ. Press.

McElhinny, M.W. & Merrill, R.T. (1975) Geomagnetic secular variation over the past 5.m.y. *Reviews of Geophysics and Space Physics*, Vol13, No.5, p687-707

Merrill, R.T. & McElhinny, M.W. (1977) Anomalies in the time averaged paleomagnetic field and their implication for the lower mantle. *Reviews of Geophysics and Space Physics*, Vol.15, No.3, p309-323

Molyneux, L. (1971) A complete result magnetometer for measuring the remanent magnetization of rocks. *Geophys. J. R. astr. Soc.*, 24, p429-433

Murthy, G.S. (1969) *Paleomagnetic studies in the Canadian shield.* Ph.D. Thesis. University of Alberta

Nagata, T., Rikitake, T., & Akasi, K. (1943) The natural remanent magnetism of sedimentary rocks. *Bull Earthqu. Res. Inst. Tokyo*, 21, p276

Nagata, T., Harada, Y., & Hirao, K. (1945) Natural remanent magnetization of sedimentary rocks. *Bull. Earthqu. Res. Inst. Tokyo*, 23, p79

- Nagata, T., Hirao, K., & Yoshikama, H. (1949) Remanent magnetism in 'Pleistocene' deposits - Paleomagnetism in Japan. *J. Geomagn. Geoelec.*, Kyoto, 1, p52-58
- Needham, J. (1962) Science and civilization in China. Vol.4, Physics and Physical Technology, 1, Physics. Cambridge Univ. Press.
- Nelson, J.H., Hurwitz, L. & Knapp, D.G. (1962) Magnetism of the Earth. Publ. 40-1, U.S. Dept. Comn. Coast Geod. Surv., Washington
- Oberg, C.J. (1978) Quaternary paleomagnetic/geomagnetic studies in western Canada. M.Sc. Thesis. University of Alberta
- Opdyke, N.D. (1961) The paleomagnetism of the New Jersey Triassic: A field study of the inclination error in red sediments. *J. Geophys. Res.* 66, p1941-1949
- Opdyke, N.D., Ninkovich, D., Lowrie, W. & Hays, J.D. (1972) The paleomagnetism of two Aegean deep-sea cores. *Earth Planet. Sci. Lett.*, 14, p145-159
- Reid, A.B. (1972) A paleomagnetic study at 1,800 million years in Canada. Ph.D. Thesis. University of Alberta
- Roquet, J. (1954) Sur les remanences des oxydes de fer et leur interet en geomagnetisme. *Ann. Geophys.* 10, p226-247 & p282-325
- Runcorn, S.K. (1959) On the theory of the geomagnetic secular variation. *Ann. Geophys.*, 15, p87-92
- Schmidt, P.W. (1976) The non-uniqueness of the Australian Mesozoic paleomagnetic pole position. *Geophy. J. R. astro. Soc.* 52, p285-300
- Schimizu, Y. (1960) Magnetic viscosity of magnetite. *J. Geomag. Geoelect.*, Kyoto, 11, p125-138
- Skiles, D.D. (1970) A method of inferring the direction of drift of the geomagnetic field from paleomagnetic data. *Journal of Geomagnetism and Geoelectricity*, Vol.22 No.4, p441-462
- Smith, P.J. & Needham, J. (1967) Magnetic declination in Medieval China. *Nature*, 214, p1213-1214
- Symons, D.T.A. & Stupavsky, M. (1974) A rational paleomagnetic

stability index. J. Geophys. Res. Vol.79, No.11, p1718-1720

Thompson, R. (1975) Long period European geomagnetic secular variation confirmed. Geophys. J. R. astr. Soc., 432, p847-859

Ulrych, T.J. & Bishop, T.N. (1975) Maximum entropy spectral analysis and autoregressive decomposition. Reviews of Geophysics and Space Physics., 13, p183-200

Verosub, K.L. & Banerjee, S.K. (1977) Geomagnetic excursions and their paleomagnetic record. Reviews of Geophysics and Space Physics Vol.15 No.2, p145-155

Verosub, K.L. (1977) Depositional and postdepositional process in the magnetization of sediments. Reviews of Geophysics and Space Physics Vol.15 No.2, p129-143

Watson, G.S. & Irving, E. (1957) Statistical methods in rock magnetism. Mon. Not. Roy. Astr. Soc. Geophys. Supp., 7, p289-300

Westgate, J.A. & Fulton, R.J. (1975) Tephrostratigraphy of Olympia Interglacial sediments in south-central British Columbia, Canada. National Research Council Canada Vol.12, No.3, p489-502

Weyer, M.E. (1978) Pole movement and sea levels. Nature, Vol.273, p18-21

Wilson, R.L. (1970) Permanent aspects of the Earth's non-dipole magnetic field over Upper Tertiary Time. Geophys. J. R. astr. Soc., 19, p417-438

Wilson, R.L. (1971) Dipole offset - the time-averaged paleomagnetic field over the past 25 million years. Geophys. J. R. astr. Soc., 22, p491-504

Wilson, R.L. (1972) Paleomagnetic differences between normal and reversed field sources, and the problem of far-sided and right-handed pole position. Geophys. J. R. astr. Soc., 28, p295-304

Yukutake, T. (1962) The westward drift of the magnetic field of the Earth. Bull. Earthqu. Res. Inst. Tokyo, 40, 1

Yukutake, T. & Tachinaka, H. (1969) Separation of the Earth's magnetic field into the drifting and the standing parts. Bull. Earthqu. Res. Inst. Tokyo, 47, p65-97

Zijderveld, J. D. A. (1964) A.C. demagnetization in rocks: Analysis of results, in Methods in Paleomagnetism, edited by Collinson, D. W., Creer, K. M. & Runcorn, S. K., Elsevier New York, p254-286

Appendix 1

List of data used in Chapter 2

S	site
E	elevation (metres)
AF	alternating field demagnetization (mT)
D	declination (degrees)
I	inclination (degrees)
J	magnetic intensity ($\text{A.m}^2 / \text{kg}$)

S	E	AF	D	I	J	S	E	AF	D	I	J
HAA01	0.0	0.0	4.3	67.3	7.78E-05	HAE04	0.28	0.0	5.4	69.3	3.21E-05
HAA01	0.0	10.0	6.2	67.6	6.91E-05	HAE04	0.28	10.0	5.7	68.7	3.04E-05
HAA01	0.0	20.0	6.1	67.5	5.57E-05	HAE04	0.28	20.0	8.2	68.9	2.62E-05
HAA02	0.0	0.0	13.1	59.6	1.03E-04	HAF01	0.35	0.0	352.1	65.4	9.40E-06
HAA02	0.0	10.0	13.4	58.7	9.34E-05	HAF01	0.35	10.0	355.3	63.9	6.92E-06
HAA02	0.0	20.0	14.1	57.0	7.72E-05	HAF01	0.35	20.0	351.1	62.2	4.06E-06
HAA03	0.0	0.0	12.9	54.6	1.28E-04	HAF02	0.35	0.0	358.3	72.5	2.19E-05
HAA03	0.0	2.5	11.8	54.2	1.25E-04	HAF02	0.35	10.0	356.7	74.3	1.83E-05
HAA03	0.0	5.0	10.7	53.3	1.21E-04	HAF02	0.35	20.0	358.3	76.0	1.30E-05
HAA03	0.0	10.0	10.3	52.1	1.07E-04	HAF03	0.35	0.0	2.6	63.7	2.87E-05
HAA03	0.0	15.0	11.5	49.8	8.96E-05	HAF03	0.35	10.0	2.6	63.9	2.60E-05
HAA03	0.0	20.0	12.9	48.0	7.60E-05	HAF03	0.35	20.0	1.5	63.5	1.95E-05
HAA03	0.0	30.0	16.0	44.2	4.94E-05	HAF04	0.35	0.0	2.0	61.9	5.21E-06
HAA03	0.0	40.0	18.4	18.4	3.87E-05	HAF04	0.35	10.0	354.8	60.8	4.55E-06
HAA03	0.0	50.0	350.9	37.5	1.89E-05	HAF04	0.35	20.0	358.4	59.8	2.61E-06
HAA03	0.0	60.0	347.9	15.1	1.26E-05	HAG01	0.42	0.0	10.6	67.9	3.02E-05
HAA04	0.0	0.0	13.1	57.5	7.29E-05	HAG01	0.42	10.0	9.0	67.9	2.58E-05
HAA04	0.0	10.0	11.9	56.5	6.55E-05	HAG01	0.42	20.0	12.1	68.7	1.55E-05
HAA04	0.0	20.0	8.9	52.1	4.62E-05	HAG02	0.42	0.0	5.2	65.9	2.86E-05
HAB01	0.07	0.0	7.2	60.4	2.09E-04	HAG02	0.42	10.0	6.6	67.2	2.38E-05
HAB01	0.07	10.0	7.9	60.2	1.97E-04	HAG02	0.42	20.0	8.3	67.4	1.91E-05
HAB01	0.07	20.0	7.3	58.9	1.70E-04	HAG03	0.42	0.0	13.6	68.1	6.43E-05
HAB02	0.07	0.0	24.0	67.0	1.24E-04	HAG03	0.42	10.0	12.6	68.6	5.90E-05
HAB02	0.07	10.0	23.4	66.3	1.16E-04	HAG03	0.42	20.0	11.7	67.7	4.77E-05
HAB02	0.07	20.0	21.1	64.6	9.92E-05	HAG04	0.42	0.0	6.4	69.5	2.50E-05
HAB03	0.07	0.0	10.6	62.2	1.58E-04	HAG04	0.42	10.0	8.0	67.8	2.22E-05
HAB03	0.07	10.0	10.9	61.6	1.49E-04	HAG04	0.42	20.0	12.5	68.1	1.64E-05
HAB03	0.07	20.0	10.3	60.8	1.27E-04	HAH01	0.49	0.0	23.2	71.5	4.15E-04
HAB04	0.07	0.0	8.5	58.6	1.35E-04	HAH01	0.49	10.0	22.4	71.9	4.16E-04
HAB04	0.07	10.0	8.4	58.3	1.27E-04	HAH01	0.49	20.0	23.0	69.8	3.63E-04
HAB04	0.07	20.0	9.1	56.4	1.05E-04	HAH02	0.49	0.0	12.3	63.2	9.76E-05
HAC01	0.14	0.0	11.9	61.2	7.79E-05	HAH02	0.49	10.0	12.8	62.6	9.24E-05
HAC01	0.14	10.0	13.0	62.0	7.00E-05	HAH02	0.49	20.0	12.2	62.6	7.88E-05
HAC01	0.14	20.0	11.7	61.0	6.03E-05	HAH03	0.49	0.0	24.2	70.7	1.76E-04
HAC02	0.14	0.0	17.6	71.8	3.66E-05	HAH03	0.49	10.0	25.2	70.1	1.69E-04
HAC02	0.14	10.0	13.9	71.4	3.35E-05	HAH03	0.49	20.0	25.4	70.2	1.49E-04
HAC02	0.14	20.0	15.4	70.1	2.87E-05	HAH04	0.49	0.0	14.0	66.8	1.18E-04
HAC03	0.14	0.0	16.0	66.5	2.91E-05	HAH04	0.49	10.0	15.0	66.6	1.12E-04
HAC03	0.14	10.0	16.0	66.4	2.76E-05	HAH04	0.49	20.0	16.0	66.4	9.81E-05
HAC03	0.14	20.0	18.3	66.2	2.46E-05	HAJ01	0.56	0.0	359.9	64.4	8.86E-05
HAC04	0.14	0.0	20.5	65.0	3.08E-05	HAJ01	0.56	10.0	358.2	65.4	8.29E-05
HAC04	0.14	10.0	20.2	64.0	2.95E-05	HAJ01	0.56	20.0	1.2	65.3	7.01E-05
HAC04	0.14	20.0	20.4	63.4	2.58E-05	HAJ02	0.56	0.0	354.5	68.5	3.31E-05
HAD01	0.21	0.0	12.1	59.9	3.20E-05	HAJ02	0.56	10.0	356.3	67.6	2.91E-05
HAD01	0.21	10.0	13.3	59.0	2.97E-05	HAJ02	0.56	20.0	358.1	68.1	2.29E-05
HAD01	0.21	20.0	11.6	57.8	2.53E-05	HAJ03	0.56	0.0	19.4	68.2	4.26E-05
HAD02	0.21	0.0	17.8	66.6	5.90E-05	HAJ03	0.56	10.0	19.6	66.9	4.04E-05
HAD02	0.21	10.0	18.4	65.7	5.49E-05	HAJ03	0.56	20.0	20.0	68.6	3.40E-05
HAD02	0.21	20.0	18.1	64.6	4.59E-05	HAJ04	0.56	0.0	20.0	64.1	3.95E-05
HAD03	0.21	0.0	26.3	66.5	1.59E-05	HAJ04	0.56	10.0	20.1	63.9	3.69E-05
HAD03	0.21	10.0	27.3	65.0	1.36E-05	HAJ04	0.56	20.0	22.1	63.8	3.18E-05
HAD03	0.21	20.0	28.1	64.3	1.16E-05	HAK01	0.63	0.0	340.0	66.8	3.06E-05
HAD04	0.21	0.0	25.7	65.9	2.11E-05	HAK01	0.63	10.0	340.8	66.5	2.52E-05
HAD04	0.21	10.0	26.1	64.1	2.03E-05	HAK01	0.63	20.0	342.5	66.3	2.08E-05
HAD04	0.21	20.0	24.9	63.2	1.60E-05	HAK02	0.63	0.0	28.1	73.8	3.90E-05
HAEO1	0.28	0.0	4.1	70.4	2.62E-05	HAK02	0.63	10.0	25.5	73.8	3.62E-05
HAEO1	0.28	10.0	3.4	70.8	2.32E-05	HAK02	0.63	20.0	26.6	74.5	3.10E-05
HAEO1	0.28	20.0	4.6	70.8	1.88E-05	HAK03	0.63	0.0	14.7	69.7	1.88E-05
HAEO2	0.28	0.0	9.1	69.1	1.71E-05	HAK03	0.63	10.0	13.4	69.8	1.78E-05
HAEO2	0.28	10.0	9.2	70.0	1.43E-05	HAK03	0.63	20.0	17.7	67.7	1.40E-05
HAEO2	0.28	20.0	7.9	69.7	1.03E-05	HAK04	0.63	0.0	10.0	82.6	2.59E-05
HAEO3	0.28	0.0	13.7	62.4	2.25E-05	HAK04	0.63	10.0	18.8	81.0	2.32E-05
HAEO3	0.28	10.0	11.6	63.0	2.06E-05	HAK04	0.63	20.0	26.2	80.6	1.96E-05
HAEO3	0.28	20.0	13.6	62.9	1.79E-05	HAK01	0.75	0.0	3.4	74.5	1.78E-05

S	E	AF	D	I	J	S	E	AF	D	I	J
HAK01	0.75	10.0	1.9	73.3	1.16E-05	HAK04	1.07	0.0	2.3	61.5	3.46E-05
HAK01	0.75	20.0	10.7	71.5	6.47E-06	HAK04	1.07	10.0	3.1	61.4	2.93E-05
HAK02	0.75	0.0	9.8	72.0	1.59E-05	HAK04	1.07	20.0	5.1	64.3	2.21E-05
HAK02	0.75	2.5	349.7	75.8	1.79E-05	HAP01	1.14	0.0	10.7	61.2	5.05E-05
HAK02	0.75	5.0	7.1	71.5	1.56E-05	HAP01	1.14	10.0	9.5	61.6	4.05E-05
HAK02	0.75	10.0	4.3	72.6	1.19E-05	HAP01	1.14	20.0	10.7	59.6	3.00E-05
HAK02	0.75	15.0	4.4	70.6	8.28E-06	HAP02	1.14	0.0	1.1	68.6	4.38E-05
HAK02	0.75	20.0	3.8	74.1	6.64E-06	HAP02	1.14	10.0	0.1	67.3	3.94E-05
HAK02	0.75	30.0	357.5	71.3	4.28E-06	HAP02	1.14	20.0	3.0	68.3	3.12E-05
HAK02	0.75	40.0	3.6	71.4	2.85E-06	HAP03	1.14	0.0	340.1	61.6	5.66E-05
HAK02	0.75	50.0	22.8	72.1	1.91E-06	HAP03	1.14	10.0	339.2	61.5	5.11E-05
HAK02	0.75	60.0	23.2	78.0	1.34E-06	HAP03	1.14	20.0	340.5	60.6	4.10E-05
HAK02	0.75	80.0	325.2	58.7	4.39E-07	HAP04	1.14	0.0	2.5	69.5	7.90E-05
HAK02	0.75	100.0	74.3	85.4	5.02E-07	HAP04	1.14	10.0	4.2	70.9	7.19E-05
HAK02	0.75	140.0	19.1	69.5	4.30E-07	HAP04	1.14	20.0	4.8	70.9	5.83E-05
HAK02	0.75	180.0	40.7	55.2	4.22E-07	HQ01	1.21	0.0	359.9	66.8	8.90E-05
HAK03	0.75	0.0	352.4	75.7	8.87E-06	HQ01	1.21	10.0	2.5	67.0	7.49E-05
HAK03	0.75	10.0	347.1	78.1	5.15E-06	HQ01	1.21	20.0	6.4	64.6	5.32E-05
HAK03	0.75	20.0	1.4	77.4	2.73E-06	HQ02	1.21	0.0	347.6	68.3	1.29E-04
HAK04	0.75	0.0	350.8	60.6	7.91E-06	HQ02	1.21	10.0	348.3	67.7	1.16E-04
HAK04	0.75	10.0	354.4	64.1	6.11E-06	HQ02	1.21	20.0	348.7	67.2	8.43E-05
HAK04	0.75	20.0	356.5	55.5	3.31E-06	HQ03	1.21	0.0	355.1	67.6	7.23E-05
HAL01	0.93	0.0	345.9	63.3	1.68E-05	HQ03	1.21	10.0	354.3	67.8	6.49E-05
HAL01	0.93	10.0	344.2	62.7	1.18E-05	HQ03	1.21	20.0	354.7	67.1	4.99E-05
HAL01	0.93	20.0	347.8	60.8	7.13E-06	HQ04	1.21	0.0	349.8	68.6	9.62E-05
HAL02	0.93	0.0	354.6	66.9	1.39E-05	HQ04	1.21	10.0	349.1	68.3	8.57E-05
HAL02	0.93	10.0	354.2	67.0	9.46E-06	HQ04	1.21	20.0	349.5	68.5	6.69E-05
HAL02	0.93	20.0	352.8	68.7	5.59E-06	HAR01	1.28	0.0	357.8	61.5	1.74E-04
HAL03	0.93	0.0	1.5	65.6	1.42E-05	HAR01	1.28	10.0	359.7	59.8	1.64E-04
HAL03	0.93	10.0	2.9	64.7	1.05E-05	HAR01	1.28	20.0	358.6	59.5	1.38E-04
HAL03	0.93	20.0	2.5	62.7	8.20E-06	HAR02	1.28	0.0	344.1	55.4	2.07E-04
HAL04	0.93	0.0	330.9	67.4	7.90E-06	HAR02	1.28	10.0	343.9	54.8	1.95E-04
HAL04	0.93	10.0	337.9	68.5	6.83E-06	HAR02	1.28	20.0	344.9	54.8	1.58E-04
HAL04	0.93	20.0	333.5	73.6	4.91E-06	HAR03	1.28	0.0	357.5	60.8	1.61E-04
HAM01	1.00	0.0	4.4	67.9	1.47E-05	HAR03	1.28	10.0	356.1	59.7	1.45E-04
HAM01	1.00	10.0	8.1	68.3	1.17E-05	HAR03	1.28	20.0	355.7	58.9	1.09E-04
HAM01	1.00	20.0	3.6	66.4	9.23E-06	HAR04	1.28	0.0	357.7	62.9	7.30E-05
HAM02	1.00	0.0	8.3	60.2	1.01E-05	HAR04	1.28	10.0	356.6	62.3	6.79E-05
HAM02	1.00	10.0	5.9	57.8	7.18E-06	HAR04	1.28	20.0	357.4	61.5	5.65E-05
HAM02	1.00	20.0	7.9	59.3	4.20E-06	HAS01	1.35	0.0	2.1	64.9	4.16E-05
HAM03	1.00	0.0	11.5	73.8	7.46E-06	HAS01	1.35	10.0	2.3	64.6	3.72E-05
HAM03	1.00	10.0	11.6	71.7	7.28E-06	HAS01	1.35	20.0	2.2	63.8	3.03E-05
HAM03	1.00	20.0	2.8	70.6	5.56E-06	HAS02	1.35	0.0	353.4	63.1	3.74E-05
HAM04	1.00	0.0	334.6	71.4	4.50E-06	HAS02	1.35	10.0	353.5	62.4	3.36E-05
HAM04	1.00	10.0	323.5	72.5	4.70E-06	HAS02	1.35	20.0	354.9	61.5	2.69E-05
HAM04	1.00	20.0	339.4	73.4	4.02E-06	HAS03	1.35	0.0	356.3	67.9	6.90E-05
HAD01	1.07	0.0	11.3	65.3	4.75E-05	HAS03	1.35	10.0	356.2	67.8	6.35E-05
HAD01	1.07	10.0	11.1	64.1	4.11E-05	HAS03	1.35	20.0	356.1	67.4	5.14E-05
HAD01	1.07	20.0	11.1	63.6	3.18E-05	HAS04	1.35	0.0	4.7	69.0	8.91E-05
HAD02	1.07	0.0	353.5	73.7	1.26E-05	HAS04	1.35	10.0	4.4	68.7	8.24E-05
HAD02	1.07	10.0	356.0	73.6	1.16E-05	HAS04	1.35	20.0	4.9	68.1	6.92E-05
HAD02	1.07	20.0	4.0	74.7	7.27E-06	HAT01	1.42	0.0	352.6	59.1	2.24E-04
HAD03	1.07	0.0	9.2	74.0	3.56E-05	HAT01	1.42	10.0	352.7	58.1	2.01E-04
HAD03	1.07	2.5	9.0	72.8	3.41E-05	HAT01	1.42	20.0	352.8	56.6	1.57E-04
HAD03	1.07	5.0	9.4	72.4	3.37E-05	HAT02	1.42	0.0	347.2	59.7	6.54E-05
HAD03	1.07	10.0	11.3	72.8	3.14E-05	HAT02	1.42	10.0	346.9	59.6	5.90E-05
HAD03	1.07	15.0	13.5	72.9	2.76E-05	HAT02	1.42	20.0	345.7	59.2	4.59E-05
HAD03	1.07	20.0	17.9	73.1	2.42E-05	HAT03	1.42	0.0	354.5	67.6	9.23E-05
HAD03	1.07	30.0	18.1	73.6	1.59E-05	HAT03	1.42	10.0	354.0	67.1	8.37E-05
HAD03	1.07	40.0	15.2	72.4	9.22E-06	HAT03	1.42	20.0	355.9	66.8	6.76E-05
HAD03	1.07	50.0	11.2	69.1	4.54E-06	HAT04	1.42	0.0	2.0	70.4	1.36E-04
HAD03	1.07	60.0	11.1	76.4	1.89E-06	HAT04	1.42	10.0	2.7	69.7	1.21E-04
HAD03	1.07	80.0	321.4	27.4	9.25E-07	HAT04	1.42	20.0	2.1	68.5	9.62E-05
HAD03	1.07	100.0	249.6	36.1	1.02E-06	HAD01	1.49	0.0	346.9	77.2	1.18E-04

S	E	AF	D	I	J	S	E	AF	D	I	J
HAU01	1.49	10.0	346.7	76.3	9.75E-05	HAZ02	1.84	20.0	8.2	62.8	5.28E-05
HAU01	1.49	20.0	348.0	76.6	6.95E-05	HAZ03	1.84	0.0	5.9	67.4	6.14E-05
HAU02	1.49	0.0	11.1	77.2	1.71E-04	HAZ03	1.84	10.0	6.0	67.0	4.94E-05
HAU02	1.49	10.0	9.9	76.3	1.54E-04	HAZ03	1.84	20.0	7.7	66.2	4.08E-05
HAU02	1.49	20.0	9.6	76.4	1.23E-04	HAZ04	1.84	0.0	13.1	70.7	3.66E-05
HAU03	1.49	0.0	5.7	67.3	1.69E-04	HAZ04	1.84	10.0	14.7	68.3	2.84E-05
HAU03	1.49	10.0	5.4	67.3	1.45E-04	HAZ04	1.84	20.0	9.3	68.5	2.08E-05
HAU03	1.49	20.0	6.9	66.1	1.11E-04	HBA01	1.91	0.0	24.9	71.8	6.43E-05
HAU04	1.49	0.0	3.5	66.6	1.27E-04	HBA01	1.91	10.0	24.9	70.8	4.52E-05
HAU04	1.49	10.0	4.7	66.0	1.09E-04	HBA01	1.91	20.0	25.2	69.5	3.63E-05
HAU04	1.49	20.0	5.8	65.7	8.33E-05	HBA02	1.91	0.0	23.7	72.0	4.87E-05
HAV01	1.56	0.0	352.7	58.4	1.67E-04	HBA02	1.91	10.0	24.9	71.2	3.86E-05
HAV01	1.56	10.0	352.3	58.4	1.42E-04	HBA02	1.91	20.0	24.4	70.2	3.14E-05
HAV01	1.56	20.0	353.7	57.7	1.06E-04	HBA03	1.91	0.0	5.9	71.7	4.63E-05
HAV02	1.56	0.0	352.3	64.6	1.04E-04	HBA03	1.91	10.0	2.9	73.8	3.70E-05
HAV02	1.56	10.0	352.3	64.3	8.65E-05	HBA03	1.91	20.0	4.9	75.9	2.98E-05
HAV02	1.56	20.0	354.2	64.2	6.39E-05	HBA04	1.91	0.0	338.4	70.9	3.45E-05
HAV03	1.56	0.0	358.2	65.7	1.23E-04	HBA04	1.91	10.0	340.8	71.6	2.41E-05
HAV03	1.56	10.0	358.3	64.5	1.09E-04	HBA04	1.91	20.0	340.2	69.0	1.88E-05
HAV03	1.56	20.0	358.6	63.2	8.48E-05	HBB01	2.00	0.0	352.4	73.1	7.25E-05
HAV04	1.56	0.0	359.9	67.4	1.37E-04	HBB01	2.00	10.0	351.6	70.5	5.38E-05
HAV04	1.56	10.0	0.0	66.9	1.20E-04	HBB01	2.00	20.0	351.1	68.6	4.05E-05
HAV04	1.56	20.0	1.1	66.1	9.44E-05	HBB02	2.00	0.0	358.1	73.0	6.87E-05
HAW01	1.63	0.0	353.3	56.6	1.61E-04	HBB02	2.00	10.0	359.9	72.1	5.52E-05
HAW01	1.63	10.0	351.8	54.9	1.33E-04	HBB02	2.00	20.0	358.5	71.7	4.10E-05
HAW01	1.63	20.0	353.0	53.8	9.88E-05	HBB03	2.00	0.0	344.0	75.8	8.15E-05
HAW02	1.63	0.0	6.6	58.9	9.68E-05	HBB03	2.00	10.0	343.7	74.5	6.88E-05
HAW02	1.63	10.0	5.1	59.0	8.20E-05	HBB03	2.00	20.0	346.7	73.0	5.40E-05
HAW02	1.63	20.0	6.3	58.6	6.63E-05	HBB04	2.00	0.0	346.3	66.1	6.35E-05
HAW03	1.63	0.0	348.6	67.4	1.06E-04	HBB04	2.00	10.0	346.4	65.6	5.24E-05
HAW03	1.63	10.0	348.5	66.5	8.62E-05	HBB04	2.00	20.0	347.8	65.2	3.84E-05
HAW03	1.63	20.0	350.3	64.9	6.45E-05	HBC01	2.07	0.0	12.4	69.9	7.91E-05
HAW04	1.63	0.0	318.1	80.6	7.84E-05	HBC01	2.07	10.0	9.1	67.4	5.64E-05
HAW04	1.63	10.0	321.8	80.2	6.17E-05	HBC01	2.07	20.0	8.1	67.2	4.00E-05
HAW04	1.63	20.0	318.4	79.6	4.44E-05	HBC02	2.07	0.0	1.1	72.3	8.11E-05
HAX01	1.70	0.0	359.3	62.3	3.14E-04	HBC02	2.07	10.0	356.5	71.6	6.68E-05
HAX01	1.70	10.0	0.2	63.1	2.81E-04	HBC02	2.07	20.0	355.2	69.5	5.13E-05
HAX01	1.70	20.0	0.1	62.1	2.32E-04	HBC03	2.07	0.0	11.5	67.5	6.06E-05
HAX02	1.70	0.0	12.3	70.5	2.29E-04	HBC03	2.07	10.0	8.4	66.6	4.80E-05
HAX02	1.70	10.0	15.0	69.4	2.05E-04	HBC03	2.07	20.0	7.8	65.9	3.62E-05
HAX02	1.70	20.0	15.3	69.0	1.70E-04	HBC04	2.07	0.0	5.0	67.7	6.32E-05
HAX03	1.70	0.0	8.3	66.0	2.06E-04	HBC04	2.07	10.0	4.4	65.9	5.26E-05
HAX03	1.70	10.0	9.2	64.7	1.84E-04	HBC04	2.07	20.0	4.9	65.5	3.97E-05
HAX03	1.70	20.0	11.3	64.4	1.52E-04	HBD01	2.14	0.0	355.3	62.5	1.93E-04
HAX04	1.70	0.0	328.3	81.7	5.58E-05	HBD01	2.14	10.0	355.7	61.5	1.59E-04
HAX04	1.70	10.0	331.8	81.3	4.39E-05	HBD01	2.14	20.0	355.0	59.6	1.20E-04
HAX04	1.70	20.0	332.7	83.2	3.28E-05	HBD02	2.14	0.0	8.0	65.6	9.33E-05
HAY01	1.77	0.0	9.3	63.2	2.31E-04	HBD02	2.14	10.0	7.7	64.6	7.76E-05
HAY01	1.77	10.0	7.3	61.6	1.87E-04	HBD02	2.14	20.0	3.4	65.1	6.13E-05
HAY01	1.77	20.0	9.4	61.5	1.37E-04	HBD03	2.14	0.0	358.5	64.2	1.17E-04
HAY02	1.77	0.0	11.0	63.2	2.05E-04	HBD03	2.14	10.0	357.6	62.6	9.46E-05
HAY02	1.77	10.0	11.1	62.9	1.84E-04	HBD03	2.14	20.0	357.3	61.4	6.91E-05
HAY02	1.77	20.0	14.1	62.5	1.59E-04	HBD04	2.14	0.0	2.5	70.3	1.39E-04
HAY03	1.77	0.0	14.3	68.5	1.83E-04	HBD04	2.14	10.0	3.9	69.9	1.16E-04
HAY03	1.77	10.0	14.6	68.7	1.67E-04	HBD04	2.14	20.0	3.4	69.2	8.43E-05
HAY03	1.77	20.0	15.4	68.2	1.45E-04	HBE01	2.21	0.0	2.3	65.1	4.28E-04
HAY04	1.77	0.0	358.1	73.5	1.40E-04	HBE01	2.21	10.0	1.5	64.9	3.87E-04
HAY04	1.77	10.0	2.4	73.3	1.24E-04	HBE01	2.21	20.0	1.6	65.3	2.90E-04
HAY04	1.77	20.0	3.7	73.3	1.03E-04	HBE02	2.21	0.0	4.7	67.3	1.74E-04
HAZ01	1.84	0.0	354.1	69.7	1.54E-04	HBE02	2.21	10.0	2.9	67.1	1.65E-04
HAZ01	1.84	10.0	350.8	68.5	1.17E-04	HBE02	2.21	20.0	3.2	67.0	1.33E-04
HAZ01	1.84	20.0	350.3	66.9	9.28E-05	HBE03	2.21	0.0	1.4	65.9	1.14E-04
HAZ02	1.84	0.0	7.8	65.1	8.54E-05	HBE03	2.21	10.0	0.4	66.4	1.09E-04
HAZ02	1.84	10.0	7.9	65.2	6.60E-05	HBE03	2.21	20.0	2.5	66.4	9.15E-05

S	E	AF	D	I	J	S	E	AF	D	I	J
HBE04	2.21	0.0	4.5	56.6	4.64E-05	HBI04	2.49	0.0	333.9	75.0	6.53E-05
HBE04	2.21	10.0	3.8	55.6	4.43E-05	HBI04	2.49	10.0	332.6	74.4	6.07E-05
HBE04	2.21	20.0	3.8	55.0	3.79E-05	HBI04	2.49	20.0	329.8	73.5	4.85E-05
HBFO1	2.28	0.0	347.3	57.4	2.02E-04	HBJO1	2.56	0.0	3.1	73.7	2.59E-05
HBFO1	2.28	10.0	345.0	56.7	1.82E-04	HBJO1	2.56	10.0	0.0	73.1	2.20E-05
HBFO1	2.28	20.0	341.2	56.1	1.34E-04	HBJO1	2.56	20.0	1.9	73.5	1.87E-05
HBFO2	2.28	0.0	345.0	63.8	1.56E-04	HBJO2	2.56	0.0	351.8	72.7	1.64E-05
HBFO2	2.28	2.5	344.9	63.2	1.55E-04	HBJO2	2.56	10.0	349.8	75.0	1.04E-05
HBFO2	2.28	5.0	344.6	63.7	1.51E-04	HBJO2	2.56	20.0	350.6	71.4	7.80E-06
HBFO2	2.28	10.0	342.4	63.4	1.36E-04	HBJO3	2.56	0.0	1.8	73.2	2.09E-05
HBFO2	2.28	15.0	344.4	63.2	1.18E-04	HBJO3	2.56	10.0	1.1	72.7	1.71E-05
HBFO2	2.28	20.0	342.9	62.8	1.01E-04	HBJO3	2.56	20.0	4.7	70.9	1.20E-05
HBFO2	2.28	30.0	339.1	65.0	6.29E-05	HBJO4	2.56	0.0	9.5	76.9	2.15E-05
HBFO2	2.28	40.0	333.8	61.8	3.25E-05	HBJO4	2.56	10.0	5.4	77.7	1.66E-05
HBFO2	2.28	50.0	314.4	51.5	1.63E-05	HBJO4	2.56	20.0	11.6	77.4	1.15E-05
HBFO2	2.28	60.0	261.3	51.4	6.62E-06	HBK01	2.63	0.0	11.2	65.1	3.01E-05
HBFO2	2.28	80.0	328.2	19.8	3.62E-05	HBK01	2.63	10.0	9.6	64.4	2.52E-05
HBFO3	2.28	0.0	357.4	70.0	1.64E-04	HBK01	2.63	20.0	10.9	63.2	1.89E-05
HBFO3	2.28	10.0	355.8	69.1	1.50E-04	HBK02	2.63	0.0	13.7	68.8	2.77E-05
HBFO3	2.28	20.0	356.4	68.9	1.12E-04	HBK02	2.63	10.0	14.4	69.3	2.34E-05
HBFO4	2.28	0.0	354.8	56.6	1.09E-04	HBK02	2.63	20.0	10.6	66.7	1.75E-05
HBFO4	2.28	10.0	354.6	56.5	9.63E-05	HBK03	2.63	0.0	348.1	68.3	1.56E-05
HBFO4	2.28	20.0	354.6	55.3	6.87E-05	HBK03	2.63	10.0	348.2	67.5	1.22E-05
HBG01	2.35	0.0	357.4	56.0	1.88E-04	HBK03	2.63	20.0	349.0	67.0	8.27E-06
HBG01	2.35	10.0	354.8	56.2	1.70E-04	HBK04	2.63	0.0	357.0	72.1	2.41E-05
HBG01	2.35	20.0	356.1	56.0	1.24E-04	HBK04	2.63	10.0	357.3	70.5	2.00E-05
HBG02	2.35	0.0	349.6	68.9	1.09E-04	HBK04	2.63	20.0	359.8	69.9	1.40E-05
HBG02	2.35	10.0	349.5	68.1	1.04E-04	HBL01	2.70	0.0	23.6	69.3	1.97E-05
HBG02	2.35	20.0	347.8	69.6	8.60E-05	HBL01	2.70	10.0	19.7	68.4	1.27E-05
HBG03	2.35	0.0	3.2	74.8	1.32E-04	HBL01	2.70	20.0	34.1	67.9	1.03E-05
HBG03	2.35	10.0	3.6	75.3	1.27E-04	HBL02	2.70	0.0	359.2	71.1	2.31E-05
HBG03	2.35	20.0	3.3	74.7	1.11E-04	HBL02	2.70	10.0	0.4	72.9	2.12E-05
HBG04	2.35	0.0	3.0	75.6	9.88E-05	HBL02	2.70	20.0	359.3	73.0	1.32E-05
HBG04	2.35	10.0	3.7	75.3	9.50E-05	HBL03	2.70	0.0	339.8	78.3	2.38E-05
HBG04	2.35	20.0	1.8	75.7	8.31E-05	HBL03	2.70	10.0	342.3	77.9	2.11E-05
HBN01	2.42	0.0	336.7	73.3	5.77E-05	HBL03	2.70	20.0	341.9	76.7	1.58E-05
HBN01	2.42	10.0	340.9	71.8	5.09E-05	HBL04	2.70	0.0	16.5	73.7	1.63E-05
HBN01	2.42	20.0	336.9	70.5	3.84E-05	HBL04	2.70	10.0	19.0	71.2	1.42E-05
HBN02	2.42	0.0	344.4	78.7	6.43E-05	HBL04	2.70	20.0	22.5	72.0	8.97E-06
HBN02	2.42	10.0	345.7	78.1	5.89E-05	HBN01	2.79	0.0	14.3	68.2	2.07E-05
HBN02	2.42	20.0	345.0	76.5	4.79E-05	HBN01	2.79	10.0	18.5	67.1	1.65E-05
HBN03	2.42	0.0	345.9	71.6	6.04E-05	HBN01	2.79	20.0	17.7	67.5	1.34E-05
HBN03	2.42	10.0	345.2	70.9	5.57E-05	HBN02	2.79	0.0	27.1	74.7	1.39E-05
HBN03	2.42	20.0	343.6	71.3	4.49E-05	HBN02	2.79	10.0	24.7	73.6	1.24E-05
HBN04	2.42	0.0	345.0	74.2	5.98E-05	HBN02	2.79	20.0	24.2	72.9	7.42E-06
HBN04	2.42	10.0	345.4	72.9	5.71E-05	HBN03	2.79	0.0	40.9	65.8	1.40E-05
HBN04	2.42	20.0	343.9	72.8	4.92E-05	HBN03	2.79	10.0	41.0	65.1	1.13E-05
HBI01	2.49	0.0	353.3	69.1	7.08E-05	HBN03	2.79	20.0	39.1	64.2	7.65E-06
HBI01	2.49	2.5	352.4	68.7	6.96E-05	HBN04	2.79	0.0	41.0	77.6	1.46E-05
HBI01	2.49	5.0	354.1	68.7	6.80E-05	HBN04	2.79	10.0	39.9	76.3	1.26E-05
HBI01	2.49	10.0	352.9	67.7	6.29E-05	HBN04	2.79	20.0	30.5	77.6	8.77E-06
HBI01	2.49	15.0	350.2	67.2	5.47E-05	HBN01	2.86	0.0	358.9	63.7	2.83E-05
HBI01	2.49	20.0	351.5	66.4	4.65E-05	HBN01	2.86	10.0	355.9	62.2	2.40E-05
HBI01	2.49	30.0	351.1	65.7	3.32E-05	HBN01	2.86	20.0	354.1	61.4	2.10E-05
HBI01	2.49	40.0	357.9	65.8	2.12E-05	HBN02	2.86	0.0	5.9	64.3	1.62E-05
HBI01	2.49	50.0	354.6	71.0	1.29E-05	HBN02	2.86	10.0	7.8	66.9	1.36E-05
HBI01	2.49	60.0	312.4	77.6	5.72E-06	HBN02	2.86	20.0	11.9	68.1	8.03E-06
HBI01	2.49	80.0	129.9	43.6	2.25E-06	HBN03	2.86	0.0	26.4	70.3	1.55E-05
HBI02	2.49	0.0	338.7	67.5	9.70E-05	HBN03	2.86	10.0	24.1	70.2	1.29E-05
HBI02	2.49	10.0	339.9	66.1	8.74E-05	HBN03	2.86	20.0	22.5	70.2	1.00E-05
HBI02	2.49	20.0	338.8	65.9	6.70E-05	HBN04	2.86	0.0	5.6	69.8	1.73E-05
HBI03	2.49	0.0	343.3	72.2	5.49E-05	HBN04	2.86	10.0	8.7	68.9	1.34E-05
HBI03	2.49	10.0	341.7	71.3	4.89E-05	HBN04	2.86	20.0	9.6	70.1	1.17E-05
HBI03	2.49	20.0	326.4	67.1	3.84E-05	HBO01	2.93	0.0	19.3	65.2	1.71E-05

S	E	AF	D	I	J
HB001	2.93	10.0	20.6	64.2	1.31E-05
HB001	2.93	20.0	15.0	66.2	7.50E-06
HB002	2.93	0.0	39.0	65.4	1.99E-05
HB002	2.93	10.0	40.2	64.5	1.51E-05
HB002	2.93	20.0	45.1	69.7	7.61E-06
HB003	2.93	0.0	35.1	60.0	1.61E-05
HB003	2.93	10.0	34.5	60.0	1.19E-05
HB003	2.93	20.0	37.2	62.1	6.38E-06
HB004	2.93	0.0	28.9	62.3	1.73E-05
HB004	2.93	10.0	28.7	64.0	1.38E-05
HB004	2.93	20.0	25.7	63.8	9.08E-06
HB001	3.00	0.0	17.2	70.4	2.09E-05
HB001	3.00	10.0	18.3	68.7	1.58E-05
HB001	3.00	20.0	18.9	67.9	1.01E-05
HB002	3.00	0.0	38.3	64.6	1.54E-05
HB002	3.00	10.0	37.5	63.3	1.21E-05
HB002	3.00	20.0	36.9	64.2	8.37E-06
HB003	3.00	0.0	8.7	61.0	1.64E-05
HB003	3.00	10.0	7.9	60.0	1.21E-05
HB003	3.00	20.0	4.0	61.6	8.15E-06
HB004	3.00	0.0	17.8	66.5	1.66E-05
HB004	3.00	10.0	15.5	65.6	1.31E-05
HB004	3.00	20.0	18.6	67.3	6.91E-06
HBQ01	3.07	0.0	15.2	67.4	1.88E-05
HBQ01	3.07	10.0	13.3	66.9	1.47E-05
HBQ01	3.07	20.0	11.2	68.2	8.92E-06
HBQ02	3.07	0.0	20.9	68.9	1.59E-05
HBQ02	3.07	10.0	21.5	69.8	1.18E-05
HBQ02	3.07	20.0	21.0	70.0	8.61E-06
HBQ03	3.07	0.0	21.9	57.2	1.48E-05
HBQ03	3.07	10.0	20.9	56.1	1.22E-05
HBQ03	3.07	20.0	21.4	56.0	7.64E-06
HBQ04	3.07	0.0	19.8	61.7	1.28E-05
HBQ04	3.07	10.0	19.6	61.5	9.82E-06
HBQ04	3.07	20.0	19.5	63.8	5.64E-06
HB001	3.14	0.0	18.2	70.6	2.04E-05
HB001	3.14	10.0	21.2	69.4	1.76E-05
HB001	3.14	20.0	21.3	71.5	1.15E-05
HB002	3.14	0.0	18.2	65.4	1.42E-05
HB002	3.14	10.0	14.7	65.2	1.08E-05
HB002	3.14	20.0	10.2	65.6	6.48E-06
HB003	3.14	0.0	26.6	63.8	1.53E-05
HB003	3.14	10.0	26.5	62.6	1.19E-05
HB003	3.14	20.0	27.4	62.8	8.02E-06
HB004	3.14	0.0	18.6	58.1	1.42E-05
HB004	3.14	10.0	19.0	57.1	1.07E-05
HB004	3.14	20.0	17.5	59.0	5.96E-06
HBS01	3.21	0.0	14.0	65.8	1.36E-05
HBS01	3.21	10.0	9.0	65.4	1.04E-05
HBS01	3.21	20.0	5.3	62.8	5.83E-06
HBS02	3.21	0.0	20.0	62.8	1.58E-05
HBS02	3.21	10.0	14.9	63.6	1.19E-05
HBS02	3.21	20.0	12.8	62.3	7.19E-06
HBS03	3.21	0.0	20.3	63.5	1.47E-05
HBS03	3.21	10.0	20.2	62.4	1.25E-05
HBS03	3.21	20.0	19.7	59.9	7.59E-06
HBS04	3.21	0.0	20.1	61.6	1.32E-05
HBS04	3.21	10.0	18.0	61.1	1.04E-05
HBS04	3.21	20.0	16.7	63.6	6.31E-06
HBT01	3.28	0.0	16.9	58.9	1.63E-05
HBT01	3.28	10.0	16.1	60.6	1.25E-05
HBT01	3.28	20.0	15.3	59.6	7.56E-06
HBT02	3.28	0.0	9.5	66.1	1.53E-05
HBT02	3.28	10.0	8.6	66.3	1.15E-05

S	E	AF	D	I	J
HBT02	3.28	20.0	10.9	67.3	6.96E-06
HBT03	3.28	0.0	17.0	63.4	1.78E-05
HBT03	3.28	10.0	15.9	61.3	1.04E-05
HBT03	3.28	20.0	13.3	61.1	6.17E-06
HBT04	3.28	0.0	6.2	58.9	2.04E-05
HBT04	3.28	2.5	12.5	57.0	1.91E-05
HBT04	3.28	5.0	14.6	57.3	1.88E-05
HBT04	3.28	10.0	15.1	58.4	1.53E-05
HBT04	3.28	15.0	13.1	58.8	1.14E-05
HBT04	3.28	20.0	10.0	57.4	8.90E-06
HBT04	3.28	30.0	12.7	58.3	5.14E-06
HBT04	3.28	40.0	15.4	54.6	2.53E-06
HBT04	3.28	50.0	11.5	62.5	1.80E-06
HBT04	3.28	60.0	12.6	53.6	9.47E-07
HBT04	3.28	80.0	306.7	44.4	5.99E-07
HBT04	3.28	100.0	92.2	74.2	2.43E-07
HBU01	3.35	0.0	10.9	59.1	2.04E-05
HBU01	3.35	10.0	9.2	58.3	1.41E-05
HBU01	3.35	20.0	7.6	59.0	9.00E-06
HBU02	3.35	0.0	22.3	57.8	1.76E-05
HBU02	3.35	10.0	20.4	58.3	1.31E-05
HBU02	3.35	20.0	16.1	57.8	6.38E-06
HBU03	3.35	0.0	8.8	57.4	1.57E-05
HBU03	3.35	10.0	8.4	59.6	1.09E-05
HBU03	3.35	20.0	11.0	60.4	6.70E-06
HBU04	3.35	0.0	22.9	62.5	1.38E-05
HBU04	3.35	10.0	20.2	62.2	1.02E-05
HBU04	3.35	20.0	21.2	62.8	6.62E-06
HBU01	3.42	0.0	7.1	61.7	1.68E-05
HBU01	3.42	10.0	3.2	61.5	9.77E-06
HBU01	3.42	20.0	1.3	57.7	6.70E-06
HBU02	3.42	0.0	22.4	67.5	1.75E-05
HBU02	3.42	10.0	19.5	68.2	1.23E-05
HBU02	3.42	20.0	20.2	60.9	7.14E-06
HBU03	3.42	0.0	11.9	53.6	1.61E-05
HBU03	3.42	10.0	10.3	52.7	1.25E-05
HBU03	3.42	20.0	13.9	55.3	6.84E-06
HBU04	3.42	0.0	9.6	57.2	1.49E-05
HBU04	3.42	10.0	8.2	57.3	1.25E-05
HBU04	3.42	20.0	7.9	60.8	6.92E-06
HBW01	3.49	0.0	9.4	65.2	1.60E-05
HBW01	3.49	10.0	8.5	63.2	1.04E-05
HBW01	3.49	20.0	8.6	63.5	7.82E-06
HBW02	3.49	0.0	18.5	65.8	1.24E-05
HBW02	3.49	10.0	17.7	63.2	9.26E-06
HBW02	3.49	20.0	23.3	65.2	6.57E-06
HBW03	3.49	0.0	16.4	66.8	1.55E-05
HBW03	3.49	10.0	13.4	65.0	1.06E-05
HBW03	3.49	20.0	19.4	68.7	6.71E-06
HBW04	3.49	0.0	9.8	67.8	1.17E-05
HBW04	3.49	10.0	9.0	66.3	9.26E-06
HBW04	3.49	20.0	8.7	66.5	6.90E-06
HBX01	3.56	0.0	17.7	61.3	1.67E-05
HBX01	3.56	10.0	16.6	60.2	1.10E-05
HBX01	3.56	20.0	18.7	62.1	6.87E-06
HBX02	3.56	0.0	11.0	61.8	1.45E-05
HBX02	3.56	10.0	9.1	62.1	1.04E-05
HBX02	3.56	20.0	6.9	64.3	4.92E-06
HBX03	3.56	0.0	359.9	54.2	1.73E-05
HBX03	3.56	10.0	359.4	54.3	1.16E-05
HBX03	3.56	20.0	359.6	57.9	6.74E-06
HBX04	3.56	0.0	1.6	60.4	9.98E-06
HBX04	3.56	10.0	3.5	57.9	7.19E-06
HBX04	3.56	20.0	4.0	58.3	4.65E-06

S	E	AF	D	I	J	S	E	AF	D	I	J
HBV01	3.63	0.0	354.5	56.5	1.65E-05	HCD02	3.98	10.0	349.9	54.2	7.40E-06
HBV01	3.63	10.0	356.1	55.3	1.15E-05	HCD02	3.98	20.0	349.6	52.8	4.54E-06
HBV01	3.63	20.0	354.5	56.6	7.12E-06	HCD03	3.98	0.0	339.5	76.5	2.49E-05
HBV02	3.63	0.0	6.4	48.9	1.20E-05	HCD03	3.98	10.0	311.4	72.9	1.24E-05
HBV02	3.63	10.0	6.7	46.1	8.50E-06	HCD03	3.98	20.0	319.7	65.1	7.21E-06
HBV02	3.63	20.0	6.0	46.5	3.83E-06	HCD04	3.98	0.0	6.1	50.0	9.16E-06
HBV03	3.63	0.0	15.3	61.3	1.30E-05	HCD04	3.98	10.0	6.7	43.4	6.31E-06
HBV03	3.63	10.0	15.1	59.0	9.14E-06	HCD04	3.98	20.0	5.3	42.5	3.36E-06
HBV03	3.63	20.0	13.0	58.5	5.76E-06	HCE01	4.05	0.0	8.3	49.3	9.37E-06
HBV04	3.63	0.0	10.3	59.5	1.62E-05	HCE01	4.05	10.0	5.9	45.4	5.57E-06
HBV04	3.63	10.0	8.2	59.1	1.28E-05	HCE01	4.05	20.0	8.9	41.9	2.36E-06
HBV04	3.63	20.0	5.9	58.2	9.16E-06	HCE02	4.05	0.0	6.2	56.2	8.70E-06
HBZ01	3.70	0.0	359.8	58.3	9.40E-06	HCE02	4.05	2.5	4.8	55.0	9.00E-06
HBZ01	3.70	10.0	352.8	53.5	6.47E-06	HCE02	4.05	5.0	5.1	55.0	8.23E-06
HBZ01	3.70	20.0	348.4	51.1	3.21E-06	HCE02	4.05	10.0	4.4	54.1	6.26E-06
HBZ02	3.70	0.0	1.7	52.9	8.80E-06	HCE02	4.05	15.0	7.6	52.4	4.63E-06
HBZ02	3.70	10.0	358.2	50.9	5.43E-06	HCE02	4.05	20.0	357.6	49.4	3.35E-06
HBZ02	3.70	20.0	354.4	32.6	3.55E-06	HCE02	4.05	30.0	358.2	47.3	1.70E-06
HBZ03	3.70	0.0	10.9	58.2	9.91E-06	HCE02	4.05	40.0	3.1	48.1	9.25E-07
HBZ03	3.70	10.0	5.7	56.7	6.39E-06	HCE02	4.05	50.0	22.0	40.8	3.97E-07
HBZ03	3.70	20.0	6.8	53.3	4.24E-06	HCE02	4.05	60.0	13.0	8.1	2.77E-07
HBZ04	3.70	0.0	355.2	41.4	1.05E-05	HCE03	4.05	0.0	356.9	51.7	8.06E-06
HBZ04	3.70	10.0	355.8	38.8	7.39E-06	HCE03	4.05	10.0	357.7	53.2	3.91E-06
HBZ04	3.70	20.0	357.0	36.0	4.14E-06	HCE03	4.05	20.0	357.6	52.2	3.37E-06
HCA01	3.77	0.0	353.6	60.2	1.11E-05	HCE04	4.05	0.0	1.3	61.1	3.39E-05
HCA01	3.77	10.0	351.7	57.3	7.47E-06	HCE04	4.05	10.0	3.5	57.2	2.04E-05
HCA01	3.77	20.0	350.4	55.5	3.83E-06	HCE04	4.05	20.0	3.8	56.5	1.07E-05
HCA02	3.77	0.0	351.7	50.7	1.58E-05	HCF01	4.12	0.0	355.1	62.1	4.36E-05
HCA02	3.77	10.0	350.7	48.3	1.14E-05	HCF01	4.12	10.0	352.9	57.9	2.84E-05
HCA02	3.77	20.0	351.6	51.8	4.79E-06	HCF01	4.12	20.0	353.1	59.4	1.45E-05
HCA03	3.77	0.0	343.3	73.3	1.44E-05	HCF02	4.12	0.0	7.9	76.5	2.95E-05
HCA03	3.77	10.0	344.0	72.5	1.00E-05	HCF02	4.12	10.0	21.8	73.9	1.74E-05
HCA03	3.77	20.0	346.4	72.0	6.11E-06	HCF02	4.12	20.0	18.7	72.5	1.18E-05
HCA04	3.77	0.0	359.4	51.1	9.04E-06	HCF03	4.12	0.0	352.1	63.7	3.18E-05
HCA04	3.77	10.0	356.7	48.3	6.00E-06	HCF03	4.12	10.0	353.6	60.5	1.96E-05
HCA04	3.77	20.0	354.9	49.4	2.94E-06	HCF03	4.12	20.0	0.8	57.1	1.05E-05
HCB01	3.84	0.0	348.9	63.8	1.19E-05	HCF04	4.12	0.0	347.5	72.7	3.37E-05
HCB01	3.84	10.0	345.0	63.4	7.61E-06	HCF04	4.12	10.0	348.4	69.1	1.97E-05
HCB01	3.84	20.0	341.6	62.8	3.84E-06	HCF04	4.12	20.0	352.8	68.5	1.17E-05
HCB02	3.84	0.0	357.8	61.4	1.17E-05	HCG01	4.19	0.0	0.4	54.6	6.24E-05
HCB02	3.84	10.0	351.8	63.2	6.62E-06	HCG01	4.19	10.0	359.4	51.7	4.41E-05
HCB02	3.84	20.0	347.9	63.7	4.58E-06	HCG01	4.19	20.0	0.1	53.2	2.23E-05
HCB03	3.84	0.0	10.4	68.7	9.64E-06	HCG02	4.19	0.0	354.8	54.5	4.49E-05
HCB03	3.84	10.0	5.9	64.9	7.48E-06	HCG02	4.19	10.0	354.2	52.6	3.18E-05
HCB03	3.84	20.0	328.1	76.2	2.64E-06	HCG02	4.19	20.0	353.0	52.6	1.92E-05
HCB04	3.84	0.0	3.0	47.2	8.52E-06	HCG03	4.19	0.0	359.9	45.8	3.96E-05
HCB04	3.84	10.0	0.5	43.1	7.34E-06	HCG03	4.19	10.0	359.7	46.1	2.78E-05
HCB04	3.84	20.0	359.6	41.0	4.01E-06	HCG03	4.19	20.0	359.0	45.8	1.67E-05
HCC01	3.91	0.0	16.2	61.1	1.01E-05	HCG04	4.19	0.0	9.9	61.3	3.47E-05
HCC01	3.91	10.0	15.9	58.9	5.99E-06	HCG04	4.19	10.0	9.8	58.8	2.45E-05
HCC01	3.91	20.0	15.9	59.7	3.02E-06	HCG04	4.19	20.0	10.2	58.7	1.44E-05
HCC02	3.91	0.0	351.5	61.9	7.86E-06	HCH01	4.26	0.0	12.1	66.3	1.37E-05
HCC02	3.91	10.0	345.5	60.4	4.17E-06	HCH01	4.26	10.0	9.7	63.7	8.64E-06
HCC02	3.91	20.0	346.1	58.9	2.58E-06	HCH01	4.26	20.0	14.2	61.6	5.17E-06
HCC03	3.91	0.0	341.8	74.9	2.24E-05	HCH02	4.26	0.0	0.4	55.1	1.85E-05
HCC03	3.91	10.0	328.3	76.7	1.31E-05	HCH02	4.26	10.0	358.2	51.6	1.05E-05
HCC03	3.91	20.0	317.1	73.3	6.72E-06	HCH02	4.26	20.0	1.9	53.1	6.57E-06
HCC04	3.91	0.0	15.0	48.0	6.08E-06	HCH03	4.26	0.0	4.4	56.1	1.52E-05
HCC04	3.91	10.0	14.5	39.9	4.96E-06	HCH03	4.26	10.0	4.4	57.9	8.96E-06
HCC04	3.91	20.0	11.9	39.4	2.65E-06	HCH03	4.26	20.0	5.5	57.1	5.77E-06
HCD01	3.98	0.0	16.5	63.6	1.09E-05	HCH04	4.26	0.0	11.2	54.3	1.85E-05
HCD01	3.98	10.0	10.6	64.9	7.77E-06	HCH04	4.26	10.0	12.1	53.5	1.29E-05
HCD01	3.98	20.0	20.5	66.4	3.21E-06	HCH04	4.26	20.0	13.2	54.4	7.04E-06
HCD02	3.98	0.0	354.7	60.7	8.59E-06	HCI01	4.33	0.0	4.6	56.6	1.35E-05

S	E	AF	D	I	J	S	E	AF	D	I	J
HCI01	4.33	10.0	4.5	54.0	9.13E-06	HCO02	4.68	20.0	22.8	63.8	4.47E-06
HCI01	4.33	20.0	4.9	51.7	6.08E-06	HCO03	4.68	0.0	2.4	56.3	8.59E-06
HCI02	4.33	0.0	344.1	47.3	1.20E-05	HCO03	4.68	10.0	1.6	58.1	5.25E-06
HCI02	4.33	10.0	341.2	42.8	1.18E-05	HCO03	4.68	20.0	7.2	55.1	3.79E-06
HCI02	4.33	20.0	339.1	42.0	3.62E-06	HCO04	4.68	0.0	6.9	59.2	8.66E-06
HCI03	4.33	0.0	2.7	60.0	1.29E-05	HCO04	4.68	10.0	4.3	57.2	5.29E-06
HCI03	4.33	10.0	2.5	56.2	9.05E-06	HCO04	4.68	20.0	0.3	55.1	3.24E-06
HCI03	4.33	20.0	2.7	56.0	6.41E-06	HCO01	4.75	0.0	16.1	59.5	1.03E-05
HCI04	4.33	0.0	7.7	61.4	1.60E-05	HCO01	4.75	10.0	9.8	61.3	6.58E-06
HCI04	4.33	10.0	9.4	58.6	1.16E-05	HCO01	4.75	20.0	13.3	59.7	4.20E-06
HCI04	4.33	20.0	10.8	57.7	5.80E-06	HCO02	4.75	0.0	15.5	62.1	9.30E-06
HCI01	4.40	0.0	10.8	51.0	1.82E-05	HCO02	4.75	10.0	19.2	64.3	6.30E-06
HCI01	4.40	10.0	8.3	48.9	1.40E-05	HCO02	4.75	20.0	16.9	64.9	5.71E-06
HCI01	4.40	20.0	9.4	48.2	7.64E-06	HCO03	4.75	0.0	11.6	57.4	6.25E-06
HCI02	4.40	0.0	3.0	64.7	1.58E-05	HCO03	4.75	10.0	15.0	51.4	3.94E-06
HCI02	4.40	10.0	8.3	62.6	1.15E-05	HCO03	4.75	20.0	7.5	66.2	2.48E-06
HCI02	4.40	20.0	8.2	62.6	7.04E-06	HCO04	4.75	0.0	11.0	59.8	9.60E-06
HCI03	4.40	0.0	16.8	57.6	1.41E-05	HCO04	4.75	2.5	6.5	58.6	7.84E-06
HCI03	4.40	10.0	20.9	52.5	1.14E-05	HCO04	4.75	5.0	10.7	61.5	6.45E-06
HCI03	4.40	20.0	19.1	54.3	6.44E-06	HCO04	4.75	10.0	15.1	60.6	4.80E-06
HCI04	4.40	0.0	12.8	61.0	1.51E-05	HCO04	4.75	15.0	14.3	62.8	3.80E-06
HCI04	4.40	10.0	13.1	56.9	1.07E-05	HCO04	4.75	20.0	9.5	62.8	3.70E-06
HCI04	4.40	20.0	12.9	56.7	5.73E-06	HCO04	4.75	30.0	16.2	58.7	1.94E-06
HCK01	4.47	0.0	18.6	56.2	1.97E-05	HCO04	4.75	40.0	25.5	61.4	2.17E-06
HCK01	4.47	10.0	15.0	54.6	1.50E-05	HCO04	4.75	50.0	330.8	79.7	1.94E-06
HCK01	4.47	20.0	16.5	53.8	7.98E-06	HCO04	4.75	60.0	116.3	61.4	8.78E-07
HCK02	4.47	0.0	30.8	63.2	1.96E-05	HCP01	4.82	0.0	6.7	66.0	4.50E-06
HCK02	4.47	10.0	25.5	65.8	1.20E-05	HCP01	4.82	10.0	13.4	57.2	3.33E-06
HCK02	4.47	20.0	32.3	62.0	5.74E-06	HCP01	4.82	20.0	27.7	62.5	1.99E-06
HCK03	4.47	0.0	14.0	60.8	1.63E-05	HCP02	4.82	0.0	17.0	64.5	5.73E-06
HCK03	4.47	10.0	15.3	58.4	1.38E-05	HCP02	4.82	10.0	17.6	64.8	2.74E-06
HCK03	4.47	20.0	16.4	56.6	6.99E-06	HCP02	4.82	20.0	16.7	59.6	1.97E-06
HCK04	4.47	0.0	14.3	56.7	1.99E-05	HCP03	4.82	0.0	23.8	67.0	2.55E-05
HCK04	4.47	10.0	13.4	55.3	1.51E-05	HCP03	4.82	10.0	23.6	66.3	2.34E-05
HCK04	4.47	20.0	13.1	53.8	8.62E-06	HCP03	4.82	20.0	20.9	66.5	2.18E-05
HCL01	4.54	0.0	13.8	52.0	1.61E-05	HCP04	4.82	0.0	7.0	61.5	6.32E-06
HCL01	4.54	10.0	13.9	49.7	1.26E-05	HCP04	4.82	10.0	5.9	58.0	3.84E-06
HCL01	4.54	20.0	17.4	49.2	6.59E-06	HCP04	4.82	20.0	8.9	62.4	2.53E-06
HCL02	4.54	0.0	3.4	53.4	1.88E-05	HCR01	4.89	0.0	16.9	65.4	5.40E-06
HCL02	4.54	10.0	2.5	50.7	1.39E-05	HCR01	4.89	10.0	19.6	65.4	3.89E-06
HCL02	4.54	20.0	6.9	51.2	5.14E-06	HCR01	4.89	20.0	16.6	65.5	3.01E-06
HCL03	4.54	0.0	7.9	54.5	1.86E-05	HCR02	4.89	0.0	18.4	64.7	2.94E-06
HCL03	4.54	10.0	7.2	52.4	1.39E-05	HCR02	4.89	10.0	15.2	59.1	1.69E-06
HCL03	4.54	20.0	7.7	52.0	7.88E-06	HCR02	4.89	20.0	22.0	50.8	8.91E-07
HCL04	4.54	0.0	6.2	50.0	1.89E-05	HCR03	4.89	0.0	20.2	62.4	5.98E-06
HCL04	4.54	10.0	8.0	48.2	1.38E-05	HCR03	4.89	10.0	21.8	59.5	5.27E-06
HCL04	4.54	20.0	8.0	48.5	7.87E-06	HCR03	4.89	20.0	20.9	60.1	2.85E-06
HCM01	4.61	0.0	360.0	48.4	1.21E-05	HCR04	4.89	0.0	20.0	62.9	8.81E-06
HCM01	4.61	10.0	355.0	46.2	7.33E-06	HCR04	4.89	10.0	19.7	63.7	7.31E-06
HCM01	4.61	20.0	357.4	49.8	4.53E-06	HCR04	4.89	20.0	19.6	65.3	5.60E-06
HCM02	4.61	0.0	359.8	52.6	7.62E-06	HCR01	4.96	0.0	21.7	67.0	1.06E-05
HCM02	4.61	10.0	358.9	48.4	5.92E-06	HCR01	4.96	10.0	13.9	66.8	1.02E-05
HCM02	4.61	20.0	357.7	50.0	3.71E-06	HCR01	4.96	20.0	9.8	67.3	6.05E-06
HCM03	4.61	0.0	7.0	48.8	1.13E-05	HCR02	4.96	0.0	9.8	61.5	3.57E-05
HCM03	4.61	10.0	4.7	45.8	7.75E-06	HCR02	4.96	10.0	9.5	60.1	3.17E-05
HCM03	4.61	20.0	3.7	48.6	4.36E-06	HCR02	4.96	20.0	8.1	59.1	2.45E-05
HCM04	4.61	0.0	13.6	61.0	1.35E-05	HCR03	4.96	0.0	17.2	70.1	7.23E-06
HCM04	4.61	10.0	12.1	54.9	9.54E-06	HCR03	4.96	10.0	15.7	68.1	5.38E-06
HCM04	4.61	20.0	10.5	56.0	5.73E-06	HCR03	4.96	20.0	8.2	68.8	1.99E-06
HCO01	4.68	0.0	24.7	61.5	1.06E-05	HCR04	4.96	0.0	14.3	68.4	1.93E-05
HCO01	4.68	10.0	24.2	60.0	6.31E-06	HCR04	4.96	10.0	13.4	67.3	1.71E-05
HCO01	4.68	20.0	25.7	62.2	2.57E-06	HCR04	4.96	20.0	13.0	67.4	1.39E-05
HCO02	4.68	0.0	15.0	65.4	8.37E-06	HCS01	5.03	0.0	14.5	65.7	1.68E-05
HCO02	4.68	10.0	15.6	62.4	4.96E-06	HCS01	5.03	10.0	26.9	66.9	9.94E-06

S	E	AF	D	I	J	S	E	AF	D	I	J
HCS01	5.03	20.0	15.0	64.3	4.73E-06	HGX03	5.38	0.0	19.4	71.2	1.07E-04
HCS02	5.03	0.0	15.3	59.3	9.59E-06	HGX03	5.38	10.0	18.8	70.7	9.71E-05
HCS02	5.03	10.0	18.2	53.8	6.73E-06	HGX03	5.38	20.0	16.6	70.6	7.52E-05
HCS02	5.03	20.0	15.0	55.7	5.09E-06	HGX04	5.38	0.0	15.0	76.6	5.26E-05
HCS03	5.03	0.0	17.6	71.7	2.86E-05	HGX04	5.38	10.0	12.3	75.5	4.93E-05
HCS03	5.03	10.0	19.8	74.7	2.15E-05	HGX04	5.38	20.0	14.4	75.6	4.12E-05
HCS03	5.03	20.0	19.8	72.9	1.26E-05	HGY01	5.45	0.0	4.5	63.7	4.85E-05
HCS04	5.03	0.0	15.3	67.4	2.14E-05	HGY01	5.45	10.0	5.1	62.9	4.36E-05
HCS04	5.03	10.0	12.8	68.0	1.28E-05	HGY01	5.45	20.0	5.0	61.5	3.69E-05
HCS04	5.03	20.0	16.3	68.7	7.21E-06	HGY02	5.45	0.0	333.8	70.9	8.55E-06
HCT01	5.10	0.0	22.2	71.9	2.28E-05	HGY02	5.45	10.0	336.5	70.4	6.37E-06
HCT01	5.10	10.0	13.2	69.6	1.32E-05	HGY02	5.45	20.0	350.0	73.6	3.33E-06
HCT01	5.10	20.0	18.2	67.8	6.67E-06	HGY03	5.45	0.0	279.0	85.8	7.96E-06
HCT02	5.10	0.0	27.3	67.3	1.86E-05	HGY03	5.45	10.0	233.4	84.2	5.50E-06
HCT02	5.10	10.0	31.7	64.6	8.63E-06	HGY03	5.45	20.0	239.9	80.6	4.07E-06
HCT02	5.10	20.0	23.5	63.7	6.79E-06	HGY04	5.45	0.0	9.6	67.3	5.82E-05
HCT03	5.10	0.0	5.3	60.2	2.09E-05	HGY04	5.45	10.0	6.9	67.3	5.06E-05
HCT03	5.10	10.0	0.9	62.5	1.49E-05	HGY04	5.45	20.0	9.6	67.6	3.48E-05
HCT03	5.10	20.0	3.6	61.6	1.00E-05	HGZ01	5.52	0.0	357.2	66.5	3.21E-05
HCT04	5.10	0.0	13.9	71.0	1.97E-05	HGZ01	5.52	10.0	357.9	64.3	2.80E-05
HCT04	5.10	10.0	12.0	68.2	1.24E-05	HGZ01	5.52	20.0	357.8	62.7	2.37E-05
HCT04	5.10	20.0	13.5	66.2	7.40E-06	HGZ02	5.52	0.0	356.7	69.7	7.39E-06
HCU01	5.17	0.0	5.0	69.3	1.94E-05	HGZ02	5.52	10.0	0.3	65.2	5.22E-06
HCU01	5.17	10.0	2.0	68.2	1.07E-05	HGZ02	5.52	20.0	354.4	67.6	3.53E-06
HCU01	5.17	20.0	2.4	65.4	5.53E-06	HGZ03	5.52	0.0	350.0	75.7	7.22E-06
HCU02	5.17	0.0	14.0	66.1	3.42E-05	HGZ03	5.52	10.0	351.4	73.7	4.95E-06
HCU02	5.17	10.0	17.2	64.7	2.29E-05	HGZ03	5.52	20.0	344.2	72.0	3.30E-06
HCU02	5.17	20.0	19.1	62.4	1.78E-05	HGZ04	5.52	0.0	23.0	69.8	2.83E-05
HCU03	5.17	0.0	19.8	62.3	2.56E-05	HLZ04	5.52	10.0	24.0	69.0	2.61E-05
HCU03	5.17	10.0	21.8	61.7	1.70E-05	HLZ04	5.52	20.0	23.1	68.5	2.11E-05
HCU03	5.17	20.0	15.1	64.9	9.97E-06	HDA01	5.59	0.0	353.8	65.2	1.04E-05
HCU04	5.17	0.0	15.3	65.5	2.62E-05	HDA01	5.59	10.0	356.6	61.7	8.34E-06
HCU04	5.17	10.0	16.6	65.8	1.82E-05	HDA01	5.59	20.0	356.1	62.9	5.92E-06
HCU04	5.17	20.0	15.3	63.4	1.21E-05	HDA02	5.59	0.0	13.2	63.2	1.63E-05
HCV01	5.24	0.0	12.8	60.9	5.62E-05	HDA02	5.59	10.0	16.6	64.0	1.07E-05
HCV01	5.24	10.0	8.8	62.9	4.27E-05	HDA02	5.59	20.0	21.8	63.7	1.01E-05
HCV01	5.24	20.0	9.1	64.6	2.91E-05	HDA03	5.59	0.0	23.3	72.2	1.64E-05
HCV02	5.24	0.0	1.8	65.6	4.97E-05	HDA03	5.59	10.0	27.6	69.9	1.31E-05
HCV02	5.24	10.0	3.8	67.5	3.49E-05	HDA03	5.59	20.0	27.8	68.2	1.18E-05
HCV02	5.24	20.0	7.4	66.0	2.38E-05	HDA04	5.59	0.0	305.2	88.8	7.93E-06
HCV03	5.24	0.0	13.6	70.3	3.31E-05	HDA04	5.59	10.0	205.6	87.6	5.81E-06
HCV03	5.24	10.0	13.4	63.3	2.33E-05	HDA04	5.59	20.0	342.1	87.5	4.27E-06
HCV03	5.24	20.0	9.2	63.4	1.71E-05	HDB01	5.66	0.0	0.7	65.9	1.29E-05
HCV04	5.24	0.0	17.0	74.4	3.04E-05	HDB01	5.66	10.0	1.0	63.2	9.01E-06
HCV04	5.24	10.0	15.0	71.5	2.16E-05	HDB01	5.66	20.0	1.7	61.6	7.58E-06
HCV04	5.24	20.0	14.2	69.5	1.42E-05	HDB02	5.66	0.0	356.5	76.9	7.46E-06
HCW01	5.31	0.0	5.1	72.1	2.74E-05	HDB02	5.66	10.0	354.5	73.4	4.70E-06
HCW01	5.31	10.0	4.9	74.9	1.92E-05	HDB02	5.66	20.0	355.1	72.3	2.69E-06
HCW01	5.31	20.0	7.7	72.0	1.68E-05	HDB03	5.66	0.0	350.9	73.9	1.16E-05
HCW02	5.31	0.0	11.6	66.1	3.21E-05	HDB03	5.66	10.0	351.5	72.0	7.87E-06
HCW02	5.31	10.0	11.5	62.2	2.57E-05	HDB03	5.66	20.0	351.7	72.2	4.31E-06
HCW02	5.31	20.0	14.6	62.6	1.74E-05	HDB04	5.66	0.0	13.8	81.5	2.92E-05
HCW03	5.31	0.0	17.5	58.6	1.74E-04	HDB04	5.66	10.0	18.3	79.0	2.47E-05
HCW03	5.31	10.0	17.4	59.1	1.60E-04	HDB04	5.66	20.0	19.0	77.8	2.02E-05
HCW03	5.31	20.0	17.9	57.7	1.26E-04	HDC01	5.73	0.0	357.2	70.2	7.93E-06
HCW04	5.31	0.0	6.8	63.7	3.49E-05	HDC01	5.73	10.0	357.6	67.8	6.49E-06
HCW04	5.31	10.0	5.2	62.6	3.23E-05	HDC01	5.73	20.0	358.3	65.4	4.47E-06
HCW04	5.31	20.0	8.3	61.7	2.66E-05	HDC02	5.73	0.0	358.3	66.7	9.67E-06
HGX01	5.38	0.0	3.5	56.9	8.99E-05	HDC02	5.73	10.0	359.4	64.2	6.59E-06
HGX01	5.38	10.0	3.0	56.4	8.19E-05	HDC02	5.73	20.0	1.2	63.6	4.87E-06
HGX01	5.38	20.0	4.7	55.0	6.33E-05	HDC03	5.73	0.0	359.0	71.7	9.93E-06
HGX02	5.38	0.0	23.6	59.8	3.15E-05	HDC03	5.73	10.0	3.6	70.3	8.88E-06
HGX02	5.38	10.0	22.3	58.5	2.89E-05	HDC03	5.73	20.0	0.2	71.8	4.86E-06
HGX02	5.38	20.0	19.4	57.9	2.31E-05	HDC04	5.73	0.0	1.6	72.6	7.77E-06

S	E	AF	D	I	J	S	E	AF	D	I	J
HDC04	5.73	10.0	358.8	68.3	5.15E-06	HDC03	6.08	10.0	356.8	67.5	1.33E-05
HDC04	5.73	20.0	4.4	68.8	3.89E-06	HDC03	6.08	20.0	356.6	66.3	8.41E-06
HDD01	5.80	0.0	353.8	70.0	1.16E-05	HDC04	6.08	0.0	6.0	73.5	1.33E-05
HDD01	5.80	10.0	351.7	68.9	7.60E-06	HDC04	6.08	10.0	10.3	71.2	1.03E-05
HDD01	5.80	20.0	353.6	65.7	5.04E-06	HDC04	6.08	20.0	1.4	70.7	4.95E-06
HDD02	5.80	0.0	9.7	68.5	1.33E-05	HDI01	6.15	0.0	357.9	65.9	1.81E-05
HDD02	5.80	2.5	6.5	68.5	1.22E-05	HDI01	6.15	10.0	357.5	63.5	1.44E-05
HDD02	5.80	5.0	3.8	68.6	1.01E-05	HDI01	6.15	20.0	355.0	63.2	1.17E-05
HDD02	5.80	10.0	8.0	66.7	7.64E-06	HDI02	6.15	0.0	5.1	70.8	3.32E-05
HDD02	5.80	15.0	9.5	64.5	5.49E-06	HDI02	6.15	10.0	6.8	68.0	2.33E-05
HDD02	5.80	20.0	9.2	64.3	4.48E-06	HDI02	6.15	20.0	356.0	54.6	2.92E-05
HDD02	5.80	30.0	13.0	60.8	2.66E-06	HDI03	6.15	0.0	10.8	73.6	2.12E-05
HDD02	5.80	40.0	22.7	54.7	2.10E-06	HDI03	6.15	10.0	8.9	73.0	1.65E-05
HDD02	5.80	50.0	6.6	58.7	8.04E-07	HDI03	6.15	20.0	5.5	72.0	1.16E-05
HDD02	5.80	60.0	47.4	2.0	1.25E-06	HDI04	6.15	0.0	16.6	75.3	1.27E-05
HDD03	5.80	0.0	1.2	66.4	1.03E-05	HDI04	6.15	10.0	18.5	74.2	9.66E-06
HDD03	5.80	10.0	4.0	63.3	5.79E-06	HDI04	6.15	20.0	9.3	72.6	5.97E-06
HDD03	5.80	20.0	0.8	62.9	2.77E-06	HDI01	6.22	0.0	0.6	72.0	1.02E-05
HDD04	5.80	0.0	0.1	67.3	8.56E-06	HDI01	6.22	10.0	352.8	72.5	5.41E-06
HDD04	5.80	10.0	5.6	66.7	5.61E-06	HDI01	6.22	20.0	359.6	73.4	2.81E-06
HDD04	5.80	20.0	356.8	63.1	3.66E-06	HDI02	6.22	0.0	0.2	73.4	3.09E-05
HDE01	5.87	0.0	2.3	71.8	7.42E-06	HDI02	6.22	10.0	0.8	70.3	2.47E-05
HDE01	5.87	10.0	348.0	69.4	4.49E-06	HDI02	6.22	20.0	359.3	69.3	1.74E-05
HDE01	5.87	20.0	10.8	65.7	2.53E-06	HDI03	6.22	0.0	7.8	75.5	7.63E-06
HDE02	5.87	0.0	5.5	70.6	1.03E-05	HDI03	6.22	10.0	7.7	74.1	3.93E-06
HDE02	5.87	10.0	2.9	68.0	4.21E-06	HDI03	6.22	20.0	7.5	73.2	1.78E-06
HDE02	5.87	20.0	10.7	65.9	3.64E-06	HDI04	6.22	0.0	11.0	78.3	9.63E-06
HDE03	5.87	0.0	7.7	74.7	9.83E-06	HDI04	6.22	10.0	7.5	74.5	8.16E-06
HDE03	5.87	10.0	358.0	72.0	4.47E-06	HDI04	6.22	20.0	11.8	72.4	5.00E-06
HDE03	5.87	20.0	5.7	69.9	2.40E-06	HDK01	6.29	0.0	14.6	74.7	1.30E-05
HDE04	5.87	0.0	346.4	70.4	7.66E-06	HDK01	6.29	10.0	12.4	74.6	6.93E-06
HDE04	5.87	10.0	345.3	70.6	5.08E-06	HDK01	6.29	20.0	1.9	72.1	3.83E-06
HDE04	5.87	20.0	351.6	71.8	4.50E-06	HDK02	6.29	0.0	1.1	66.9	1.50E-05
HDF01	5.94	0.0	22.4	73.4	1.33E-05	HDK02	6.29	10.0	8.0	62.7	1.07E-05
HDF01	5.94	10.0	15.1	70.4	6.75E-06	HDK02	6.29	20.0	10.3	65.3	6.78E-06
HDF01	5.94	20.0	18.9	70.0	4.31E-06	HDK03	6.29	0.0	5.2	68.0	9.65E-06
HDF02	5.94	0.0	2.9	71.3	1.20E-05	HDK03	6.29	10.0	5.2	64.4	5.64E-06
HDF02	5.94	10.0	13.0	67.8	6.82E-06	HDK03	6.29	20.0	7.5	59.0	2.93E-06
HDF02	5.94	20.0	12.7	65.2	3.20E-06	HDK04	6.29	0.0	7.4	69.1	1.33E-05
HDF03	5.94	0.0	15.9	73.2	1.15E-05	HDK04	6.29	10.0	7.5	67.7	1.03E-05
HDF03	5.94	10.0	17.3	71.2	7.19E-06	HDK04	6.29	20.0	1.1	66.8	7.45E-06
HDF03	5.94	20.0	26.1	72.0	4.96E-06	HDL01	6.36	0.0	2.3	65.1	4.21E-05
HDF04	5.94	0.0	1.2	72.4	1.21E-05	HDL01	6.36	10.0	1.8	61.5	3.09E-05
HDF04	5.94	10.0	356.9	69.6	8.32E-06	HDL01	6.36	20.0	3.5	57.5	2.06E-05
HDF04	5.94	20.0	3.2	70.4	5.76E-06	HDL02	6.36	0.0	0.5	63.5	3.10E-05
HDG01	6.01	0.0	1.0	63.8	1.51E-05	HDL02	6.36	10.0	1.0	60.9	2.28E-05
HDG01	6.01	10.0	2.6	61.1	8.06E-06	HDL02	6.36	20.0	2.6	61.0	1.62E-05
HDG01	6.01	20.0	4.9	60.9	4.40E-06	HDL03	6.36	0.0	18.2	73.1	1.79E-05
HDG02	6.01	0.0	11.1	67.2	1.43E-05	HDL03	6.36	10.0	16.4	71.6	1.31E-05
HDG02	6.01	10.0	7.8	68.3	1.28E-05	HDL03	6.36	20.0	22.5	70.3	9.75E-06
HDG02	6.01	20.0	7.9	68.6	5.04E-06	HDL04	6.36	0.0	11.2	77.1	1.90E-05
HDG03	6.01	0.0	2.4	72.0	1.20E-05	HDL04	6.36	2.5	8.4	74.6	1.53E-05
HDG03	6.01	10.0	354.7	69.6	9.02E-06	HDL04	6.36	5.0	10.4	74.3	1.34E-05
HDG03	6.01	20.0	355.7	68.3	3.55E-06	HDL04	6.36	10.0	15.8	70.9	1.03E-05
HDG04	6.01	0.0	3.4	74.8	1.04E-05	HDL04	6.36	15.0	17.1	67.3	8.50E-06
HDG04	6.01	10.0	4.2	70.6	6.87E-06	HDL04	6.36	20.0	19.9	71.1	6.92E-06
HDG04	6.01	20.0	6.9	70.5	4.12E-06	HDL04	6.36	30.0	26.1	64.2	4.55E-06
HDH01	6.08	0.0	1.4	70.7	2.86E-05	HDL04	6.36	40.0	37.5	64.1	3.14E-06
HDH01	6.08	10.0	0.8	69.0	2.24E-05	HDL04	6.36	50.0	248.0	73.0	2.29E-06
HDH01	6.08	20.0	359.4	66.0	1.53E-05	HDL04	6.36	60.0	351.0	58.5	8.61E-07
HDH02	6.08	0.0	9.3	72.2	1.08E-05	HDM01	6.43	0.0	4.7	64.6	8.74E-05
HDH02	6.08	10.0	6.9	71.7	7.25E-06	HDM01	6.43	10.0	4.1	64.7	7.14E-05
HDH02	6.08	20.0	9.0	71.6	6.98E-06	HDM01	6.43	20.0	3.5	64.9	5.16E-05
HDH03	6.03	0.0	359.6	68.2	1.97E-05	HDM02	6.43	0.0	9.2	70.5	7.89E-05

S	E	AF	D	I	J
HDM02	6.43	10.0	10.1	69.2	6.20E-05
HDM02	6.43	20.0	9.7	67.2	4.39E-05
HDM03	6.43	0.0	12.9	75.1	6.20E-05
HDM03	6.43	10.0	12.7	74.1	5.16E-05
HDM03	6.43	20.0	15.7	73.3	3.94E-05
HDM04	6.43	0.0	15.2	68.6	7.79E-05
HDM04	6.43	10.0	16.4	68.1	6.28E-05
HDM04	6.43	20.0	22.5	67.0	4.52E-05
HDM01	6.50	0.0	1.2	71.5	1.10E-04
HDM01	6.50	10.0	0.5	71.7	9.55E-05
HDM01	6.50	20.0	1.3	71.2	7.53E-05
HDM02	6.50	0.0	4.0	73.8	7.96E-05
HDM02	6.50	10.0	7.4	74.9	6.49E-05
HDM02	6.50	20.0	4.8	75.0	4.84E-05
HDM03	6.50	0.0	19.5	75.5	7.13E-05
HDM03	6.50	10.0	18.9	74.0	5.50E-05
HDM03	6.50	20.0	22.8	74.0	4.05E-05
HDM04	6.50	0.0	23.5	72.5	5.58E-05
HDM04	6.50	10.0	21.9	72.0	4.45E-05
HDM04	6.50	20.0	22.1	70.1	3.40E-05
HDO01	6.57	0.0	10.6	78.7	9.73E-05
HDO01	6.57	10.0	4.1	78.5	8.28E-05
HDO01	6.57	20.0	7.1	79.7	6.40E-05
HDO02	6.57	0.0	4.9	69.4	1.02E-04
HDO02	6.57	10.0	5.2	67.7	8.31E-05
HDO02	6.57	20.0	3.8	67.3	6.39E-05
HDO03	6.57	0.0	17.8	72.1	6.06E-05
HDO03	6.57	10.0	17.3	71.9	4.94E-05
HDO03	6.57	20.0	22.4	71.8	3.59E-05
HDO04	6.57	0.0	13.8	72.3	9.41E-05
HDO04	6.57	10.0	15.3	71.9	8.21E-05
HDO04	6.57	20.0	16.5	71.5	6.56E-05
HDP01	6.64	0.0	1.1	73.6	3.67E-05
HDP01	6.64	10.0	356.8	69.7	2.38E-05
HDP01	6.64	20.0	356.4	69.8	1.46E-05
HDP02	6.64	0.0	9.7	73.0	6.41E-05
HDP02	6.64	10.0	11.8	73.8	5.02E-05
HDP02	6.64	20.0	14.2	72.5	3.74E-05
HDP03	6.64	0.0	6.7	71.4	4.14E-05
HDP03	6.64	10.0	5.7	72.2	3.33E-05
HDP03	6.64	20.0	5.6	69.7	2.66E-05
HDP04	6.64	0.0	23.8	72.4	1.80E-05
HDP04	6.64	10.0	18.4	72.0	1.05E-05
HDP04	6.64	20.0	14.3	69.0	6.98E-06
HDR01	6.71	0.0	1.2	68.7	1.96E-05
HDR01	6.71	10.0	3.5	67.6	1.02E-05
HDR01	6.71	20.0	5.6	63.0	7.19E-06
HDR02	6.71	0.0	357.2	65.8	1.99E-05
HDR02	6.71	10.0	357.9	59.6	1.25E-05
HDR02	6.71	20.0	1.6	54.7	6.14E-06
HDR03	6.71	0.0	348.0	67.0	2.57E-05
HDR03	6.71	10.0	346.9	62.4	1.46E-05
HDR03	6.71	20.0	347.8	61.1	1.28E-05
HDR04	6.71	0.0	5.3	74.5	1.94E-05
HDR04	6.71	10.0	1.1	74.4	1.43E-05
HDR04	6.71	20.0	5.1	73.4	9.68E-06

Appendix 2

Carved	specimen	data
S	specimen	
E	elevation	(metres)
AF	alternating field	demagnetization (mT)
D	declination	(degrees)
I	inclination	(degrees)
J	intensity	(A.m ² / kg)

S	E	AF	D	I	J	S	E	AF	D	I	J
HEA01	5.73	0.0	5.1	66.0	6.51E-06	HEE01	1.32	10.0	355.2	68.1	1.07E-04
HEA01	5.73	5.0	0.9	66.3	5.75E-06	HEE01	1.32	20.0	358.0	68.2	9.14E-05
HEA01	5.73	10.0	2.6	66.3	4.87E-06	HEE02	1.32	0.0	350.1	60.3	2.51E-04
HEA01	5.73	20.0	358.5	63.6	3.19E-06	HEE02	1.32	5.0	349.1	63.2	2.40E-04
HEA02	5.73	0.0	5.4	68.7	1.02E-05	HEE02	1.32	10.0	349.6	65.1	2.26E-04
HEA02	5.73	5.0	3.5	69.8	9.04E-06	HEE02	1.32	20.0	353.0	66.3	1.90E-04
HEA02	5.73	10.0	4.9	68.9	8.24E-06	HEE03	1.32	0.0	341.0	66.0	1.99E-04
HEA02	5.73	20.0	3.3	70.4	5.83E-06	HEE03	1.32	5.0	342.6	66.8	2.16E-04
HEA03	5.73	0.0	7.5	64.4	6.89E-06	HEE03	1.32	10.0	346.0	67.2	1.85E-04
HEA03	5.73	5.0	5.5	66.1	5.80E-06	HEE03	1.32	20.0	352.4	66.9	1.56E-04
HEA03	5.73	10.0	5.5	64.6	4.91E-06	HEE04	1.32	0.0	322.3	59.6	2.20E-04
HEA03	5.73	20.0	13.1	64.8	3.29E-06	HEE04	1.32	5.0	323.9	62.0	2.05E-04
HEA04	5.73	0.0	351.8	68.7	7.26E-06	HEE04	1.32	10.0	330.1	64.3	1.85E-04
HEA04	5.73	5.0	349.9	69.8	6.14E-06	HEE04	1.32	20.0	337.7	65.6	1.46E-04
HEA04	5.73	10.0	348.9	69.4	5.26E-06	HEF01	1.34	0.0	348.2	66.9	1.65E-04
HEA04	5.73	20.0	348.4	67.7	3.72E-06	HEF01	1.34	5.0	351.4	66.2	1.59E-04
HEB01	2.21	0.0	9.9	64.3	9.14E-05	HEF01	1.34	10.0	353.1	66.0	1.51E-04
HEB01	2.21	5.0	10.5	64.8	9.08E-05	HEF01	1.34	20.0	357.8	65.5	1.26E-04
HEB01	2.21	10.0	10.5	64.5	8.78E-05	HEF02	1.34	0.0	336.9	64.6	1.15E-04
HEB01	2.21	20.0	10.3	65.1	7.39E-05	HEF02	1.34	5.0	340.0	65.4	1.13E-04
HEB02	2.21	0.0	14.2	66.9	2.65E-05	HEF02	1.34	10.0	345.3	65.2	1.06E-04
HEB02	2.21	5.0	12.1	67.7	2.78E-05	HEF02	1.34	20.0	351.6	64.9	8.97E-05
HEB02	2.21	10.0	12.2	67.5	2.67E-05	HEF03	1.34	0.0	359.6	65.8	1.78E-04
HEB02	2.21	20.0	12.2	67.5	2.32E-05	HEF03	1.34	5.0	358.8	66.0	1.71E-04
HEB03	2.21	0.0	13.0	65.1	6.31E-05	HEF03	1.34	10.0	0.2	65.6	1.62E-04
HEB03	2.21	5.0	12.3	64.8	6.29E-05	HEF03	1.34	20.0	2.5	65.1	1.36E-04
HEB03	2.21	10.0	12.7	64.3	6.04E-05	HEF04	1.34	0.0	342.2	65.5	1.66E-04
HEB03	2.21	20.0	12.7	65.2	5.04E-05	HEF04	1.34	5.0	345.7	65.3	1.57E-04
HEB04	2.21	0.0	12.1	66.4	5.85E-05	HEF04	1.34	10.0	348.1	65.2	1.47E-04
HEB04	2.21	5.0	12.6	66.2	5.88E-05	HEF04	1.34	20.0	350.4	64.3	1.21E-04
HEB04	2.21	10.0	13.0	66.0	5.75E-05	HEG01	1.35	0.0	342.3	61.8	1.93E-04
HEB04	2.21	20.0	12.1	66.4	4.90E-05	HEG01	1.35	5.0	342.1	63.1	1.89E-04
HEC01	1.29	0.0	344.4	69.8	1.90E-04	HEG01	1.35	10.0	344.0	64.5	1.82E-04
HEC01	1.29	5.0	349.6	68.9	1.86E-04	HEG01	1.35	20.0	350.9	64.4	1.55E-04
HEC01	1.29	10.0	351.5	67.7	1.82E-04	HEG01	1.35	25.0	352.7	66.0	1.33E-04
HEC01	1.29	20.0	353.3	65.9	1.57E-04	HEG01	1.35	30.0	352.2	64.6	1.13E-04
HEC02	1.29	0.0	336.4	69.6	9.72E-05	HEG01	1.35	35.0	353.1	63.5	9.12E-05
HEC02	1.29	5.0	341.8	69.5	9.66E-05	HEG01	1.35	40.0	7.5	62.2	7.10E-05
HEC02	1.29	10.0	343.0	67.4	9.20E-05	HEG01	1.35	50.0	0.2	70.4	4.24E-05
HEC02	1.29	20.0	346.6	66.3	7.99E-05	HEG02	1.35	0.0	340.7	66.4	1.40E-04
HEC03	1.29	0.0	6.9	72.0	1.68E-04	HEG02	1.35	5.0	343.0	66.7	1.35E-04
HEC03	1.29	5.0	5.4	70.3	1.65E-04	HEG02	1.35	10.0	344.4	67.2	1.28E-04
HEC03	1.29	10.0	5.1	69.1	1.61E-04	HEG02	1.35	20.0	348.4	67.6	1.07E-04
HEC03	1.29	20.0	5.7	67.3	1.41E-04	HEG02	1.35	25.0	2.3	56.6	9.90E-05
HEC04	1.29	0.0	307.9	79.1	2.10E-04	HEG02	1.35	30.0	357.0	68.2	7.59E-05
HEC04	1.29	5.0	317.3	78.8	2.09E-04	HEG02	1.35	35.0	357.1	68.4	6.19E-05
HEC04	1.29	10.0	319.2	78.2	2.01E-04	HEG02	1.35	40.0	359.7	67.3	4.87E-05
HEC04	1.29	20.0	328.9	77.2	1.72E-04	HEG02	1.35	50.0	13.1	70.2	2.51E-05
HED01	1.31	0.0	340.2	62.9	2.48E-04	HEG03	1.35	0.0	340.4	66.8	2.42E-04
HED01	1.31	5.0	338.4	65.7	2.37E-04	HEG03	1.35	5.0	340.7	67.1	2.32E-04
HED01	1.31	10.0	341.0	66.4	2.23E-04	HEG03	1.35	10.0	343.2	65.6	2.20E-04
HED01	1.31	20.0	345.2	67.6	1.86E-04	HEG03	1.35	20.0	350.8	64.5	1.87E-04
HED02	1.31	0.0	351.2	61.0	1.82E-04	HEG03	1.35	25.0	351.9	64.5	1.60E-04
HED02	1.31	5.0	351.1	63.2	1.73E-04	HEG03	1.35	30.0	354.3	63.6	1.36E-04
HED02	1.31	10.0	350.8	64.0	1.64E-04	HEG03	1.35	35.0	356.4	64.3	1.11E-04
HED02	1.31	20.0	351.2	64.5	1.40E-04	HEG03	1.35	40.0	245.3	78.4	1.17E-04
HED03	1.31	0.0	351.7	60.9	1.61E-04	HEG03	1.35	50.0	214.2	62.3	6.41E-05
HED03	1.31	5.0	350.5	62.9	1.54E-04	HEG04	1.35	0.0	260.1	68.0	2.90E-04
HED03	1.31	10.0	350.5	63.8	1.45E-04	HEG04	1.35	5.0	264.0	71.1	2.77E-04
HED03	1.31	20.0	350.5	64.3	1.24E-04	HEG04	1.35	10.0	272.9	73.6	2.55E-04
HED04	1.31	0.0	353.6	61.5	1.51E-04	HEG04	1.35	20.0	306.7	75.7	2.05E-04
HED04	1.31	5.0	353.2	62.4	1.44E-04	HEG04	1.35	25.0	321.1	74.6	1.73E-04
HED04	1.31	10.0	351.8	63.2	1.37E-04	HEG04	1.35	30.0	330.7	74.0	1.44E-04
HED04	1.31	20.0	353.6	63.0	1.16E-04	HEG04	1.35	35.0	332.8	72.3	1.21E-04
HEE01	1.32	0.0	356.1	66.0	1.16E-04	HEG04	1.35	40.0	337.0	71.2	9.72E-05
HEE01	1.32	5.0	354.0	67.3	1.12E-04	HEG04	1.35	50.0	321.0	73.2	4.71E-05

Appendix 3

Viscous remanent magnetization data

t time in hours

VRM^a viscous remanent magnetization acquired (A.m²)

AF AF demagnetization (mT)

VRM^b viscous remanent magnetization remaining
after AF demagnetization (A.m²)

HAA03

t	VRM ^a	AF	VRM ^b
0.07	54.62E-08	0.0	334.51E-08
1.0	116.31E-08	2.5	254.63E-08
2.0	142.74E-08	5.0	209.42E-08
4.0	165.18E-08	10.0	160.84E-08
7.0	191.36E-08	15.0	132.16E-08
24.0	253.08E-08	20.0	115.20E-08
44.5	285.51E-08	30.0	80.66E-08
48.0	283.69E-08	40.0	52.15E-08
72.0	310.36E-08	50.0	29.91E-08
96.0	327.65E-08	60.0	18.06E-08

HAK02

t	VRM ^a	AF	VRM ^b
0.15	18.06E-08	0.0	40.61E-08
1.1	23.19E-08	2.5	22.50E-08
2.1	23.34E-08	5.0	15.60E-08
4.1	27.18E-08	10.0	11.90E-08
7.1	26.41E-08	15.0	7.12E-08
24.1	32.32E-08	20.0	6.03E-08
44.6	35.47E-08	30.0	4.25E-08
48.1	34.83E-08	40.0	2.99E-08
72.1	38.84E-08	50.0	1.38E-08
96.1	37.14E-08	60.0	0.91E-08

HBI01

t	VRM ^a	AF	VRM ^b
0.27	21.76E-08	0.0	63.61E-08
1.2	28.59E-08	2.5	43.88E-08
2.2	30.03E-08	5.0	38.58E-08
4.2	32.94E-08	10.0	31.58E-08
7.2	37.30E-08	15.0	24.54E-08
24.2	48.14E-08	20.0	21.54E-08
44.7	54.30E-08	30.0	17.19E-08
48.2	52.01E-08	40.0	13.20E-08
72.2	60.52E-08	50.0	6.03E-08
96.2	61.72E-08	60.0	6.26E-08

HCO04

t	VRM ^a	AF	VRM ^b
0.37	10.53E-08	0.0	19.51E-08
1.3	11.80E-08	2.5	11.37E-08
2.3	12.67E-08	5.0	10.19E-08
4.3	11.17E-08	10.0	6.69E-08
7.3	13.61E-08	15.0	4.10E-08
24.3	15.65E-08	20.0	3.03E-08
44.8	19.26E-08	30.0	2.18E-08
48.3	15.75E-08	40.0	1.77E-08
72.3	20.69E-08	50.0	1.52E-08
96.3	18.95E-08	60.0	1.42E-08

Appendix 4

IRM build-up data

F field (T)

J IRM intensity (A.m² / kg)

HAH04

F	J
0	1.86E-06
0.015	6.24E-04
0.058	9.18E-03
0.113	2.47E-02
0.167	2.71E-02
0.227	2.77E-02
0.278	2.79E-02
0.360	2.84E-02
0.415	2.83E-02
0.484	2.82E-02
0.547	2.82E-02
0.669	2.85E-02
0.780	2.86E-02
0.886	2.87E-02
0.972	2.86E-02
1.046	2.86E-02
1.109	2.87E-02

HAS04

F	J
0	1.57E-06
0.015	1.00E-03
0.067	3.40E-02
0.118	7.22E-02
0.169	8.01E-02
0.226	8.20E-02
0.284	8.27E-02
0.354	8.33E-02
0.421	8.17E-02
0.487	8.23E-02
0.550	8.27E-02
0.676	8.25E-02
0.787	8.29E-02
0.888	8.30E-02
0.976	8.29E-02
1.050	8.28E-02
1.116	8.30E-02

HAR04

F	J
0	1.23E-05
0.015	1.13E-03
0.060	2.88E-02
0.115	7.09E-02
0.169	7.99E-02
0.226	8.18E-02
0.280	8.30E-02
0.357	8.35E-02
0.419	8.37E-02
0.489	8.35E-02
0.552	8.39E-02
0.674	8.40E-02
0.786	8.37E-02
0.887	8.40E-02
0.976	8.40E-02
1.050	8.41E-02
1.116	8.42E-02

HBB02

F	J
0	4.55E-06
0.015	1.64E-04
0.066	1.93E-02
0.116	3.47E-02
0.169	3.73E-02
0.233	3.85E-02
0.279	3.89E-02
0.350	3.91E-02
0.418	3.92E-02
0.481	3.93E-02
0.550	3.92E-02
0.671	3.93E-02
0.785	3.94E-02
0.888	3.93E-02
0.976	3.92E-02
1.050	3.93E-02
1.114	3.90E-02

Appendix 5

High temperature data

T temperature C

J intensity ($\text{A.m}^2 / \text{kg}$)

HAH02		HAR03	
T	J	T	J
21.0	7.89E-05	20.5	1.15E-04
27.0	6.99E-05	29.0	1.11E-04
53.5	7.24E-05	42.0	1.10E-04
103.0	7.14E-05	53.5	1.12E-04
153.0	6.84E-05	98.0	9.75E-05
197.5	6.17E-05	142.5	9.56E-05
246.0	5.05E-05	201.5	8.05E-05
302.5	3.76E-05	255.0	6.65E-05
350.0	2.75E-05	305.0	4.88E-05
400.0	1.16E-05	354.0	3.32E-05
450.0	2.81E-06	403.5	2.00E-05
500.0	1.73E-06	449.5	3.96E-06
551.0	1.70E-06	499.0	2.07E-06
600.0	1.61E-06	548.0	1.92E-06
585.0	5.09E-07	599.0	1.06E-06
506.5	1.80E-06	574.5	6.13E-06
452.0	1.10E-06	492.5	1.39E-06
400.0	1.40E-06	446.0	1.93E-06
367.0	8.26E-07	398.0	1.53E-06
339.0	3.84E-07	351.5	7.92E-07
291.0	8.06E-07	309.0	2.61E-06
248.5	2.36E-07	300.0	2.05E-06
197.0	2.95E-07	245.0	3.14E-06
173.0	1.03E-06	196.0	1.21E-06
102.5	3.46E-07	149.0	3.18E-06
24.5	9.74E-07	101.0	2.22E-06
HEG05		52.5	3.14E-06
T	J	32.0	4.16E-06
19.5	2.17E-04	28.0	2.59E-06
27.0	2.28E-04	HBB03	
47.5	2.11E-04	T	J
98.0	2.03E-04	19.9	5.94E-05
151.0	1.82E-04	25.0	6.23E-05
200.0	1.57E-04	42.5	5.99E-05
252.0	1.21E-04	52.5	6.17E-05
300.5	8.82E-05	103.5	6.28E-05
350.5	5.07E-05	148.0	5.99E-05
400.0	2.15E-05	200.0	4.89E-05
450.0	5.26E-06	250.0	3.90E-05
500.0	1.24E-06	300.0	3.06E-05
549.5	2.14E-06	354.5	1.60E-05
599.0	1.74E-06	398.0	8.89E-06
585.0	1.28E-06	446.0	2.28E-06
510.0	6.24E-07	495.0	1.74E-06
450.0	8.86E-07	551.0	2.33E-06
403.0	1.48E-06	599.5	2.62E-06
389.0	9.61E-07	598.5	7.54E-07
341.0	1.46E-06	553.0	5.62E-07
289.0	8.65E-07	507.0	3.09E-07
250.0	5.91E-07	450.0	4.74E-07
182.0	4.24E-07	402.5	2.08E-06
134.5	3.02E-07	351.0	1.48E-06
75.0	5.29E-07	301.5	3.75E-06
53.0	8.07E-07	248.5	2.75E-06
34.0	4.86E-07	200.0	4.51E-06
		154.0	3.51E-06
		101.0	2.49E-06
		19.0	4.41E-06

B30214